# Using Mesoscale Meteorological Models to Assess Wind Energy Potential

A thesis

submitted in fulfillment

of the requirements for the

Masters of Science in Environmental Science

from the

University of Canterbury

by

Michael Green

University of Canterbury

2005

# Table of Contents

# List of Figures

# List of Tables

# Acknowledgements

First I would like to acknowledge Katie Brown who gave me the inspiration to take on this thesis. I am grateful for her support and encouragement more than she will ever know.

My supervisors Professor Andy Sturman and Dr Peyman Zawar-Reza were always there when I needed them. Their support and wisdom was and continues to be very much appreciated. Thanks also to John Thyne and Graham Furness from the University of Canterbury Geography Department for their help in obtaining and formatting data, and to Margaret Paterson for her help with referencing.

Windflow Technology Ltd provided wind data from their current Windflow 500 turbine site at Gebbies Pass. Geoff Henderson also helped set the scene for me at the very beginning of this journey.

Finally thanks to my family who have given me support in so many ways during this time.

# Abstract

As the demand for safe and clean electricity increases, the New Zealand wind energy industry seems poised to expand. Many generating companies have projects in the planning stage and there are likely to be many more potential sites yet to be identified. Reliable wind climate predictions over a wide area and for different heights above grounds are often vital to determine the viability of wind farm projects. This study investigates the use of meteorological mesoscale models to determine the wind and energy resource, particularly in areas of complex terrain. Complex terrain environments are likely to be typical of where New Zealand wind energy developments will take place.

Using the prognostic mesoscale meteorological model TAPM (The Air Pollution Model), regions of relatively high mean wind speed were identified for a number of regions, including Banks Peninsula and parts of Canterbury and Otago. The simulations were conducted for a one-year period (2001) and at different heights above ground level. Depending on the resolution of the model calculations, speed-up effects from the forcing of some topographic features were accounted for by this model. Where the modelling was considered reliable, hourly wind data were obtained from grid points within the inner grid and used as input data for the industry-standard wind energy assessment model WAsP (The Wind Atlas Analysis and Application Program). As WAsP is able to account for detailed topography and surface roughness features, wind and energy predictions at a specific site or over a wider area surrounding the site were made.

Limitations of both models in complex terrain were identified. These limitations were due to a number of factors, including the grid spacing used for mesoscale model calculations, the complexity of the terrain, and difficulties in modelling some regional scale airflow regimes. Being aware of when and where model limitations are likely to occur is important in being able to overcome and account for them.

# Chapter 1

## Introduction

### 1.1 Background

As energy demands have increased, wind energy has become a favourable option for the generation of electricity in New Zealand, and in many other countries. The proposed Meridian West Wind development near Wellington alone will power up to 110,000 homes in the Wellington region. Greenpeace (2005) also suggests that West Wind will avoid the emission of 520,000 tonnes of carbon dioxide per year, therefore addressing global warming concerns.

It is vital to have reliable estimates of the wind climate at different heights above the ground to determine the feasibility of wind energy developments. These wind climates in the past have tended to be dependent on long-term wind observations, which in many places are sparse and/or unreliable. There are many current methods to predict the mean climate for a specific location or height above ground level. Some techniques use simple empirical formula and interpolation techniques, while other use sophisticated computer-based statistical and numerical type models.

Atmospheric modelling in the wind energy industry has tended to be dominated by the use of The Wind Atlas Analysis and Application Program (WASP). The WAsP model was developed at the Riso National Laboratory, Denmark as a result of economic and environmental interest in wind energy in Europe, and a desire for reliable wind resource information, such as presented in the European Wind Atlas (Troen and Petersen, 1989). The WAsP model is based on using wind data from one site and then applying this to a predicted site or region. This is often a reliable method for making wind and energy predictions, but sometimes there are limitations, particularly if the observed and predicted sites are located in different climate and topographic environments. The WAsP model is known to have problems when applied to particularly complex terrain.

Mesoscale meteorological models can be classified into two types, diagnostic and prognostic. Diagnostic models such as WAsP use interpolated wind fields (from a given wind database) that are then adjusted to satisfy the laws of mass conservation when forced by topography or other physical constraints. Prognostic models provide an evolving state of mesoscale features of the atmosphere through the integration of conservation equations for mass, motion, heat and water. They are initialised by meteorological data available at a coarse resolution, but can

provide predictions at much higher resolutions in areas where no data currently exist. This thesis combines the use of both of these model types to investigate whether reliable wind and energy predictions can be made in the absence of actual wind data. There has been an emphasis in undertaking such predictions in regions of complex terrain, since this is where many wind energy developments are likely to be in New Zealand. It is in these locations that topographic features often enhance the wind speed.

The prognostic modelling addresses two primary goals of this study. First, by simulating the airflow over a region over the period of one year, the spatial variation of mean wind speed will be obtained. Areas of higher mean wind speed can be identified and quantified through this process. Second, in the absence of reliable actual wind data, it is possible to obtain hourly wind data from the prognostic model for anywhere within the modelled area.

The diagnostic model WAsP was used to make wind and energy predictions at a case study site at Gebbies Pass on Banks Peninsula. The WAsP model is able to resolve the speed-up and slow-down effects that result from the interaction of airflow with small-scale terrain and roughness features. These effects are not fully accounted for in the relatively low resolution prognostic modelling. The main goal in this part of the study is to use wind data from a number of different sites and sources (including from the prognostic mesoscale model) to determine the relative accuracy of the wind and energy predictions at the case study site at Gebbies Pass.

The limitations of airflow simulation in complex terrain are commonly acknowledged in the literature on mesoscale meteorological models. There is therefore an emphasis in this study on being able to identify the extent of these limitations, so that attempts can be made to overcome them.

To be able to predict the wind climate at a site without the erecting a 50 m mast for a long period of time could save wind farm developers significant time and money. Model validation against observation data is still likely to be required, but this could be for a shortened period merely to confirm the reliability of the prognostic model results.

## 1.2 Thesis aim and objectives

The overall aim of this thesis is to investigate the application of atmospheric modelling techniques to assessing the wind resource for the establishment of wind farms in New Zealand.

The specific objectives of this research are to:

1. Evaluate the application of a mesoscale meteorological model to the identification of good potential wind energy generating areas in complex terrain.
2. Develop a methodology that uses mesoscale meteorological model wind output data to drive an industry standard wind energy model, so that the wind and energy generation potential can be identified and quantified.
3. Investigate the limitations of the models used, and develop processes to assess and predict such limitations.
4. Develop useful resources for use in planning and development of wind energy projects.

## 1.3 Thesis structure

This thesis has four main sections. Chapter 2 first sets the scene by briefly outlining the development of the wind energy industry in New Zealand and worldwide. The following section makes links between wind and energy concepts, many of which are referred to in later chapters. Following that, the interaction of topographic features on airflow is reviewed – an important factor when making decisions about the potential locations for wind farm development. Finally in this chapter, methods for predicting wind speeds across horizontal distances and at different heights above the ground are reviewed and discussed.

Chapter 3 covers the methodology and validation processes for the prognostic and diagnostic modelling techniques. There is a focus on limitations of modelling airflow in complex terrain using the diagnostic model WAsP.

Chapter 4 presents the prognostic results for the Canterbury, Otago and Banks Peninsula regions. The higher resolution modelling results for mean wind speed and annual energy production for the Gebbies Pass site and the surrounding area are then described.

Model limitations are discussed further in this chapter. Finally, a wind farm simulation is given as an application of the combined prognostic-diagnostic modelling technique.

The conclusions chapter provides some recommendations for the use meteorological mesoscale models for the assessment of wind energy potential in a complex terrain environment, and ways of overcoming limitations of the models used in this study.

# Chapter 2

## Background information

This chapter is divided into four sections. First, an overview is provided of the wind energy industry from both a local and global perspective, together with some background on past and current New Zealand wind energy assessment studies. The second section examines links between wind and energy. The third section looks at the interaction of airflow and the shape of the terrain from a New Zealand perspective, and the final part provides an overview of wind modelling theory and prediction techniques. The aim of these background sections is to provide the research context and background information from which the methodology and results of this research have developed.

### 2.1 Wind energy – setting the scene

This section provides information on the development and current status of the wind energy industry, both at a global and New Zealand level. Although the New Zealand wind energy industry is relatively young compared to some countries in Europe, it has long been recognised as having a vast wind energy resource.

#### 2.1.1 A global overview

Most of the 20th century energy developments were dominated initially by the use of the steam engine followed by more recent technological advances in the conversion of fossil fuels to useful energy. Until the very end of the last century, for many it seemed that the role of wind energy generation in the future would be insignificant. Increasing awareness of the enhanced greenhouse effect, oil shocks, and electricity supply and demand issues have all contributed to making wind a potentially significant and accepted form of energy generation.

The recent wind energy revolution is based on five key concepts, the first of which is the basic need for energy, especially with the finite reserves of fossil fuels and a general concern regarding the use of nuclear energy in many countries. There is also increasing concern that the burning of fossil fuels using existing energy generation methods is contributing to global warming. Second, there has been increasing realisation of the potential of wind energy around the globe. Wind exists everywhere in the world, and in some places with considerable intensity. Third, the technological developments in the wind energy field, particularly with

turbines, have made it economically competitive with other energy conversion methods. The final two concepts are the emotional acceptance of the vision for using wind in energy generation, and the higher level political will to make it happen.

The worldwide rate of growth of electricity generation from wind power is impressive. However, this growth is relative to a small base. It is the potential of what this industry could provide for the world's future energy requirements that is most impressive. Wind energy utilises an unlimited resource while producing minimal quantities of greenhouse gases, a topical issue in the world today and in the future.

From 1990 to 2000, the world wind energy capacity doubled every three years. This is likely to have made it the fastest growing energy technology (Milborrow, 2002). In 2002, it was estimated that the world wind power capacity was 27,000 MW, of which the United States contributed 4265 MW (16%), producing 11.2 billion kilowatt-hours of electricity annually. However, this was only 1% of the national total (Winters, 2003). By the beginning of 2005, the total global installed capacity had reached 46,853 MW, a 19% increase since the start of 2004. Germany had the highest installed capacity, with 16,626 MW at the beginning of 2005, contributing about 35% of the global total. Denmark also utilises its windy climate, with wind energy accounting for about 18% of all electricity consumed (Winters, 2003). Both of these countries have set a goal of generating 50% of their electricity from the wind by 2030 (Dvorak, 2001). The European Union has been pushing to develop alternatives to burning of fossil fuels. It wants 22% of its electricity to come from renewable resources by 2010, to meet its commitments to the Kyoto Protocol (Simmon, 2002). In fact, Europe is very progressive in wind energy contributing 74% of the global total (New Zealand Wind Energy Association, 2005c).

A large percentage of the United States electricity production comes from the burning of fossil fuels, such as coal and oil. It is therefore not surprising that they have refused to ratify the Kyoto Protocol. It is the cost of energy production that has the greatest impact on how electricity is going to be produced. Winters (2003) estimated that it costs about 3 US cents per kilowatt-hour for a gas-fired electricity production plant, while current wind farms produce electricity for about 5 US cents per kilowatt-hour. However, the cost of generating electricity from the wind today is only about 10% of what it was 20 years ago, due to rapid advances in technology. The Chief Executive Officer of Vestas, one of the largest turbine manufacturers

in the world has stated that he expects turbine costs to decline at a rate of 3-5% per year for the foreseeable future (New Zealand Wind Energy Association, 2005a).

Even without taking into account carbon charges for fossil fuel powered forms of electricity, the New Zealand wind industry is competitive with fossil-fuel forms of generation, at less than 6c per KWh. (New Zealand Wind Energy Association, 2005a). However, in a June 2004 study by the Australian Wind Energy Association (AUSWEA), there was still found to be a significant difference between wind and thermal fuel generation costs in that country. This gap is steadily narrowing, especially when carbon costs and high oil prices are accounted for. With increased production of turbines and more efficient technology, the cost of wind power will fall and this is essential for wind powered electricity production to be a viable option or alternative.

### 2.1.2 A New Zealand specific overview

The demand for electricity in New Zealand is growing at rate of two to three percent per year. If this demand is to be met, then installation of between 150 and 300 MW of new electricity generation is required every year (New Zealand Wind Energy Association, 2005g). It is most likely that such energy production will have to be met through either wind turbines, coal or natural gas, especially with limited future hydro and geothermal generation options. Harnessing the wind for electricity production is fast becoming a favourable option that satisfies the desire for an environmentally safe and cost effective way of meeting New Zealand's electricity requirements.

Although only 132 MW of wind turbines was installed in 2004 (compared to 2037 MW in Germany), for global wind turbine installation per capita, New Zealand was ranked fourth in the world behind Spain, Ireland and Luxembourg. For wind turbine installations relative to land area, New Zealand was ranked 22nd in the world for 2004 (New Zealand Wind Energy Association, 2005c). This last statistic suggests that there is much scope to expand the industry, especially considering the wind resource available. The National Energy Efficiency and Conservation Strategy (NEECS) set a target to increase energy supply by renewable resources by 8333 GWh by 2012, relative to 2000. This equates to about 2380 1MW turbines over New Zealand, if this target is met(New Zealand Wind Energy Association, 2005a).

In 2003, New Zealand generated about 63% of its electricity needs from hydropower stations, 26% from burning of gas and coal, and 7% from geothermal sources (Reuters News Service,

2003). Since then, wind energy generation capacity has increased from 40 MW to 168 MW, which is a large increase, but still a small proportion of the total electricity generation. Increasing the proportion of wind energy generation capacity further has a number of benefits to New Zealand, including significant reductions in carbon dioxide emissions and utilising a positive relationship between wind and hydro electricity generation. These two factors will be described briefly below.

On February 2005, the Kyoto Protocol came into force after Russia announced in October 2004 that it would ratify (New Zealand Wind Energy Association, 2005d). The Kyoto Protocol is a multi-national treaty recognising that human activities are affecting the global climate, and putting in place mechanisms for encouraging reductions in greenhouse gas emissions. Such mechanisms include a carbon market in which emitting industries are required to buy permits if a certain level of emissions is exceeded, while carbon credits can be gained by industries that do not emit greenhouse gases. Based on 2003 emissions arising from electricity generation, if New Zealand were to install 1000 MW of wind turbines, carbon dioxide equivalent emissions would be reduced by just over 18% or about 3 million tonnes (New Zealand Wind Energy Association, 2005d). Accounting for carbon credits makes wind energy an even more feasible energy generation option, financially and environmentally.

One common perception of wind energy is that it is intermittent and therefore unreliable. However, wind turbines and hydro power stations work together very effectively. If the wind is blowing, then the water in the hydro lakes can be stored. There has even been discussion that wind turbines could be used to pump water back in storage lakes when wind-generated electricity is not required on the national grid.

It is not clear yet just how much of New Zealand's electricity generation can come from the wind, as there has been no detailed research into this topic. There are a number of issues that will influence this, the first being the integration of an intermittent and fluctuating power source into the national grid. Effective localised wind and power forecasting models will help improve the management of this problem. Another issue is the 'back-up' cost that would be necessary if wind energy generation increased. These 'back-up' costs become significant when wind energy reaches a certain percentage level of the total electricity generation, usually around 10-15% (New Zealand Wind Energy Association, 2005g). New Zealand's electricity infrastructure and generation methods are unique and care needs to be taken when using studies from overseas as a guide to the limitations in the use of wind power in this country.

New technology in the future is likely to relax the constraints on the amount of wind power that can be incorporated into the generation mix.

At the beginning of 2005 there were five wind farms in the North and South Islands (or seven if you count Tararua and Hau Nui developments as separate sites). The details and location of each of these wind farms are provided in Table 2.1 and Figure 2.2. The installed capacity of 168 MW is enough to meet the needs of approximately 75,000 average households (New Zealand Wind Energy Association, 2005b). In comparison, Australia has 380 MW of installed wind energy capacity at the same time.

**Table 2.1: Details of current New Zealand Wind Energy Farms (New Zealand Wind Energy Association, 2005b).**

| Name | Year Commissioned | Region | Number of turbines | Turbine capacity | Project capacity |
|---|---|---|---|---|---|
| **Te Apiti** | 2004 | Manawatu | 55 | 1.65 MW | 90.8 MW |
| **Tararua 2** | 2004 | Manawatu | 55 | 660 kW | 36.3 MW |
| **Hau Hau 2** | 2004 | Manawatu | 8 | 600 kW | 4.8 MW |
| **Gebbies Pass** | 2003 | Canterbury | 1 | 500 kW | 500 kW |
| **Tararua 1** | 1999 | Manawatu | 48 | 660 kW | 31.7 MW |
| **Hau Hau 1** | 1996 | Manawatu | 7 | 550 kW | 3.9 MW |
| **Brooklyn** | 1993 | Wellington | 1 | 225 kW | 225 kW |
| **Total** | | | 175 | | 168.2 MW |


**Figure 2.2: Location of current New Zealand wind farms (New Zealand Wind Energy Association, 2005e).**

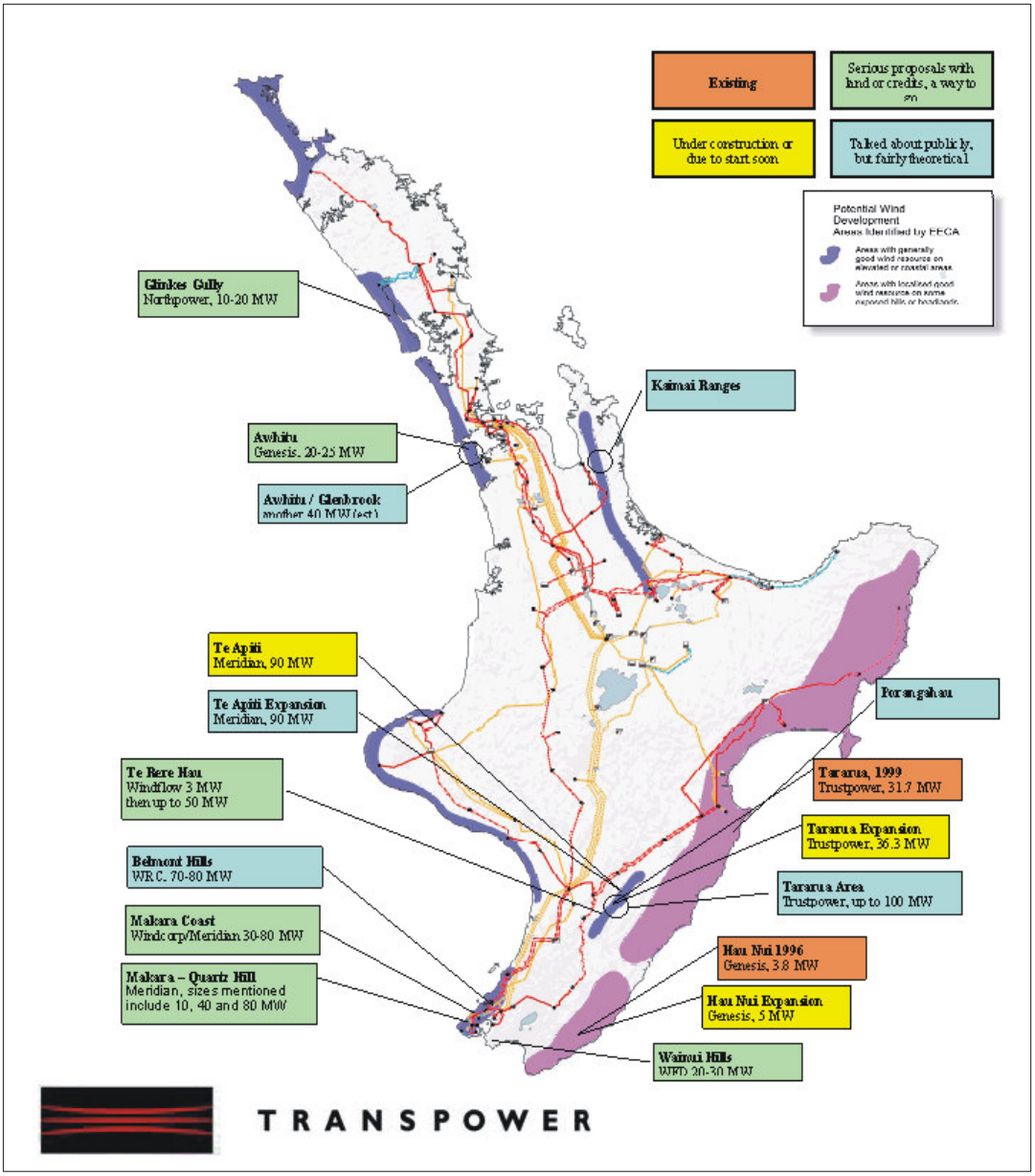


**Figure 2.3: Location of known potential and possible future wind farm developments in the North Island (New Zealand Wind Energy Association, 2005f).**

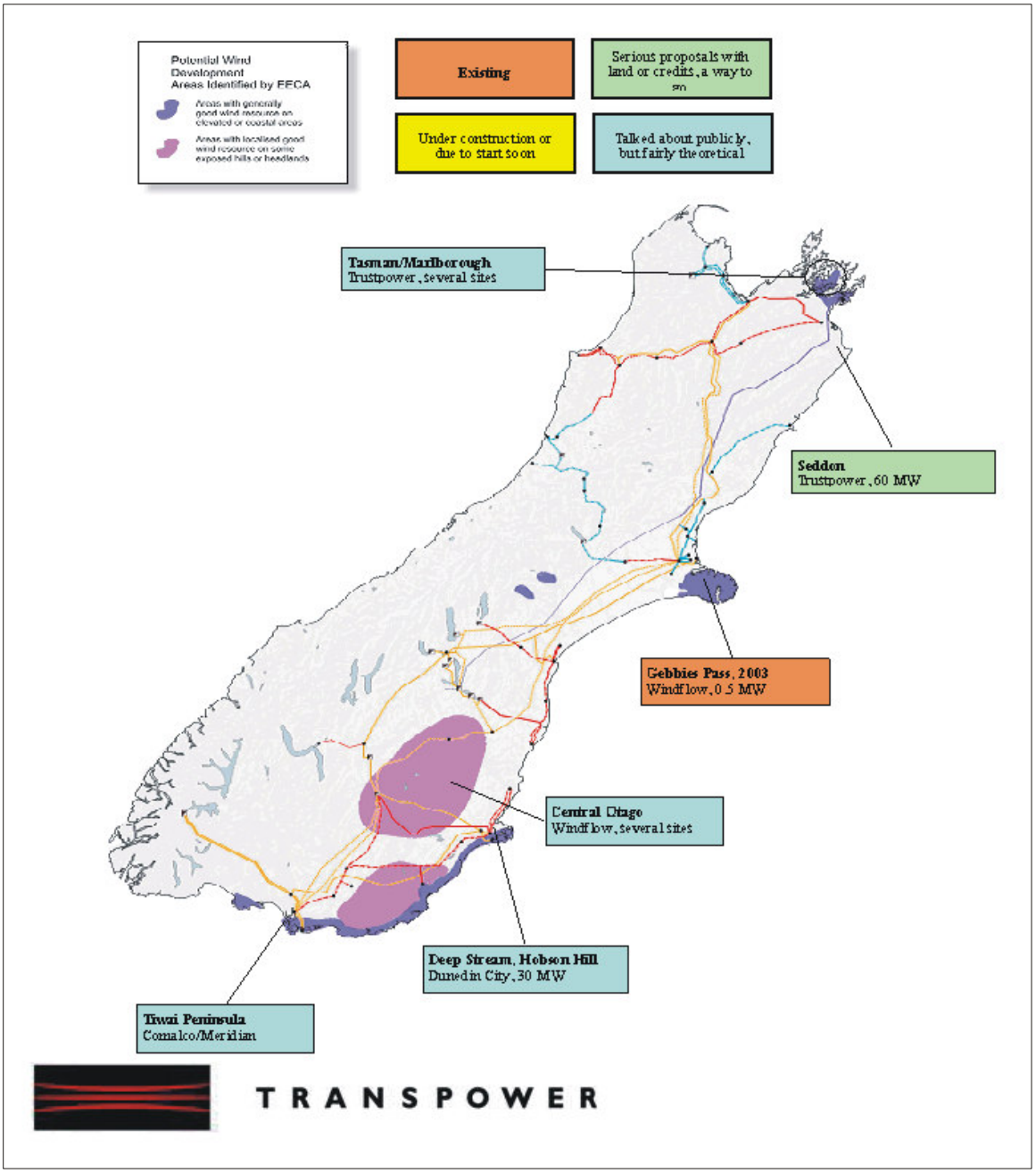


**Figure 2.4: Location of known potential and possible future wind farm developments in the South Island (New Zealand Wind Energy Association, 2005f).**

At the New Zealand Wind Energy Association (NZWEA) conference in July 2004, Transpower identified known possible and probable wind farm developments in New Zealand (Figures 2.3 and 2.4). The maps provide an indication of where wind farms may be located in the future, but there is likely to be much work done to determine (and predict) the wind and power resource at many of these and other so far unidentified locations.

This brief overview of the wind energy generation in New Zealand illustrates the potential for the growth of this industry. New Zealand is demanding more energy generation and at the same time wants this energy source to be environmentally clean and safe. Wind energy is an obvious option for this country, and one that complements existing energy generation methods.

### 2.1.3 Previous and current New Zealand wind energy studies

Existing and prospective wind energy generation companies are conducting many wind energy resource studies confidentially. Some of these studies are identified in the Transpower maps above. Interest has been expressed by the NZWEA in the production of a low-resolution wind map of New Zealand to identify general regions of higher mean wind speed, but without providing sufficient detail to compromise current or future business interests.

A comprehensive wind energy survey of New Zealand was conducted during the 1980's (Cherry, 1987), using a database of surface and upper level wind data from the New Zealand Meteorological Service. There were also special regional surveys conducted for parts of Canterbury and Otago.

In this study, an estimate of the 'well exposed' mean wind speed at 50 m above ground level was made for each observation site. A height of 50 m was regarded as a good level to focus on for future wind energy developments, as it approximated the hub height of commonly available wind turbines. A 'well exposed' site was classified as having a surface roughness length[1] of 0.01m, which is associated with smooth open flat areas or smooth rounded ridge crests. It was found that the seasonal and diurnal characteristics of the mean wind speed varied significantly, depending on proximity to the coast and altitude above sea level.

[1] Surface roughness length is defined as the height above the ground at which the wind speed is zero. Surface roughness length increases with increasing surface roughness.

Elevated sites tend to have winter and night maxima, while lower and coastal generally have spring/summer and afternoon maxima, with the exception of North Island west coast sites which have a winter maxima (Cherry, 1987). Part of the results in this study investigates the seasonal variation of modelled winds over the Banks Peninsula region.

Cherry (1987) created a map to identify areas of good wind energy potential. The map was based on 'well exposed' 50m above ground mean wind speed predictions. It was considered that 'favourable' sites (or areas) were those where the mean wind speed at 50m exceeded 7 m $s^{-1}$. The list below (and Figure 2.5) identifies 16 potentially good wind farm areas in New Zealand identified by Cherry (1987):

1. Far North
2. Campbell and Chatham Islands (not in map area)
3. West of Auckland area – from Murawai to Wuiuku.
4. Coromandel – Kaimai Range (labelled Te Aroha on map)
5. Taranaki coast
6. Manawatu Ranges
7. Wellington hills and coast (labelled Makara Hills on map)
8. Wairarapa hills and coast
9. Farewell Spit (not identified on the map)
10. Marlborough Sounds and hills
11. Marlborough hills and coast (combined with Marlborough Sounds on map)
12. Banks Peninsula
13. Canterbury river gorges
14. Elevated Otago (labelled as Rocklands on map)
15. Coastal Otago (not identified on map)
16. Foveaux Strait and southeast hills

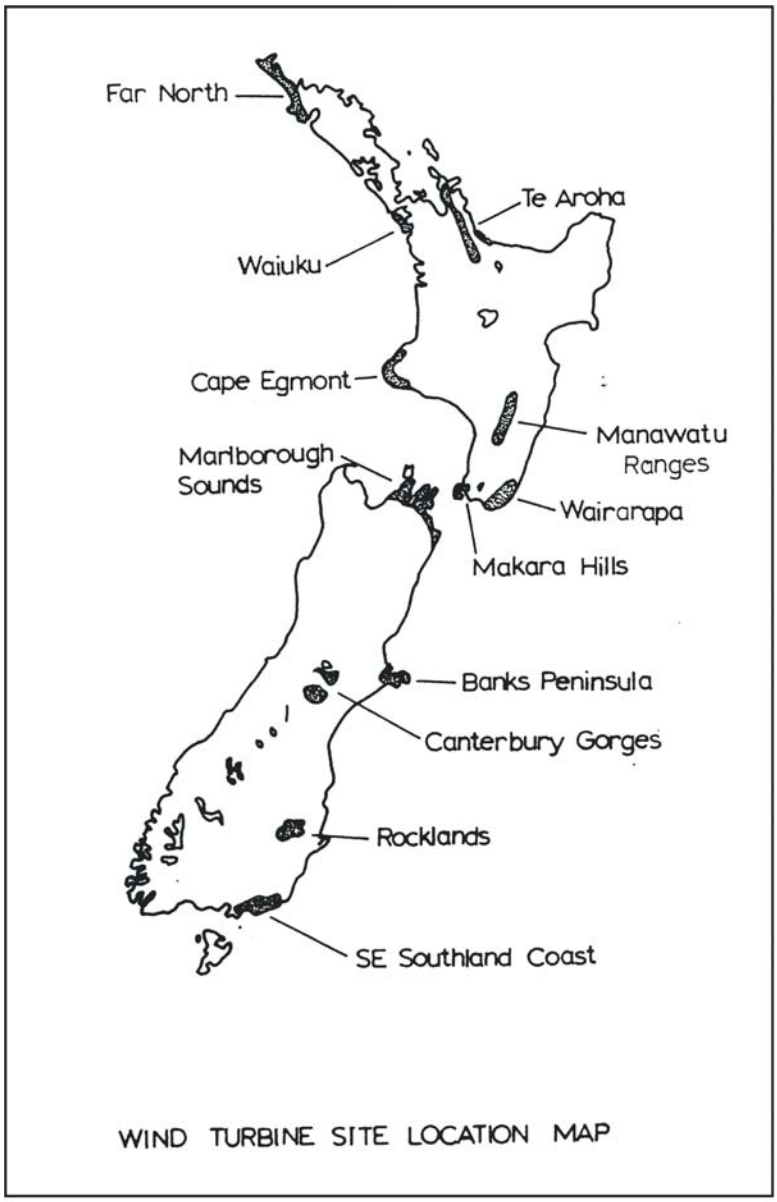


**Figure 2.5: Map showing good potential areas for wind energy development as identified from *The Wind Energy Resource Survey of New Zealand* completed in 1987 (Cherry, 1987).**

## 2.2 Wind and energy

The aim of this section is to provide background information on the theory of wind energy and to cover terminology used in following sections. There is an emphasis on the importance of the mean speed when assessing wind energy generation potential.

### 2.2.1 Energy and power

Since there is often confusion between energy and power, a brief description of each of them is given below.

**Energy**

Since in theory, energy is neither be created or destroyed, it is correct to refer to wind turbines as wind energy converters. A system is commonly defined as having energy if it has the capacity of doing work. Energy can be classified as kinetic and potential, and may exist in many forms, such as heat, electrical, sound and wind, for example. Both wind and electricity are forms of kinetic energy, although electricity can be stored as potential energy in the form of water behind dams in hydropower stations.

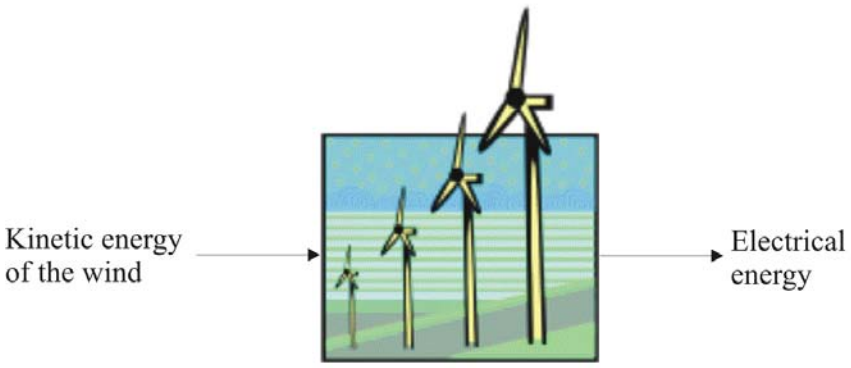


**Figure 2.6: Schematic view of wind energy conversion.**

The kilowatt-hour (kWh) is a commonly used unit of energy in the electricity sector (rather than the Joule which is used in the scientific literature). It is easily confused with kilowatt (kW), which is a unit of power. Power is the rate of energy conversion, rather than the amount of energy converted. In electricity bills, consumers are charged for the kilowatt-hours of energy converted (or the total work done). For example, if a 100W light is left on for 200 hours then 20000Wh (20kWh) of energy is converted or work done.

**Power**

The performance of a wind turbine is measured in terms of the rate of work done or energy transferred over a given period of time. With a wind turbine, kinetic energy of the wind is converted into electrical energy. Energy is usually measured in kilowatt-hours (kWh), which accumulated over a certain time period, such as an hour, day or year provides a measure of

power output. If a wind turbine has a rated power of 1000kW, then it has the capability of converting 1000kWh of energy per hour when running at maximum performance.

### 2.2.2 The 'Power of the wind' equation

The power from the wind can be given as equation (1):

$$P = \frac{1}{2}\rho A V^3 \qquad (1)$$

This shows that the power (*P)* of the wind is a function of air density ( $\rho$ ), the area swept by the turbine blades (*A*), and the velocity of the wind (*V).* As any one of these factors increase, so does the power available from the wind. Each variable in the power of the wind equation are described below.

**Mean wind speed**

In the long term, the mean annual wind speed at a particular site provides a good indication of the amount of energy likely to be captured by the wind. In general, it is said that the energy content of the wind is directly proportional to the cube of the wind speed, as indicated in equation (1) above. That is, if the wind speed is doubled, it will produce eight times the amount of energy captured by the wind turbine. However, the ability of a wind turbine to capture this energy is not perfect. For low wind speed sites, the relationship between energy capture and wind speed is nearer to being squared, rather than cubed (Corbet, 1993).

Wind energy is generally only considered cost effective for sites with relatively high mean annual wind speeds. For example, in the United Kingdom, it is generally recognised that wind energy projects in areas with mean annual wind speeds of less than 7.5 m $s^{-1}$ are not economical (Corbet, 1993). In New Zealand, locations with mean annual wind speed above 7 m $s^{-1}$ have been considered as potential wind farm sites (Sims, 1992). As a rough guide, wind farm developments on sites with mean annual wind speeds of 8 m $s^{-1}$ will yield electricity at a third of the cost for a 5 m $s^{-1}$ site (Milborrow, 2002). In a wind resource analysis of New Zealand, it was estimated that the annual mean wind speeds at some coastal sites in New Zealand exceeds 10 m $s^{-1}$. Compared to a site with an annual mean wind speed of 6 m $s^{-1}$, (which is not unusual for European wind farms), this would trebled the wind energy output (Sims, 1992).

Areas of high wind energy potential can be identified in a number of ways. The most obvious approach is to use existing 'windy' regions. Such regions will be exposed to prevailing wind

directions and are also likely to be affected by the enhancement of airflow speed by topographic features. Another way to capture higher wind speeds is to avoid effects of the wind shear near the Earth's surface, and raise the height of the hub of wind turbines. The trade-off with raising the hub height is the extra cost of constructing the tower and overall turbine structure. There is also the potential for increased maintenance due to the effects of increased vertical shear on blades with longer diameters.

**Air density**

Air density varies with temperature and air pressure, so that air density is higher for cold temperatures and low elevations. Increasing the air density increases the resistance of the wind turbine blades in the air, hence increasing the turbine's ability to generate power. The higher air density at sea level is one reason why offshore wind farms are becoming more popular. Although the effects of air density are small compared to the annual mean wind speed at that site, a wind farm at 1200 m elevation will result in approximately 20% less annual energy production.

**Area swept**

The final variable in the 'power from the wind' equation is the area swept by the turbine blades. As this increases, so the energy captured increases by the same proportion. So if the area swept by the turbine blades is doubled, so will the potential power from the wind. It is therefore clear that either increasing the number of turbines or the individual blade diameters can increase the total 'area swept' for a wind farm and hence the power output.

**The power coefficient**

For any wind turbine, the power output must also incorporate another term in the power of the wind equation, called the power coefficient ($c_p$). Therefore, the power from a turbine can be given as:

$$P = c_p \frac{1}{2} \rho A V^3 \qquad (2)$$

The power coefficient is the ratio of net generated power to the available power of the undisturbed flow through the wind swept area. The power coefficient can be seen a measure of the turbine's efficiency. However, due to the deliberate 'waste' of energy conversion at higher wind speeds (when the wind speed exceeds the design specifications of the turbine and it is closed down), it is not a true measure of a turbine's efficiency. Figure 2.7 below gives an example of the power coefficient for a typical Danish wind turbine.

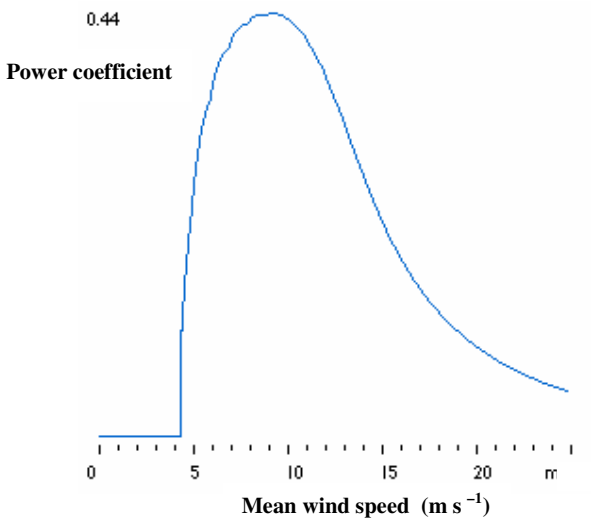


**Figure 2.7: Example of a power coefficient curve showing a maximum energy capture of 44%. (Danish Wind Energy Association, 2005b).**

For this turbine, the mechanical efficiency is maximised near 9 m $s^{-1}$ at 44%. This would be a deliberate choice of the designers, so that the efficiency is maximised near the wind speed where most energy will be converted. In fact, the theoretical maximum fraction power that can be extracted from the wind is 16/27 or about 59% of the maximum available power from the wind. This is called the Betz maximum (Dundar and Inan, 1996).

### 2.2.3 Calculating the energy capture from the wind

Below are some important factors to consider when energy conversion calculations are performed. These factors are used in the Wind Atlas and Analysis Application Program (WAsP) (Troen and Petersen, 1989) to predict the energy conversion at a given site from an observed wind climate.

***The power curve***

Power curves are used directly in energy conversion estimates. They indicate how large the electrical power output will be for a turbine at different wind speeds. Figure 2.8 shows the power curve for a 1 MW rated turbine. Note that this turbine has a cut-in wind speed near 4 m $s^{-1}$ and reaches the rated power output (1MW) at a wind speed near 14 m $s^{-1}$, after which the power output remains constant until the cut-out wind speed. The cut-out wind speed, at 25 m $s^{-1}$, is a safety mechanism to avoid turbine damage in strong winds. Power curves are empirically derived by using wind measurements, air density, and other characteristics of the turbine such as the generator, blade diameter and the power coefficient.

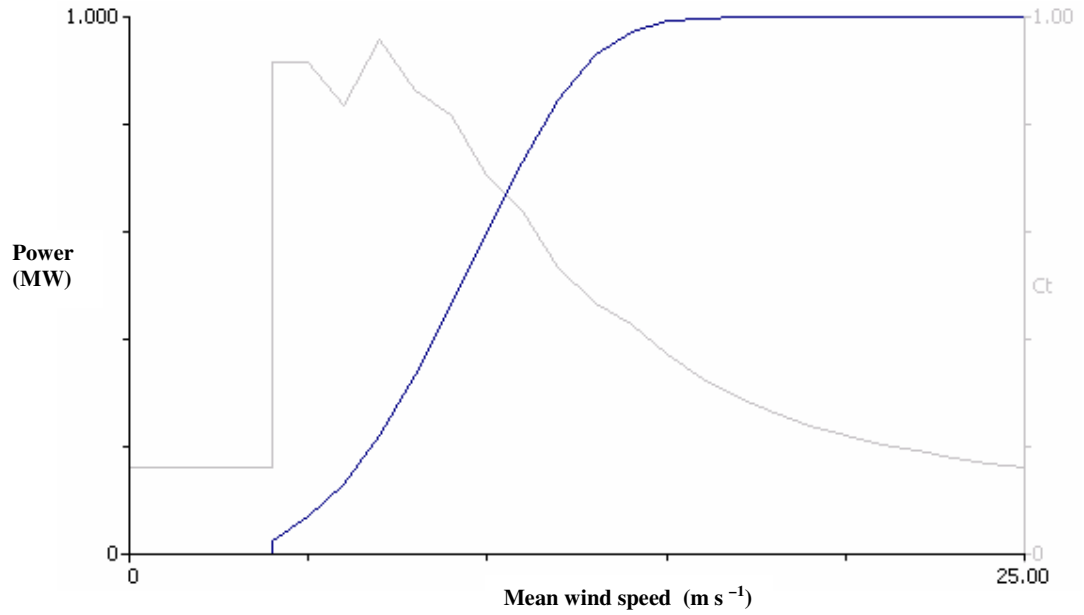


**Figure 2.8: Example of a 1 MW turbine power curve (blue) and thrust curve (grey).**

***The thrust curve***

The thrust curve or thrust coefficient is also used in energy conversion calculations. While the power curve shows the power output verses wind speed, the thrust curve indicates a 'thrust factor' against wind speed. Like the power coefficient, the 'thrust factor' is given as a coefficient, $c_t$, as shown by the grey curve in Figure 2.8. The thrust factor is used in wake interference calculations and is the ratio of the thrust force on the rotor to the available thrust force of the wind in the rotor plane. It essentially gives an indication of how much the wind speed will be reduced and disturbed by a turbine upwind of another turbine.[2]

***The Weibull distribution***

The Weibull distribution is a two-parameter probability density function that best models the observed or predicted frequency distribution of wind speeds at a particular site. It represents wind speed data given initially as a histogram, to a smooth curve described by a specific formula.

[2] Personal Communication with Francis Jackson, Windflow Technology Ltd, 17 August 2004

The formula for this function is:

$$p(v) = \frac{k}{A}\left(\frac{v}{A}\right)^{k-1} \exp\left(-\left(\frac{v}{A}\right)\right)^{k} \qquad (3)$$

Here: $p(v)$ is the probability of the occurrence of a given wind speed, where $v \geq 0$,
$k$ is the shape parameter, where $k > 1$, and
$A$ is the 'scale' parameter, where $A \geq 0$.

In general, $k$ specifies how steep the peak of the curve is, while $A$ is a value close to the mean wind speed. The Weibull parameters $k$ and $A$ are empirically derived by statistical calculations based on the wind data.

Figure 2.9 shows the frequency distribution of observed wind speeds and the associated Weibull curve, for wind data used in this study from Gebbies Pass. The shape ($k$) and scale ($A$) parameters for the distribution fit are given, along with the mean wind speed and mean power output.

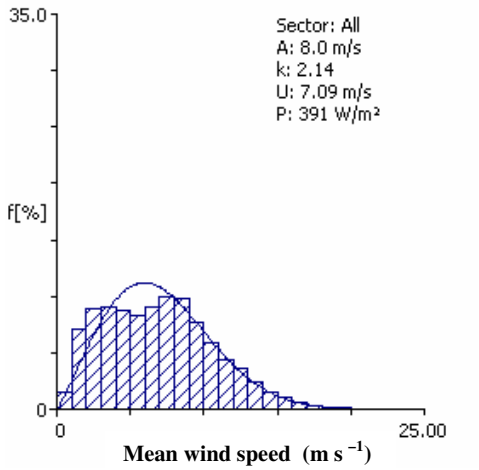


**Figure 2.9: An example of histogram and Weibull curve generated by WAsP for observed wind data at the Gebbies Pass case study site.**

Many wind speed distributions in temperate regions can be adequately described with a shape parameter ($k$) of 2. When this is the case, the distribution is a special case of the Weibull distribution, called the Rayleigh distribution. Wind turbine manufacturers often give standard performance figures for their machines using the Rayleigh distribution (Danish Wind Energy Association, 2005a). For a shape parameter of 1 the distribution is exponential, while a shape parameter of 3.5 gives approximately the normal distribution.

***The relationship between power density and wind speed***

The graphs in Figure 2.10 show the predicted power density and mean wind speed at 50m above ground level for a site on Banks Peninsula. The diagram illustrates the importance of mean wind speed on the power output from a turbine. Most of the energy from the wind comes from wind speed significantly higher than the mean wind speed of 7.7 m $s^{-1}$ (Figure 2.10b). For the 1 MW turbine used in this simulation, the power density maximised close to 11.4 m $s^{-1}$ (Figure 2.10a), even though such speeds occur at a much lower frequency compared to wind speeds closer to the mean. The difference in distribution shape is due to the cubed relationship between the wind speed and power. Some of this effect is also due to characteristics of the turbine used in the simulation.

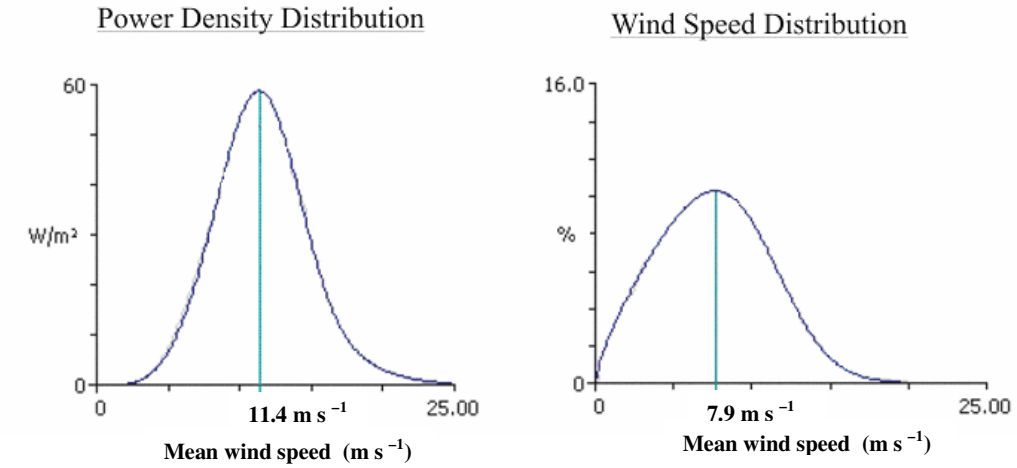


**Figure 2.10: Distributions of (a) power density and (b) wind speed generated by WAsP for observed wind data at the Gebbies Pass case study site, and showing the effect of increased power of wind at higher wind speeds.**

***Annual energy production***

Annual Energy Production (AEP) is the total amount of energy produced by the wind turbine over the period of one year. It might be more suitable to call AEP annual electrical energy conversion, since energy is converted from one form to another. The power curve for a turbine and the Weibull curve for the wind climate of a particular site are combined by multiplying the probably that small increments of wind speeds occur, with corresponding values from the power curve. The result is then multiplied by the number of hours in a year (8760) to get the resulting annual energy production estimate. AEP is measured in terms of giga-Watt hours (GWh), since the numbers get large (note that 1 GWh is equal to 1,000,000,000 Wh).

## 2.3 Wind enhancement due to terrain features

Wind energy conversion schemes aim to utilise locations with the highest possible mean wind speeds. This section provides a review of the interaction of atmospheric processes with the topographic characteristics that endow New Zealand with excellent wind energy generating potential. It also provides some background concerning when and why current airflow modelling techniques have difficulty reproducing observed winds in complex terrain.

Much of New Zealand lies within latitudes that are affected by strong prevailing westerly winds. While the approximate perpendicular alignment of New Zealand's major topographic features (most notably the Southern Alps in the South Island) to the prevailing westerly winds provides sheltering for some areas, these barriers result in regional scale enhancement of airflow over certain parts of the country. Localised acceleration of wind occurs at elevated sites, such as on hills and ridges, and also due to channelling of winds by local terrain features. A combination of these elevation and channelling effects determines the distribution of the best wind energy generation sites over the country.

### 2.3.1 Terrain forced airflows

Terrain forcing can cause an airflow approaching a mountain barrier to be carried over the barrier, around the barrier, through gaps in the barrier or be blocked by the barrier. (Whiteman, 2000) stated that there are three factors that determine the behaviour of an approaching flow in response to a downstream barrier:

1. The stability of the air approaching the barrier,
2. The speed of the air approaching the barrier, and
3. The topographic characteristics of the underlying terrain.

Barry (1992) suggested that the vertical profile of the wind speed and direction relative to the barrier orientation are also important to the resulting air motion. The above factors can vary a lot over New Zealand, in both time and space, resulting in complex interactions between atmospheric processes and topography.

Terrain forced airflow phenomena can therefore be divided into two types: channelling of air around and through topographic features, and flow over terrain features. Although these two phenomena are often discussed separately, there are close interactions between them. Both

have a significant impact on the resulting wind climate of New Zealand, and hence on the location of existing and future wind farms.

***Channelling***

Airflow channelling by terrain is caused by the forced convergence of air into a space (or volume), as a result of the interaction of airflow with topographic features. A stable vertical profile enhances this effect by capping the vertical displacement of the air. Under stable conditions, winds tend to split around topographic features such as an isolated mountain, so that strong wind zones are produced around the edges that are tangential to the flow, as shown in Figure 2.11 (Whiteman, 2000). When air is forced by more than one terrain feature, the interacting channelled airflows can enhance wind speeds further.

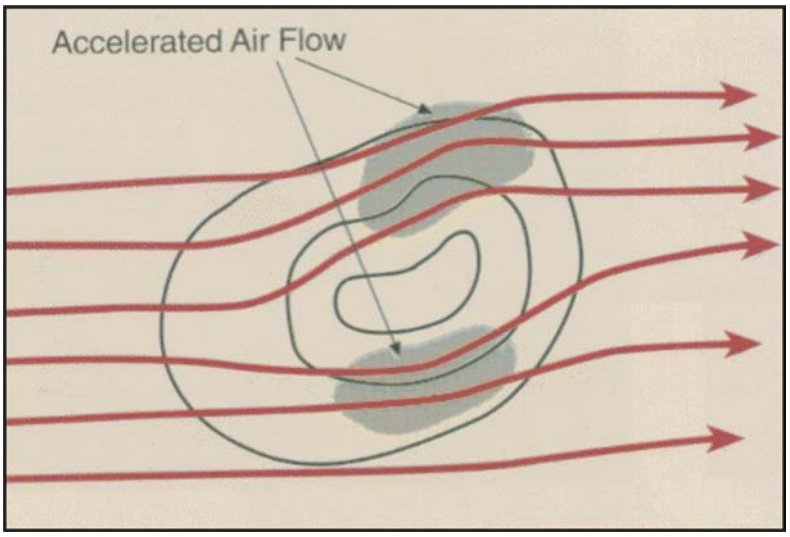


**Figure 2.11: Under stable conditions, airflow can be split around an isolated mountain resulting in strong wind zones on the edges of the mountains (source (Whiteman, 2000)).**

The height of the region of accelerated flow is dependent on the position of the dividing line between the low level air that splits around the barrier and the higher-level flow, which tends to be carried over the barrier (Figure 2.12, (Whiteman, 2000)). The height of the strongest wind zone is also dependent on atmospheric stability, the vertical wind profile approaching the barrier, and the topography and surface roughness characteristics of the area. If the topography of an area is complicated, the resulting flow patterns also increase in complexity.

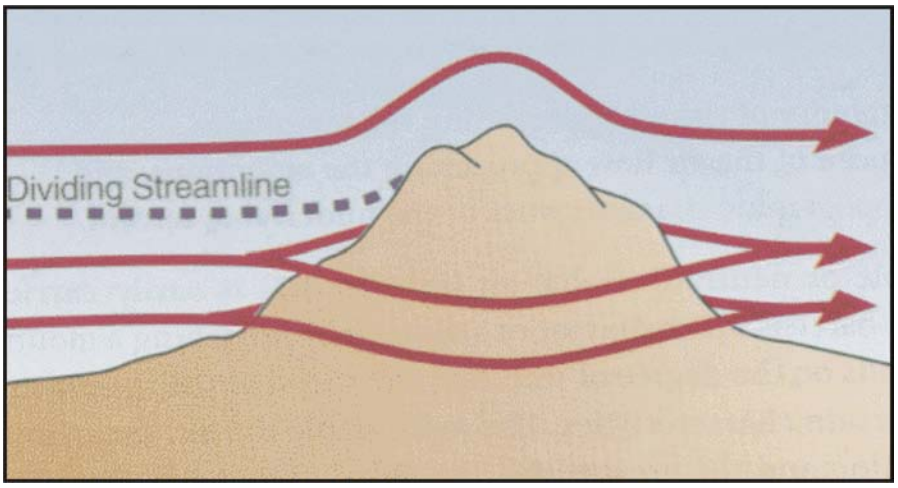


**Figure 2.12: The dividing streamline height is at the boundary between the low level split flow and a higher-level flow over the barrier (source (Whiteman, 2000)).**

The amount of energy required for air to flow over a long mountain barrier, such as the Southern Alps, is much greater than that of over a small hill. That is, more energy is required to flow around an extended barrier than for an isolated peak (Whiteman, 2000). Atmospheric stability at and below the mountain barrier level also has a significant impact on these energy requirements. Unstable air will readily rise over a mountain barrier or hill, resulting in very different airflow patterns compared to that in a stable environment.

The channelling of airflow at a range of scales is common over New Zealand, from around isolated hills to over and around large-scale barriers. The Southern Alps and the North Island mountains can have a significant impact on the synoptic and mesoscale isobaric pattern, and hence the winds over New Zealand, especially when the wind direction is perpendicular to the major topography features. Cook and Foveaux Straits provide significant gaps in the mountain barrier, and both of these areas experience strong winds as a result of channelling in such situations.

Northeast barrier winds are a common occurrence on the west coast of the South Island in strong stable onshore flows (see Figure 2.13 below). These barrier winds have a distinctive structure with strong directional shear from the northwest flow above barrier level to the northeast winds below. The lower level flow often has a jet like core (McCauley and Sturman, 1999). Strong low level winds observed near the end of the barrier (such as at Puysegur Point and in the Foveaux Strait area) are likely to occur as a result of reinforcement by this barrier jet effect. Also, westerly airflows are generally enhanced near the south coast of the South

Island from the channelling of winds through Foveaux Strait and around coastal hills, making this region very favourable for future wind energy developments.

While Cook Strait winds might sometimes be affected by a barrier jet driven by the hills to the north of the area, the strong winds experienced here are mostly due to the convergence of the airflows through a narrow gap characterised by low surface roughness. McCauley and Sturman (1999) suggest that in situations when the northeast barrier jet occurs along the west coast of the South Island, flow splitting is likely to occur somewhere north Westport, so that the resulting southwest flow is also channelled through Cook Strait. Strong wind situations near Cook Strait can also result from 'pressure-driven channelling' caused by strong horizontal pressure gradients across the area (Whiteman and Doran, 1993). The Manawatu Gorge experiences high mean wind speeds due to the channelling of prevailing westerly winds by surrounding terrain features through a relatively low part of a long hill barrier. All these effects combine to make the southern North Island experience some of the highest low level mean wind speeds in New Zealand, as discussed by Cherry (1987).

On the lee side of mountain ranges, strong winds often result due to pressure driven forces. The pressure difference threshold for these winds to 'break through' is dependent on the height and extent of the barrier, position of any gaps in the barrier and also on the stability at and below the ridge level. Further enhancement of winds occurs due to localised channelling, such as near river gorges. The Rakaia and Rangitata gorges experience such reinforced wind regimes during westerly-type weather situations.

The effects of channelling on low-level wind patterns are specific to each location and for each synoptic situation. Sturman and Kossmann (2003) discuss the complex interaction of factors that effect the channelling of airflows in valley systems. These include the valley characteristics (shape, width and depth), atmospheric stability, and the implications that baroclinic situations have on the resulting low-level wind flow.

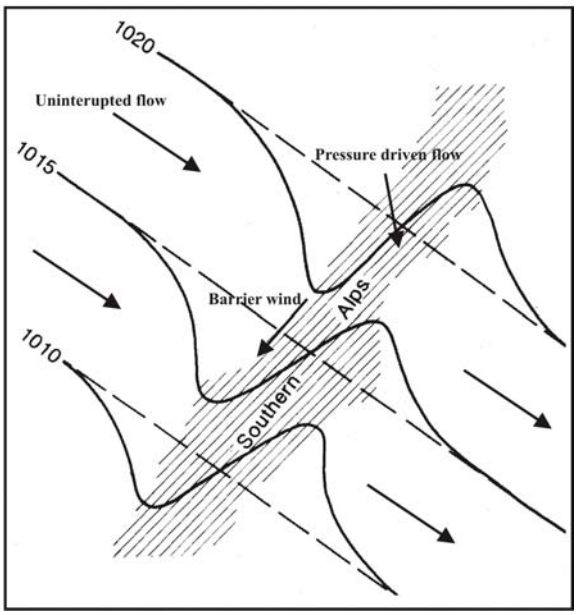


**Figure 2.13: Isobar distortion in northwest flow across the South Island. Note the northeast barrier jet along the West Coast and an example of pressure driven channelling across the Southern Alps (adapted from (Neale, 1987)).**

***Effects of airflow over elevated terrain***

Wind speeds over elevated terrain are often higher than surrounding areas for two reasons:

1. The vertical wind shear within and above the boundary layer.
2. The speed-up effects of the wind over topographic features.

There are models describing the airflow over simple hill structures. However, airflow patterns over steep or complex terrain are difficult to simulate, and this remains a limitation for high resolution wind modelling in complex terrain.

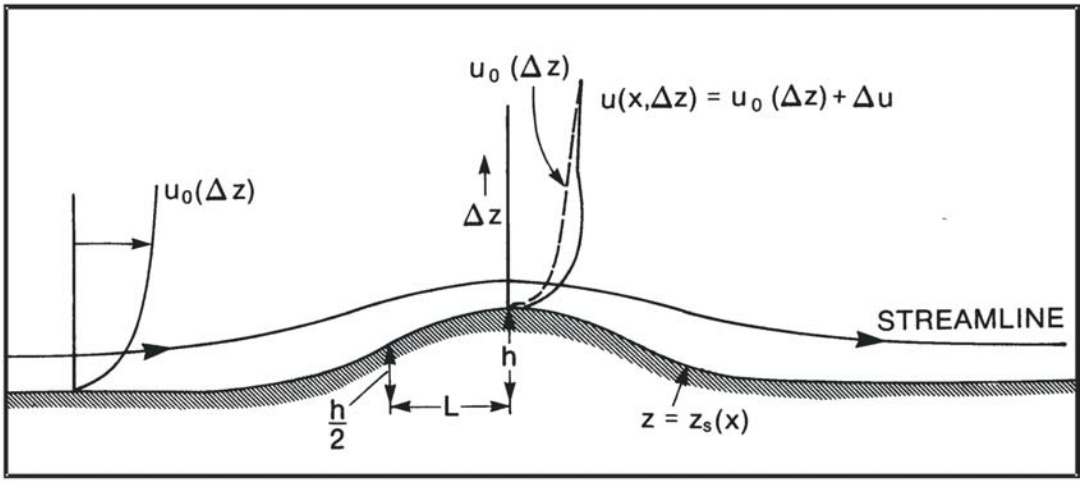


**Figure 2.14: Illustration of the vertical 'speed-up' profile over a hill. Definitions of L, h, $\Delta u$, $u_o(\Delta z)$, $\Delta z$, and $z_s$ are provided in the text (Taylor et al., 1987).**

Figure 2.14 illustrates the effect of a low hill on the vertical wind 'speed-up' profile in a neutrally stratified boundary layer flow. The diagram shows definitions of the velocity perturbations $\Delta u$, at a height, $\Delta z$, above the local terrain roughness, $z_s$, and relative to the upstream profile $u_o(\Delta z)$. L is defined as horizontal length from the hilltop to the upstream point where the elevation is half its maximum, and h is the height of the hill (Taylor et al., 1987). Note that the upstream vertical wind speed profile is logarithmic and is modified near the top of the hill. The speed-up increases from the surface to a point where maximum relative speed-up is achieved, above which the wind profile is almost constant until it matches the upstream profile again at a height of 2L.

The relative vertical speed up $((u - u_0)/u_0)$ is often used to quantify the fractional speed up ratio $(\Delta S)$ over small-scale topographic features. Typical speed up ratios can be summarised as given by (Hunt, 1980) and (Taylor et al., 1987):

$\Delta S_{max} \approx 2h/L$ for two dimensional ridges (negative for valleys);

$\Delta S_{max} \approx 1.6h/L$ for three dimensional axisymmetric hills;

$\Delta S_{max} \approx 0.8h/L$ for two-dimensional scarps[3].

[3] A scarp is defined as a long steep slope or cliff at the edge of a plateau or ridge.

These estimates apply for winds greater than 6 m $s^{-1}$, near neutral stability, and with horizontal terrain scales of less than 1 km, and with the h/L ratio less than 0.5.

It is also important to look at the horizontal relative speed-up profile over terrain features. Figure 2.15 illustrates the relative speed-up ratio over the Askervien hill at 10 m above ground level for a wind direction almost perpendicular to the ridge. Measurements are given by dots and the results from the orographic (BZ) model used in WAsP (Wind Atlas Analysis and and Application Program) as squares. Measurements from two other models are given by the full and dashed lines (Mortensen, 2003).

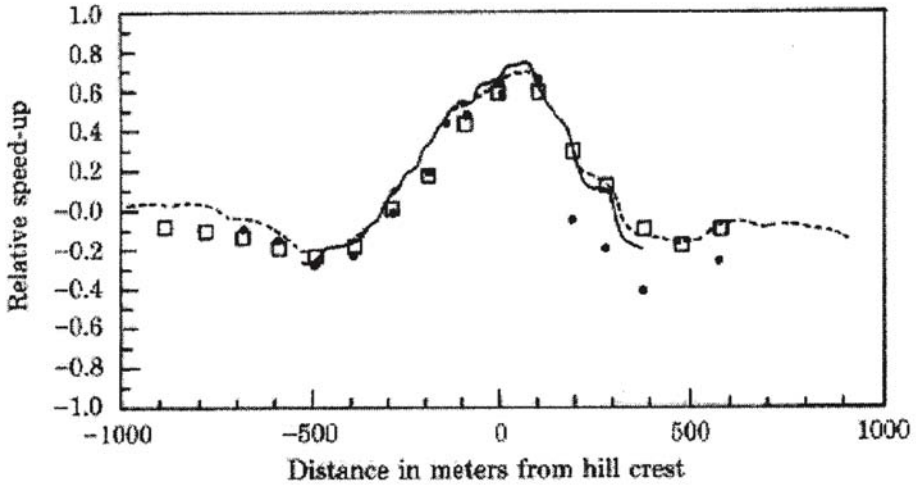


**Figure 2.15: Horizontal relative speed-up over Askervien Hill (Mortensen, 2003).**

The maximum relative speed-up near the crest is about 80% compared to the undisturbed upstream mean wind speed. Negative speed up (speed-down) is experienced in the front and lee of the hill with reductions of 20 to 40% of the mean wind speed.

In reality, hills are not smooth, rounded, isolated and located in neutrally stable air, as in the case study in Figure 2.15. Potential wind energy sites, especially those in New Zealand, are more likely to be located in complex terrain characterised by sharp breaks, changing surface roughness, with interacting flow structures from surrounding hills. A study by Miller (1996) concluded that velocity speed-ups in complex terrain are less than when compared to those found above isolated hills or ridges.

While hills can enhance the wind speed over them, flow separation over hills can result in large reductions in mean wind speed and increase the variance in flow components. Separation occurs at a critical height above the surface where the surface stress becomes zero,

and this will depend on the surface roughness and slope of the hill (Taylor et al., 1987). Flows are also more likely to remain attached in a stable environment. Coppin (1994) found that stable stratification can increase any speed-up over a hill by a factor of two (unless blocking occurs).

Flow separation can sometimes cause eddies and a return flow component. This can cause added stress on wind turbines and needs to be considered in the viability of wind farm developments. Figure 2.16 shows an example of flow separation (and flow joining again at J) occurring near a cliff feature. In New Zealand, there is the likelihood of wind energy developments at high elevations, such as in Central Otago and inland Canterbury. Here, airflow is relatively unobstructed from small-scale surface roughness effects and exposed to the stronger high-level mean wind speeds typical of mid-latitude westerly winds. However, significant flow separation and severe turbulence resulting from rugged upstream mountain ranges must be considered for these wind farm developments.

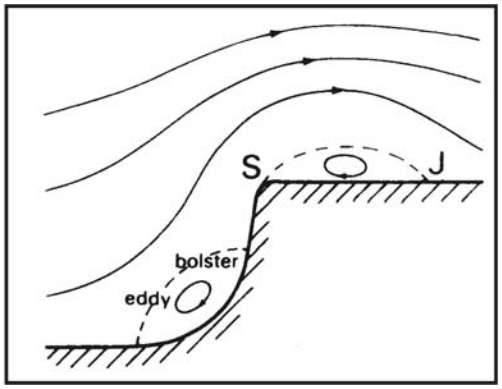


**Figure 2.16: Separation of flow by a cliff feature (Barry, 1992)**.

As discussed above, there is a number of factors that determine when flow separation will occur. Observations from a study at Blashaval suggest that flow separation occurs on slopes greater than 20 degrees (Mason and King, 1984). Wood (1995) suggested that the critical slope for flow separation to occur is above 0.3. The value of 0.3 is used later in this study to identify and quantify potential errors due to flow separation not being accounted for by the WAsP model.

Another consideration of the influence of topography on airflow patterns is the extent of any wake area downwind. Due to flow separation, this area is generally characterised by relatively lower wind speeds, but with increased gustiness. Angle (1991) suggested that this slow-down

distance is about 15 times the obstacle height. However, turbulent effects may extend further from the obstacle.

Taylor (1987) suggested that in theory, linear models under-estimate wind speed reduction in the lee of topographic features. As computing power increases, models (or more non-linear models) are likely to improve the simulation of airflow over complex terrain.

## 2.4 Predicting the wind

In the previous section, it was shown that to optimise the energy production from the wind, it is essential to find and utilise the 'windiest' locations. As the wind has become an economically viable source of energy, the methods of determining where the optimal sites are have come under increased interest and research.

The cubic relationship between mean wind speed and energy output means that a relatively small increase in the mean wind speed can make a significant difference in energy output. Therefore, subtle differences in the mean wind speed might determine whether a wind energy conversion project is viable or not. For example, if the wind speed at a site is increased by 10%, the energy output will be approximately 30% higher. Geoff Henderson of WindFlow Technology suggested that knowing the mean annual wind speed to within 0.5 m $s^{-1}$ is very important for gaining an accurate indication of energy output and hence the viability of a particular site.[4]

Also, given favourable size, orientation and shape, topographic features can increase wind energy yield potential by up to 100% (Coppin et al., 2000). In most locations in New Zealand that have been identified with high mean speeds, the airflow speed is modified and enhanced by topography, as discussed in Section 2.3. The interaction between topographic features and airflow patterns is complex and difficult to model, although there is significant interest in undertaking research in this area. The aim of such work is to gain more accurate predictions of wind energy potential in regions of complex terrain.

Ultimately, the wind energy industry needs reliable tools for estimating mean wind speeds at selected heights for locations and wider areas where data are sparse. This would allow wind farm developments to proceed in less time, without the need to collect years of actual wind

[4] Personal communication with Geoff Henderson, Windflow Technology Ltd, 14 February 2003

data for specific sites under investigation. However, such methods are required to be accurate enough to ensure confidence that power generation will be close to the predictions.

Below is a summary of some of the methods used to estimate the wind climatology for the assessment of wind energy generation potential. These methods vary from empirical techniques (derived from experimental knowledge) to theoretically based methods, and from statistical based models to numerical models. A review will be provided of some key aspects of these methods in the following sections. One other important consideration when using any model to determine an accurate picture of the wind climate is to be sure that the period of data used to base this prediction on gives an accurate representation of the actual long-term wind climate. Cyclic variations of climate, such as El Niño or just the seasons can have a significant impact on the overall character of the wind climate. The use of longer periods of wind data will reduce the impact of cyclic climate variations. In the wind energy industry, one year's data is considered to be the minimum to base predictions on.

### 2.4.1 Theoretical vertical wind speed profile models in the atmospheric boundary layer

The mean horizontal wind speed is zero at the Earth's surface and increases with height in the atmospheric boundary layer. The atmospheric boundary layer is defined as the lower layer of the atmosphere that is directly affected by friction and heating at the Earth's surface. If instantaneous measurements of the vertical wind velocity were taken at a single point, there would be many variations of wind speed through the atmospheric boundary layer, arising from turbulent eddies of varying magnitude. These turbulent variations result from the interaction of surface roughness features, wind speed and atmospheric stability at that time. Averaging such wind measurements over a longer time period reveals a steady profile, referred to as the vertical wind profile.

The overall wind climatology at a site is a function of the surface roughness ($z_0$), and the thermal stability climate of the site. The later factor is not normally available, as it requires long-term observations of the temperature profile. The thermal stability is accounted for to a large extent by the surface mean wind speed, which is an inverse function of the mean thermal stability (Cherry, 1987).

In surface layer theory, the surface roughness length is defined as the height above the ground at which the wind speed is zero (Lalas et al., 1996). Values of surface roughness length are

empirically derived. Table below gives some examples of approximate values of the surface roughness length or height $z_0$ (m) used in a study by (Rohatgi, 1996)

**Table 2.2: Examples of surface roughness lengths.**

| Terrain Description | Surface Roughness (m) |
|---|---|
| Calm open sea | 0.0002 |
| Rough Pasture | 0.01 |
| Few tress | 0.1 |
| Forest or woodlands | 0.5 |
| Suburbs | 1.5 |

There are two simple models that are both functions of the surface roughness near to the site of interest, that are commonly used to estimate the vertical wind profile over regions of homogeneous, flat terrain, such as fields, deserts and ice (Rohatgi, 1996). Due to the lack of better methods, these models are used to estimate vertical wind profiles in more complex terrain. These simple models, and adaptations of them, are used in computer models for wind predictions above surfaces with varying surface roughness characteristics.

***Equation of the Power Law Vertical Wind Profile***

The Power Law model uses an empirical equation (4) to describe the vertical wind speed profile. It is commonly used in wind engineering because it is simple and direct to apply. In its most general form it is:

$$\frac{v_2}{v_1} = \left(\frac{z_2}{z_1}\right)^{\alpha} \qquad (4)$$

Here $v_2$ is the mean wind speed at some unknown height, $z_2$, and $v_1$ is the known mean wind speed from some known height $z_1$. The exponent $\alpha$ is the key parameter that determines the shape of the wind profile.

Early assumptions by von Karman showed that under certain conditions $\alpha$ is equal to $1/7$. This value is often used in practical situations to estimate the vertical wind profile.[5]

[5] Personal communication with Geoff Henderson, Windflow Technology Ltd February 14 2003

However, studies have shown that $\alpha$ can change from less than $1/7$ during the day to more than $1/2$ at night for the same terrain (Rohatgi and Nelson, 1994). In fact, the value of the exponent will vary depending on the time of day, season, nature of terrain, wind speed, temperature and various thermal and mechanical mixing parameters.

In general, however, $\alpha$ can be expressed in terms of the surface roughness parameter $z_0$ and the mean wind speed at some level. For example, Cherry (1987) derived the following expression for the mean power law exponent in the Wind Energy Resource Survey of New Zealand:

$$\alpha = v_{10}^{-0.6}(0.78 + 0.137 \ln z_0 + 0.0098(\ln z_0)^2) \qquad (5)$$

Here $v_{10}$ is the mean annual wind speed at 10 m above ground level, and $z_0$ is the roughness length surrounding that site. He used this exponent in the power law to extrapolate the mean annual wind speed profile up to a height of 50 m above ground level.

Cook (1997) suggested that compared to the log-law model (described in the following section), the power law model fits best over the range of heights between 30 m and 300 m, and becomes less valid closer to the ground. This is a reason why is it often used in the wind energy industry due to turbine hub heights usually being within this height range.

***Equation of the logarithmic law vertical wind profile***

The logarithmic law vertical wind profile (6) is derived theoretically from the basic principles of fluid mechanics and the concept of atmospheric stability. The wind speed from a known reference height can be used to calculate the wind speed at another height using the following logarithmic formula:

$$\frac{v_1}{v_2} = \frac{\ln\left(\frac{z_1}{z_0}\right)}{\ln\left(\frac{z_2}{z_0}\right)} \qquad (6)$$

Here $v_1$ is the predicted wind speed at height $z_1$, $v_2$ is the known wind speed at a height $z_2$, and $z_0$ is the roughness length at the site of interest. The logarithmic wind profile is used in the Wind Atlas and Analysis Program (WAsP) – one of the models used in this research project.

The vertical thermal structure of the lower atmosphere is often accounted for by the addition of an empirically derived linear term, which is a function of height. This model is referred to as the log-linear wind speed profile. Such corrections arise due to the fact that the wind speeds increase less with height in an unstable environment, but faster in a stable stratification (Cook, 1997).

Cook (1997) also suggests that the log-law velocity profile is best for heights close to the surface (such as $z < 30$ m), as it satisfies the lower boundary condition at $z_0$. It is less reliable for heights more than about 200 m, as there is no upper boundary condition. Because of this, there are difficulties predicting the mean wind speed profile when the airflow moves from one form of surface roughness to another. The Deaves and Harris model is an adaptation of the log-law model that recognises a boundary condition at the top of the atmospheric boundary layer, therefore better accounting for the translation of airflows over different terrain roughness (Cook, 1997).

### 2.4.2 Computer modelling techniques

The two wind profile models described above are often used within numerical models in order to simulate the vertical wind structure within the atmospheric boundary layer. Such models are of two types, diagnostic or prognostic.

***Diagnostic modelling***

Diagnostic models are also referred to as mass-consistent models. These model types contain no time derivative and therefore specify the balance of quantities at a particular moment in time. Starting with some upper level and surface wind data, mass-consistent models firstly reconstruct the three dimensional wind fields by interpolation. The interpolated wind fields are then adjusted to satisfy the laws of mass conservation caused by forcing by topography or by other physical constraints. Mass consistent models are therefore specifically designed to predict the effects of orography on steady mean wind flow (Ratto, 1996). One advantage of diagnostic models, especially in the past, is their lesser computational demand. The Wind Atlas and Analysis Program (WAsP) is an example of a diagnostic model.

***Prognostic modelling***

Prognostic modelling is the method used by weather forecasting models. Prognostic models (also known as 'predictive' or dynamic models) are used to forecast the time evolution of the

atmospheric system through the integration of conservation equations for mass, motion, heat and water, and if necessary, other substances like gases and aerosols (Finardi et al., 1998).

Prognostic models can be used for a range of scales of motion from microscale, 2 mm-2 km (cumulus cloud structure or pollution dispersion), to mesoscale, 2-2000 km (thunderstorm or urban pollution), to synoptic scale, 500-10000 km (for weather fronts and hurricanes), to planetary scale, greater than 10000 km (global wind patterns and ozone) (Jacobson, 1999).

Prognostic models can be used to investigate the effects of synoptic scale weather systems on local scale airflow, and provide the ability to simulate such events for long time periods. While synoptic scale weather systems are driven primarily by large-scale dynamic and thermal processes, mesoscale processes are governed more by orography and irregularities of the surface energy balance (Moussiopoulos, 1996). Therefore, computer codes or models can be constructed so that atmospheric phenomena can be simulated at the scale at which they occur.

Prognostic mesoscale models are often used with nested grids, which range from a coarse to a finer scale. The outer grid can obtain boundary or initial conditions from global scale models (low resolution grid data). In the nesting procedure, output of the larger domain is used as the boundary conditions for the next inner grid, until the required resolution is gained. Output from global models is usually computed six hourly, so that the boundary conditions can be 'nudged' at these times to maintain the accuracy of the simulation. Most prognostic mesoscale models now use terrain following co-ordinate systems. This allows for easy reconstruction and analysis of the wind field features at a local scale.

There are many prognostic mesoscale models used in boundary layer meteorological studies. For example, The National Institute of Water and Atmospheric Research (NIWA) have used a range of prognostic models, including the Regional Atmospheric Modelling System - RAMS (developed by Colorado State University) and the United Kingdom Meteorological Office model (UKMO).[6] The Mesoscale Model - MM5 (developed by the Pennsylvania State University) and The Air Pollution Model - TAPM (developed by the Commonwealth Scientific and Industrial Research – Australia) are currently being used at the University of Canterbury, in air pollution and wind energy studies.

[6] Personal communication with Steve Reid, NIWA, 26 February 2003

***Model Selection***

There has been much research into the best ways of simulating the airflow close to the Earth's surface, especially in complex terrain, and many questions still remain. Diagnostic models, such as WAsP, have been most commonly used in the past, but they have recognised limitations. These model types are likely to be able to improve their calculations in complex terrain by using non-linearised equations in the model calculations (Walmsley, 1996). Prognostic models also have limitations with simulating airflow near the Earth's surface, but with increased computing power, these limitations should also become less. Some hybrid modelling techniques combine both prognostic and diagnostic techniques.

Non-hydrostatic source codes are considered to be the new generation models. In computer modelling, the hydrostatic approximation has resulted in significant reductions in computing time and expense. Effectively, this approximation neglects hydrostatic effects, and thus localised dynamical vertical accelerations. Models adopting this approach could not be applied for horizontal scales less than about 10km, because in this case non-hydrostatic effects should not be neglected (Moussiopoulos, 1996). In non-hydrostatic diagnostic and prognostic models, mesoscale pressure differences can be computed, and hence wind fields can be evaluated at a higher resolution. With greater computing capabilities, non-hydrostatic models are not only accessible to the research field, but also for more practical applications, such as in the wind energy field.

### 2.4.3 An empirical technique

The Griggs-Putnam Index describes deformation based on the permanent bending of needles, twig, branches and trunks of coniferous trees, which are visible indications of how windy a particular location is (Putnam, 1948). Hewsen (1979) applied the Griggs-Putnam Index to estimate the mean wind speed $(v)$ using the relationship:

$$v = 0.7G + 3.3 \quad (\text{root mean square error} = \pm 0.7 \text{ms}^{-1}) \qquad (7)$$

Here, G is the index value as shown in Figure 2.17. It should be noted that the effects from wind blown ice, sand, salt and snow could contribute to error in this index (Cherry, 1987). Such effects can be seen clearly on the West Coast of the South Island (see cover photo) and on the Chatham Islands. The deformation of trees can therefore serve as a simple validation tool against more sophisticated analysis techniques, and this will be illustrated later in the study.

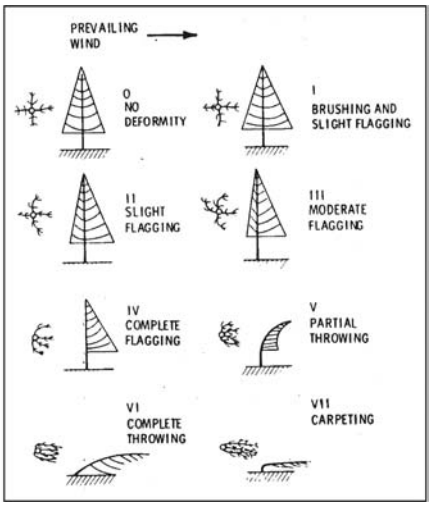


**Figure 2.17: The Griggs-Putnam Index values (Hewsen and Wade, 1979).**

### 2.4.4 Statistical modelling

The measure-correlate-predict (MCP) method has been a standard statistical procedure used to derive long term mean wind speeds at proposed wind farm sites where there is only short-term data available (Woods and Watson, 1997). This method uses wind data from a nearby meteorological station and through correlation with the smaller data set from a proposed wind farm site, predicts the wind potential. This method has been found to be reliable in simple terrain, if the regression equations used are representative of the concurrent data and the data used are representative of all wind regimes. There are variations of MCP methods that have attempted to take into account the effects of complex terrain on wind flow. Some of these are discussed below.

In complex terrain, turning in the wind direction with height and horizontal distance often occurs, making invalid any assumption that the sector wind distributions are the same for the reference site and proposed site. Woods (1997) provided a new matrix method to account for such changes in wind direction. In a study using this new technique, it was found that there was better representation of the concurrent data sets.

Walmsley and Bagg (1978) (cited in (Salmon and Walmsley, 1999)) developed a two-station correlation scheme between a reference site (meteorological station) and a target site (proposed wind farm location). The goal was to determine if short term monitoring from a site could be used to represent longer-term wind climatologies. The method involved using

simultaneous hourly data to produce a matrix of correlation coefficients for different stability, wind speed and direction classes. As described in Salmon and Walmsley (1999), the resulting correlation coefficients were used with the longer-term data from the reference site, to make a prediction of the wind climate at the target site. It was found that the target site required a minimum of 12 months of hourly wind data to obtain a representative wind climatology. Salmon (1999) modified the Walmsley-Bagg model by increasing the number of wind speed and direction bins.

In a paper by Zaphiropoulos (1999), an MCP method was used to predict the wind climatology at a potential wind farm site in complex topography using long-term data at a nearby location. In this method, the use of the Kriging methodology could make satisfactory estimates of the average wind speed in 16 wind direction sectors, given only two days of 10-minute average wind data at the proposed site.

### 2.4.5 Neural Networks

Artificial neural networks are a branch of artificial intelligence. Their strength has been identified for complex problems where there is limited theoretical knowledge or when there are complex interactions between different processes (Gardner and Dorling, 1998). Such problems occur in atmospheric science, and particularly with processes in the boundary layer.

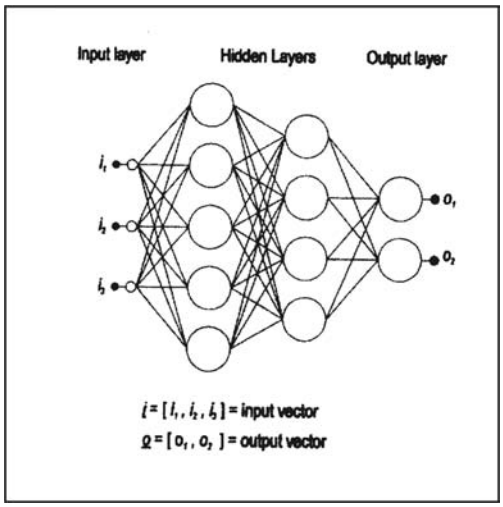


**Figure 2.18: Example of the concept of a multi-layer perceptron (Gardner and Dorling, 1998).**

One type of neural network is the multi-layer perceptron, which consists of a system of interconnected nodes (as shown in Figure 2.18). This model represents non-linear mapping between input data and output data. Once a suitable set of connecting weights and transfer functions have been selected, the neural network 'learns' using a training algorithm. Training

requires the use of many corresponding input and output data that should be representative of what is being modelled and also covers all types of different episodes. Once trained, the neural network can accurately generalise patterns when presented with new data (Gardner and Dorling, 1998).

Applications for predicting the wind climate using artificial neural networks are given in Beckrakis (2000), who used a neural network to extrapolate wind speed data observed at a low level to a higher level. Bechrakis (2000) went further and investigated predicting wind energy conversion estimates at sites in complex terrain. In both case studies in this paper, the estimates by the neural network were better than extrapolation by the power law model.

### 2.4.6 Current modelling systems for wind energy resource assessment

Below is a brief overview of three modelling techniques that are currently used for assessing the wind energy resource. Although these procedures have a similar goal, they use different models and methodologies for obtaining the predicted wind climate.

***KAMM/WAsP***

The following description of the KAMM/WAsP method was taken from (Petersen et al., 1996) and (Frank et al., 2001).

The Riso National Laboratory, in Denmark, developed the KAMM/WAsP method. The Karlsruhe Atmospheric Mesoscale Model (KAMM) is a dynamic mesoscale meteorological model used to generate a grid of geostrophic wind climatologies. The aim is to use KAMM to model processes that WAsP is not able to, such as the effects of large-scale channelling of winds by land features, and non-neutral stability.

The KAMM/WAsP method is a statistical/dynamic approach where regionalised wind climatologies are determined from particular larger scale wind regimes (light wind synoptic situations are ignored). The method first involves classifying synoptic scale situations into categories and then performing KAMM numerical simulations on each of these situations types. For each situation, low-level wind fields are corrected for roughness and orography perturbations, in a similar way as they are in the WAsP model. When the simulations are complete, Weibull curves are calculated for each sector at all of the grid points.

The result is a representative analysis of the geostrophic wind climate for each grid point over the region of interest. The overall wind climatology is obtained by combining this geostrophic analysis with the frequency of each of the situations occurring. The WAsP model then uses the resulting wind atlas files to determine the wind climate and hence energy generation potential for a site, or over an area at a higher resolution.

There is a simplifying assumption in this method in that for wind energy purposes in mid-latitudes, interest is mainly in moderate to high wind speed situations. Because this method only simulates moderate to high wind speed synoptic regimes, it ignores some mesoscale weather effects, such as sea breeze formation and thunderstorm development.

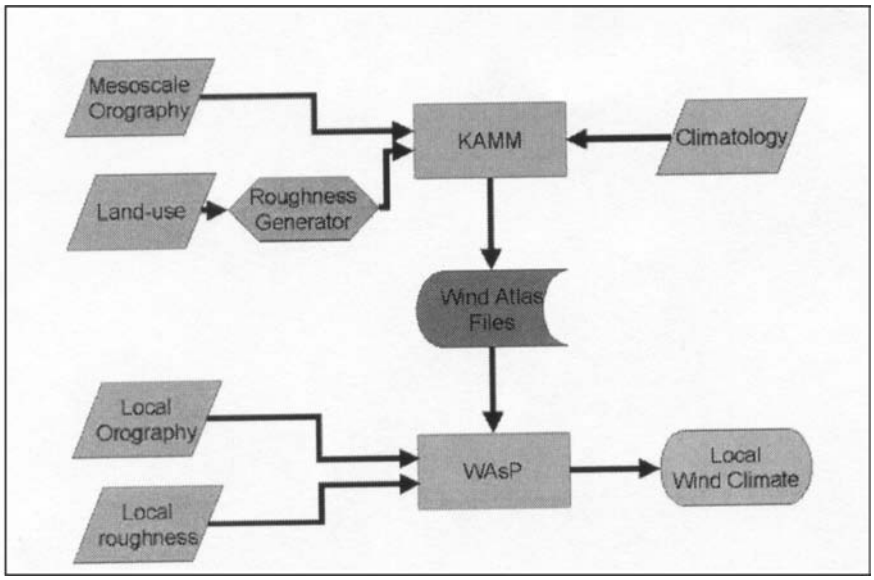


**Figure 2.19: Schematic illustration of the KAMM/WAsP method (Frank et al., 2001).**

***MesoMap***

MesoMap is a wind energy assessment tool developed by a private US company called TrueWind Solutions. The summary below is based on a report by Brower (2002). The main distinction between the KAMM/WAsP and the MesoMap prediction systems is that the MesoMap mesoscale model is run in dynamic mode. This allows for the development of mesoscale flows, such as sea breeze development, within the model domain.

The MesoMap system uses two models; the Mesoscale Atmospheric Simulation System (MASS), which is a prognostic model, and a mass conserving airflow model called WindMap. The MASS model uses two to three levels of nested grids with the highest resolution between 1000 and 3000 m. Mesomap operates on a microcale of 100 to 200m, and uses MASS output

for the initialised wind fields. MASS simulates the wind conditions for a chosen grid region for all levels of the atmosphere for 366 days randomly chosen from a 15 year period. Data are available for this 15-year period from reanalysis of global weather conditions produced by the National Center for Environmental Prediction. Output from MASS is calculated hourly, resulting in 8784 samples at each grid point.

The results of the mesoscale simulations are summarised into data files containing gridded wind rose information and Weibull statistics for 11 levels above the surface. These files are input into the WindMap model where the MASS wind fields are adjusted to account for changes in topography and land cover at a high resolution.

***Windlab Systems***

Windlab Systems is a regional wind-mapping tool developed by the Wind and Energy Research Unit, CSIRO Land and Water, in Australia. Windlab Systems now operates as a 'spin out' company of CSIRO. The Windlab Systems methodologies are not clear, although there was some background information given in a report by Steggel (2002) when the process was in its developmental stages in the CSIRO. At this stage, it was known as WindScape. This process is described below, but may not be exactly representative of the current Windlab Systems methodology.

WindScape combined the mesoscale model TAPM (The Air Pollution Model), with the fine microscale model Raptor. TAPM used two nested grids within an outer grid to obtain 3km grid point resolution winds in the inner grid. The model is run for one year, with hourly averages of wind statistics compiled for each grid point and for each of the twelve direction sectors. The mesoscale model statistics are then interpolated onto the finer scale grid. Raptor is run, typically at 100m-resolution, to calculate the speed-up and slow-down over each of the twelve direction sectors at each grid point on the microscale grid.

A non-linear version of Raptor is now likely to be used in this modelling process. This non-linear micro-scale model allows for potentially more accurate simulations of airflows in a complex terrain environment.

## 2.7 Background Summary

The first part of this chapter discussed the development of the global wind energy industry. Of particular interest to this study was potential for developments in New Zealand and also of the

actual available wind energy resource of this country. To optimise the use of this resource, wind energy developments are likely to be in a complex terrain environment. Accurately modelling wind flow patterns in such regions are important for both locating and assessing this wind energy potential. Understanding airflow patterns in complex terrain is important for the identification of high mean wind sites, and to appreciate and recognise limitations of the models used. Section 2.5 described the effects of topographic features on airflow behaviour, with a focus on New Zealand conditions.

The mean wind speed and distribution of wind speeds is a key factor in assessing the wind energy potential for a location. Section 2.4 described the relationship between wind speed and energy.

As discussed above there are many methods and models used to predict wind flow patterns, from simple empirical formulas to complicated statistical and numerical models. In following chapters the use of prognostic and diagnostic modelling techniques will be described and used in a case study to assess the wind energy potential in the Banks Peninsula region.

# Chapter 3

## Methodology

This chapter is divided into two main sections: a section describing the methodology for prognostic modelling, both low and high-resolution, and a section describing the methodology for a combined prognostic and diagnostic modelling approach. A discussion of the limitations of the combined modelling is discussed in the combined modelling methodology section. Understanding the model limitations is important when interpreting results, and also when attempting to overcome them.

### 3.1 Prognostic modelling

Prognostic modelling is used to simulate airflow over an area of interest for a given time period. There are two goals associated with the prognostic modelling section of this study:

1. To identify regions of good wind energy potential.
2. To gain hourly wind data that can be used to generate reliable wind climates[7] at sites where there are no actual wind data.

The prognostic modelling work has been divided into two sections, low-resolution (2 km grid spacing) and high-resolution (800 m grid spacing). The low and high-resolution prognostic modelling has been defined by the grid spacing of the inner grid of the model runs. Both model resolutions allow production of wind maps that can be used to identify regions of good wind energy potential. A two-step methodology in which hourly wind data are first generated by a high-resolution prognostic modelling, and then used as input to the industry-standard wind energy assessment model, The Wind Atlas Analysis and Application Program (WAsP), is described in full in Section 3.2.

#### 3.1.1 Overview of TAPM (The Air Pollution Model)

TAPM was developed by Commonwealth Scientific and Industrial Research Organisation (CSIRO), Australia. TAPM is a PC-based, three-dimensional, nestable prognostic meteorological and air pollution model. It uses global input databases that provide terrain height, land use, sea surface temperature and synoptic meteorological analysis.

[7] In this study a wind climate is represented by the distribution of hourly wind speed and direction data at a particular location and height above ground level. The longer the period of wind data, the better represented the wind climate will be for that location.

The model solutions for wind, potential temperature and specific humidity are 'nudged' towards the six hourly synoptic input values for these variables. A full technical description of TAPM Version 2 is given in (Hurley, 2002). Validation studies have shown that TAPM performs well in complex terrain for sub-tropical and mid-latitude conditions (Hurley et al., 2002). This study will use the wind data output from the model's meteorological component to both identify areas of wind energy potential, and provide input data to run the WAsP program.

TAPM predicts the local scale flow, such as sea breezes and terrain induced flows, given the larger scale synoptic meteorological fields. The model solves the momentum equations for the horizontal wind components and the incompressible continuity equation for the vertical velocity in the terrain following coordinate system. Air pressure is determined from the sum of the hydrostatic and the optional non-hydrostatic components. A Poisson equation is solved for the non-hydrostatic component. Wind data can also be assimilated into the momentum equations as nudging[8] terms (Luhar and Hurley, 2003). Assimilation of wind data into the model was not used in this study because of the potential effects they can have on computations away from the assimilation point. Since the generation of wind maps usually require a large area of the modelled inner grid, the potential effects from using assimilated wind data were avoided, and was therefore not used in this study.

As mentioned above, the non-hydrostatic mode is an optional aspect of TAPM. The hydrostatic approximation assumes that vertical velocities are small compared to horizontal motion and can therefore be ignored. Many mesoscale meteorological phenomena have non-hydrostatic effects such as surface and atmospheric heat and moisture fluxes, turbulence, convection, evaporation and condensation. Therefore non-hydrostatic processes should not be ignored. It was recommended that the non-hydrostatic option be used when the grid spacing was less that about 1000 m, and only if the terrain is steep and winds are strong. Otherwise, this option will have little effect other than increasing the processing time (Hurley, 2002).

In order to represent topography in mesoscale models, vertical terrain-following coordinate systems are incorporated into their formulations. The terrain-following vertical coordinate system in TAPM allows for easy collection of wind data at a number of levels above ground level in complicated terrain.

[8] Nudging is the process of forcing model solutions towards observed values.

TAPM uses the following datasets:

- Terrain heights at approximately 1km resolution (US Geological Survey),
- Vegetation and soil types at approximately 1 km resolution (US Geological Survey),
- Sea surface temperature at 100km spacing (US National Center for Atmospheric Research),
- Six hourly synoptic scale meteorological data at approximately 100km grid spacing. The synoptic data were derived from GASP (Global Analysis and Prediction model) re-analysis data from the Australian Bureau of Meteorology.

There is an option to edit terrain heights, sea surface temperatures and deep soil moisture content. The deep soil moisture was set at a default value due to its relative insignificance in calculating wind characteristics. There is also the ability to input user-defined databases for terrain heights (this option was used in the higher resolution simulations of this study), synoptic data, and vegetation and soil type.

### 3.1.2 Low-resolution modelling

The low-resolution modelling was conducted for large parts of the Canterbury and Otago regions. The primary goals of this modelling were to identify areas of good wind energy potential over a wide area and make some general comparisons with the results obtained in the Wind Energy Resource Survey (Cherry, 1987). Wind maps were generated for 50 m above ground level for the two regions. The 50 m above ground level was chosen since many current turbines have a hub height near this level, and also because this was the height that Cherry estimated mean wind speeds in the Wind Energy Resource Survey.

***Low-resolution modelling method***

TAPM used six hourly GASP analysis data at a grid spacing of approximately 100 km from the Bureau of Meteorology to provide the synoptic conditions, Rand's global sea surface temperatures, and terrain height data and vegetations and soil classification data from US Geological Survey databases. The model was run with a three level nested grid of 80 x 80 x 20 points at 15600 m, 6000 m and 2000 m horizontal grid spacing with default model options, including having the hydrostatic approximation option turned on. The outer grid dimensions allowed for the forcing of winds from larger scale topographic features, such as Cook and Foveaux Straits and the Southern Alps, to be accounted for in the simulations.

At a horizontal resolution of 2000 m, the model was expected to identify the effects from large-scale topographic features and simulate general wind patterns at a reasonable resolution over the region of interest. Smaller scale topographic features, such as hills and ridges that cause speed-up in the wind, will not be accounted for at this resolution.

The simulations were carried out for the year 2002. The mean wind speed at 50 m above ground level at each grid point in the inner grid was used to illustrate the wind climatology of the two regions.

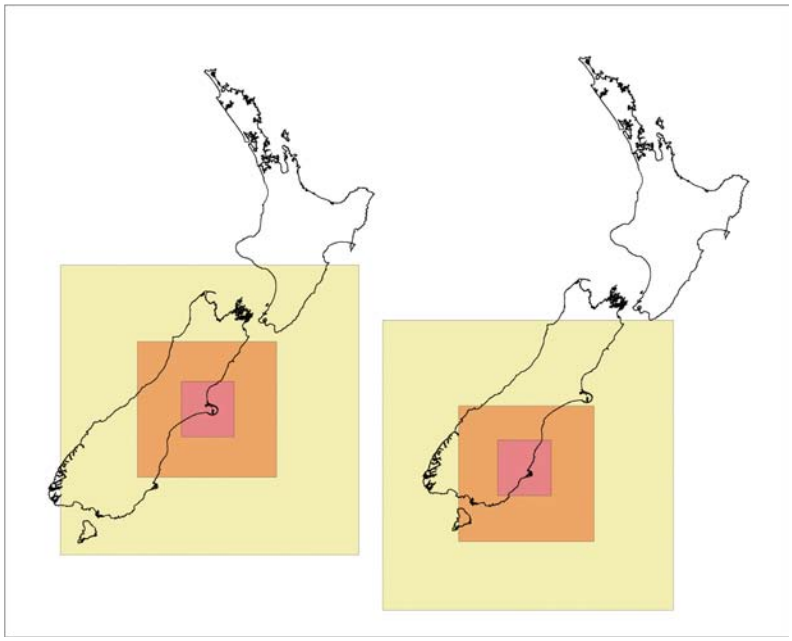

**Figure 3.1: Illustration of the grid nesting for low-resolution prognostic model runs for Canterbury and Otago. The inner grids indicate the region where mean wind speeds at 50 m above the ground were obtained at 2000 m resolution.**

***Canterbury and Otago region descriptions***

The inner grids in Figure 3.1 show the two regions modelled. The first area covers a large part of eastern Canterbury (approximately 120 km by 120 km) from near Amberley in the north to near Ashburton in the south and extending west across the Canterbury Plains to the foothills of the Southern Alps. The second region (also 120 km by 120 km) includes the coastal parts of Otago, from near Oamaru in the north and Nugget Point in the south, and extending approximately 100 km inland.

***Validation methodology (low-resolution model)***

Contour maps of the mean annual wind speed at 50 m above ground level were created from the averaged hourly wind speed data at each grid point of the inner grids (2 km grid spacing) for the Canterbury and Otago regions. Only simple comparisons of the modelled results were made with estimates of 50 m mean wind speeds from the Wind Energy Resource Survey (Cherry, 1987). The main aim of this low-resolution prognostic modelling was to identify general regions of relatively high mean wind speeds. More rigorous validation was completed for the higher resolution study in the Banks Peninsula area, where modelled winds are expected to respond to smaller-scale terrain features.

### 3.1.3 High resolution modelling

TAPM was used to model the wind climatology for the year 2002 for the Banks Peninsula region as shown in Figure 3. The modelled region had dimensions of approximately 64 km by 64 km, and included the following four sites that could be used for model validation:

1. Christchurch Airport (CHX)
2. Le Bons (LBX)
3. Gebbies Pass (GBX)
4. McQueens Valley (MQX)

At a horizontal resolution of 800 m, TAPM was expected to respond to smaller topographic features than the 2000 m-resolution model runs. This simulation was expected to account for topographic features causing speed-up and sheltering of the wind over the Banks Peninsula region. However, at 800 m grid spacing the modelled topography representation of Banks Peninsula is still inexact, creating limitations in the modelling process.

This region was chosen for this case study because it has been identified for potential wind energy developments (there is already one turbine sited there), there was access to reliable wind data, and due to the complexity of the terrain. Regarding the last point, this area provided a challenging area to 'test' the models and methodology used in this study.

***High-resolution modelling method***

TAPM used six hourly GASP analysis data at a grid spacing of approximately 100 km from the Bureau of Meteorology to provide the synoptic conditions, Rand's global sea surface temperatures, and vegetations and soil classification data from US Geological Survey database sets. Topographic data was obtained at 25 m resolution from the Landcare Digital

Elevation Model (DEM). This allowed for a better representation of the 'shape of the land' over Banks Peninsula. With an inner grid resolution of 800 m, much of the detail from the DEM data was lost, although starting with higher resolution data means that the topography is much better represented than with the default 1000 m grid heights used by TAPM.

The model was run with four nested grids of 80 x 80 x 20 points at 12000 m, 5000 m, 2000 m and 800 m horizontal grid spacing (Figure 3.2) with default model options, except for having the non-hydrostatic option turned on. It was advised that for modelling at a horizontal resolution less than 1000 m, the non-hydrostatic option be used to better resolve mesoscale processes (Hurley, 2002). TAPM was run for one-month periods to keep the data output file size below 2 Gb and also allow for easier monitoring of model output for instability errors.

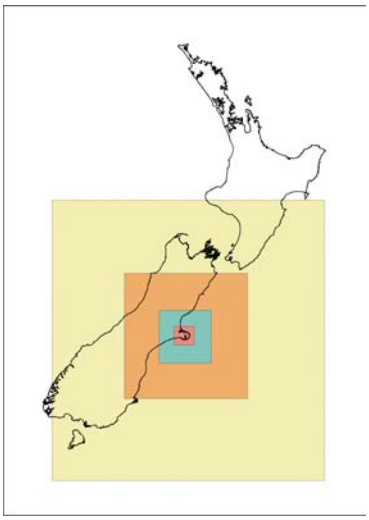

**Figure 3.2: Grid nesting for the high-resolution model run for the Banks Peninsula. The inner (red) grid is the region where wind speed data were obtained at 800 m resolution at 10 m, 25 m, 50 m and 100 m above ground level.**

Contour maps for the mean annual wind speed were created at 10 m, 25 m, 50 m and 100 m above ground level. Hourly time series data were also obtained from grid points (in the inner grid) closest to the four validation sites. A statistical analysis was carried out at these four sites to assess the performance of the model. This validation procedure was based on other validation studies previously carried out for TAPM simulations (Hurley et al., 2002). Wind rose plots were also used to compare the model output and observed data. The location and characteristics of the validation sites are given below.

***Banks Peninsula area description***

The Banks Peninsula topography is characterised by steep valleys and harbours, and exposed ridges rising to a maximum height of 919 m on Mt Herbert (see Figure 3.3). Lyttelton and

Akaroa are the largest harbours, and were formed from the erosion of long extinct volcanoes. The eastward extension and elevation of much of Banks Peninsula mean that the area is more exposed to higher winds compared to other eastern parts of Canterbury. The already complex airflow patterns of the Canterbury region are complicated further by the often steep and varying terrain of Banks Peninsula.

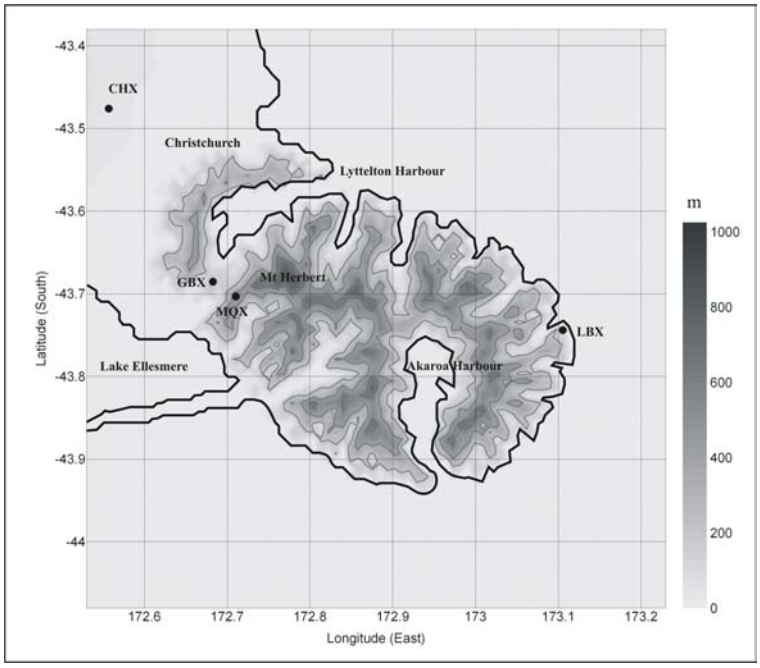


**Figure 3.3: Map of the inner grid region of the high-resolution prognostic modelling. The locations of the four validation sites are indicated by black dots. Elevation contours are given at 200 m intervals.**

***Validation methodology (high resolution model)***

Validation of the model output data was based on four sites within the inner grid where actual wind data were available. Three of the sites, Gebbies Pass (GBX), McQueens Valley (MQX) and Le Bons Bay (LBX) are located in complex terrain environments. Accurate simulation of airflow patterns near these sites was likely to be very challenging. Based on the performance of TAPM at all four sites, a measure of the confidence of the results and hence of the derived wind maps could be determined. The locations of the validation sites are shown in Figure 3.3 and a description of each is given below.

There are two components to the validation process: the first using wind rose plots to compare the overall wind direction distribution of the modelled and observed data at each site, and the second using a more rigorous statistical analysis of the hourly wind data.

## Validation site descriptions

### Christchurch Airport (CHX)

Christchurch Airport lies in the northwest part of the inner grid, as shown in Figure 3.3. The Airport site is 37 m above mean sea level and lies on the northwest fringe of the high surface roughness zone of the Christchurch city area. This site is the only validation point located in flat terrain and has good exposure to all wind directions. Wind data from the National Institute for Water and Atmospheric Research Ltd (NIWA) were available for all of 2002 at a height of 10 m above ground level. Hourly modelled 10 m winds were obtained from the nearest grid point to Christchurch Airport on the inner grid. The elevation of this grid point was 32 m above mean sea level.

### Gebbies Pass (GBX)

Gebbies Pass lies in a saddle between Lyttelton Harbour to the north and Lake Ellesmere to the south. The observation site is located on a small rise in the saddle at an elevation of about 250 m above mean sea level (this is the current site of a Windflow 500 turbine, as shown in Figure 3.4). The site is subjected to significant channelling of wind due to the northeast/southwest orientation of the saddle between the Port Hills (rising to about 400 m above mean sea level) to the west and north, and the steep terrain to the east, up to a maximum elevation of 919 m at the summit of Mount Herbert (see Figure 3.3). Other small knolls and rock outcrops close to the site are likely to cause local variations in the airflow over the saddle, especially at low levels. Observed wind data at 10 m above ground level were available from Windflow Technology Ltd for the period 1 May 2002 to December 31 2002.

**Figure 3.4: The Gebbies Pass validation site looking south showing the turbine and wind measurement mast.**

Hourly modelled predictions at 10 m winds were extracted from the nearest grid point to Gebbies Pass in the inner grid. The elevation of this grid point was 188 m and was considered to be the most representative for this site.

**McQueens Valley (MQX)**

The McQueens Valley site is located on a ridge about 3 km east of the Gebbies Pass site (Figure 3.5). The site is well exposed at an elevation about 540 m and is surrounded by steep and complex terrain. Observed 10 m wind data from Windflow Technology Ltd was available for a three-month period from 1 January 2002 to 31 March 2002.

**Figure 3.5: The approximate position of the McQueens Valley observation site looking east from Gebbies Pass.**

Hourly modelled data at 10 m were obtained from a grid point on the ridge at an elevation of 467 m. Smoothing of elevation data due to the 800 m grid spacing in the inner TAPM grid causes the lower elevation than the actual observation site. However, this grid point was considered to be the most representative for the site.

**Le Bons Bay (LBX)**

The Le Bons Bay observation site is on the eastern side of Banks Peninsula. It is located 236 m above mean sea level on a hill along a ridge on the southern side of Le Bons Bay (Figure 3.6). The terrain near the site is complex with the steep ridge and valley/harbour systems in the area, and with cliffs into the Pacific Ocean just to the east of the anemometer site. Observed wind data at 10 m above ground level was obtained from NIWA for all of 2002.

**Figure 3.6: Looking south towards the Le Bons Bay automatic weather station site.**

Hourly modelled 10 m wind data were extracted from the nearest grid point to this site. The elevation of this grid point was 209 m.

**Statistical measures**

A variety of statistical measures are used for the model evaluation, focusing on wind speed and direction. One of the statistical measures used to evaluate model performance is based on an index (the Index of Agreement). The other statistics, except for the correlation coefficient, are given in absolute terms of m $s^{-1}$.

Because wind direction has a crossover point at north between 0 and 360 degrees, standard linear methods cannot be used to calculate statistics. For model performance the wind direction data need to be split into north/south (v) and east/west (u) vector components before being analysed. The following conversion is used:

$u$ = -speed × sin(direction)
and
$v$ = -speed × cos(direction) (direction in radians)

TAPM winds are computed at 5-minute intervals and the resulting modelled hourly winds are the average of these. Due to the measuring procedure for observed winds, these data are based on the 10-minute averages from the end of each hour.

The nine statistical measures listed below were used to evaluate model performance with respect to wind speed, and the u-component and v-component of the wind. These statistics can be divided into three types, mean and global statistics, difference statistics, and skill measures.

**A) Mean and global statistics**

These statistics provide an overall summary of the model and observed wind data. These statistics (1-4 below) are also used in the calculations of other statistical measures.

1. Observed mean
2. Modelled mean
3. Observed standard deviation
4. Modelled standard deviation

**B) Difference statistics**

These statistical measures compare observed hourly data with the corresponding modelled hourly data. The three statistics used in this study are described below.

5. Root Mean Square Error (RMSE) $$\text{RMSE} = \sqrt{\frac{1}{N}\sum_{i=1}^{N}(P_i - O_i)^2}$$

The RSME can be described as the standard deviation of the difference for hourly prediction and observation pairings at a specific point. Overall, the RSME is a good overall measure of model performance, but since large errors are weighted heavily (due to squaring), its value can be distorted (ENVIRON, 2004).

6. Systematic Root Mean Square Error ($\text{RMSE}_s$) $$\text{RMSE}_S = \sqrt{\frac{1}{N}\sum_{i=1}^{N}(\hat{P}_i - O_i)^2}$$

The $\text{RMSE}_s$ is calculated as the square root of the mean square difference of hourly predictions from the regression formula and observation pairings, at a specific point. The regressed predictions are taken from the least squares formula. The $\text{RMSE}_s$ estimates the model's linear (or systematic) error. This error might be reduced through improvements of the model input or use of different grid nesting, or use of more appropriate model options (ENVIRON, 2004).

7. Unsystematic Root Mean Square Error ($\text{RMSE}_u$) $$\text{RMSE}_U = \sqrt{\frac{1}{N}\sum_{i=1}^{N}(\hat{P}_i - P_i)^2}$$

The $RMSE_u$ is calculated as the square root of the mean square difference of hourly predictions from the regression formula and model prediction value pairings, at a specific point. The $RMSE_u$ is a measure of how much of the difference between predictions and observations resulting from random processes or influences outside the legitimate range of the model. This error may require model refinement, such as new algorithms or higher resolution grids, or that the phenomena being simulated cannot be fully resolved by the model (ENVIRON, 2004).

Ultimately for 'good' model performance, the RMSE should be a low value, with most of the variation explained in the observations. Here, the systematic error $RMSE_s$ should approach zero and the unsystematic error, $RMSE_u$, should approach the RMSE since:

$$RMSE^2 = RMSE_S^2 + RMSE_u^2$$

**C) Skill measures**

Skill measure statistics are given in terms of a score, rather than in absolute terms.

8. Index of Agreement (IOA) $$IOA = 1 - \frac{\sum_{i=1}^{N}(P_i - O_i)^2}{\sum_{i=1}^{N}(|P_i - O_{mean}| + |O_i - O_{mean}|)^2}$$

The IOA is calculated using a method described in Willmott (1982). The IOA can take a value between 0 and 1, with 1 indicating perfect agreement. The IOA is the ratio of the total RMSE to the sum of two differences: the difference between each prediction and the observed mean, and the difference between each observation and observed mean. From another perspective, the IOA is a measure of the match between the departure of each prediction from the observed mean and the departure of each observation from the observed mean (ENVIRON, 2004).

(Note: $N$ is the number of observations, $P_i$ are the hourly model predictions, $O_i$ are the hourly observations, $O_{mean}$ is the observed observation mean, and $\hat{P}_i = a + bO_i$ is the linear regression fitted with intercepts $a$ and slope $b$.)

9. Correlation coefficient

The correlation coefficient provides a measure of the strength of the linear relationship between all of the corresponding hourly modelled and observed winds. The correlation coefficient can take a value between 1 and –1. For model validation a correlation coefficient of 1 indicates a perfect relationship between all of the hourly modelled and observed winds.

Emery (2001) considered that for wind speed the benchmark for IOA was greater than or equal to 0.6. Hurley (2002) referred to other prognostic modelling studies that said an IOA value of more that 0.5 was considered to be good model performance. Emery (2001) suggested that a benchmark for RMSE was less than or equal to 2 m $s^{-1}$. However, in complex terrain this value could easily be contaminated by a relatively small number of larger errors. In a validation study of TAPM in complex terrain at Cape Grim on the southwest corner of Tasmania, RMSE values of wind speed and the wind components were averaged to be 3.1 m $s^{-1}$. It was concluded that the model had performed well in predicting the observed meteorology at this site (Hurley et al., 2002).

## 3.2 Combined prognostic and diagnostic modelling

The Wind Atlas Analysis and Application Program (WAsP) is the wind energy industry-standard model used to assess the mean wind speed and energy output at a specific site, or at a high resolution over a wider area. One key requirement for a WAsP analysis is to have a site for which a reliable wind climate is available close to and in a similar environment to the prediction area. Without years of forward planning, or being fortunate enough to have a reliable wind observation site near the area of interest, this may not be available (particularly in a data sparse area like New Zealand).

The section below therefore outlines a methodology that will evaluate whether prognostic modelling can be used to provide reliable wind climates for sites within an area, which can be used as input to the diagnostic model WAsP. Limitations of the WAsP model are discussed below, particularly when it is used in complex terrain. The combined atmospheric model-WAsP model methodology aims to overcome some of these limitations by providing a source of data over areas of complex terrain (without measurement sites) that can be used to drive the WAsP model. The aims of this section are described fully in Section 3.2.3 below.

### 3.2.1 Overview of WAsP (The Wind Atlas Analysis and Application Program)

The WAsP model was developed at the Riso National Laboratory, Riso, Denmark (Troen, 2003). Its development was a result of economic and environmental interest in wind energy,

and a desire for reliable wind resource information, such as the European Wind Atlas (Troen and Petersen, 1989).

Unlike dynamic models such as MM5, TAPM and RAMS, WAsP does not represent the changing state of the atmosphere over time, but is based around the statistical description of the wind. From this climatological perspective and on small spatial scales, wind variations are affected by features of the surface of the land such as topographic changes like surface roughness variations, and obstacles, like buildings and trees. WAsP uses equations to describe these variations of the Earth's surface and their effect on wind speed and direction.

The WAsP program determines wind speed distribution parameters for twelve direction sectors at certain heights above the ground for an observation site and then transforms this wind climate to a predicted site. This is referred to as the Wind Atlas Analysis and Application approach and is described in detail in the Danish Wind Atlas (Petersen et al., 1981), and developed further in the European Wind Atlas (Petersen et al., 1996).

The method used by WAsP involves the following steps, and is shown in Figure 7 below:

1. Analysis of observed wind data into 12 direction sectors, to each of which a Weibull distribution function is fitted.

2. Elimination of the effects of terrain, roughness and obstacles on the wind climate data by the application of sub-models (described below).

3. Vertical extrapolation of the 'cleaned' wind data using the logarithmic wind profile model to obtain a regional wind climate (wind atlas) over flat homogeneous terrain for neutral atmospheric conditions. The resulting wind atlas summary is given for a number of roughness criteria and standard levels above the ground.

4. Reverse transformations are then applied to the wind atlas information to account for the terrain, roughness and obstacles surrounding the predicted site. These transformations account for the speed-up (and slow-down) of the airflow when encountering such features. The effects from topographic features are described in Section 2.3, and the effects from surface roughness and obstacles that are more specific to the WAsP model, are given below. The predicted wind climate at each site is given as a Weibull function (to model the wind speed) for each of the twelve wind

direction sectors. The probability of the occurrence of winds falling into each of the direction sectors is also given. For the production of wind maps, the reverse transformations are applied and hence predicted wind climates attained at a specified grid resolution over the map area.

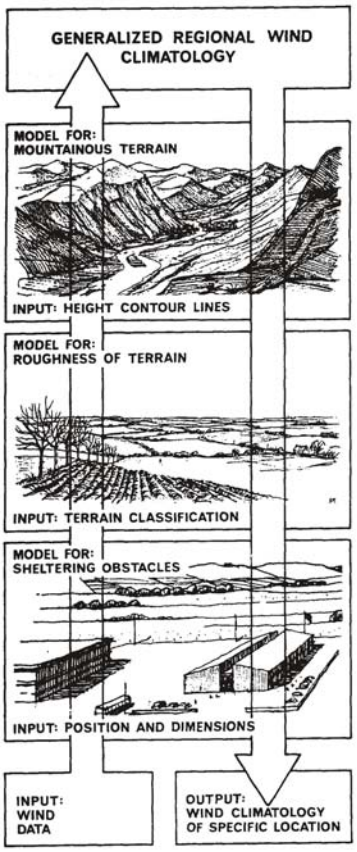


**Figure 3.7: Illustration of the wind atlas methodology used in WAsP (Troen and Petersen, 1989).**

***Description of the sub-models used in WAsP***

WAsP is built around three sub-models, incorporating effects of obstacles on airflow in the vicinity of the observation and prediction sites, surface roughness changes within the map area, and speed up and turning of the wind due to orographic effects. These sub-models are briefly described below.

**The shelter model**

Shelter is defined as the relative decrease in wind caused by an obstacle in the terrain. The shelter model used in WAsP is based on Perera (1981), where shelter by an obstacle at a particular site depends on:

- the distance between the obstacle and site
- the height of the obstacle

- the height of the point of interest at the site
- the length of the obstacle
- the porosity of the obstacle (Mortensen, 2003).

The reduction of wind speed due to shelter from an infinitely long two-dimensional obstacle of zero porosity is shown in Figure 3.8 below (based on ideas from Perera (1981). The shelter decreases with diminishing length and increasing porosity. In the shaded area the sheltering is very dependent on the detailed geometry of the obstacle. Also, wind speeds are usually increased close to and above the obstacle, similar to the speed-up effects over hills (Mortensen, 2003).

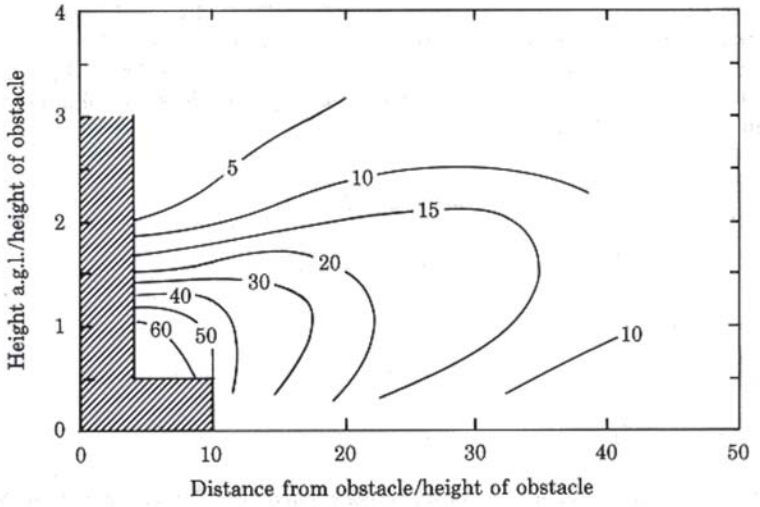


**Figure 3.8: Reduction of wind speed from a non-porous obstacle based on the ratio of the height above ground level to the height of the obstacle (Mortensen, 2003).**

WAsP considers obstacles as rectangular 'boxes'. Each obstacle is assigned a position relative to the site, its dimensions and porosity. There is a maximum of 50 obstacles that can be specified in one obstacle list.

There is often the problem of whether to classify a feature as an obstacle or roughness element (as described below). The following guidelines are given:

1. If the point of interest (turbine or anemometer) is closer than about 50 obstacle heights to the obstacle and closer than three obstacle heights to the ground, the object should be included as an obstacle.

2. If the point of interest is further away than the above conditions, the object could be included in the roughness description.

There were no obstacles to account for in any of the WAsP analyses completed in this study.

**The roughness change model**

The overall effects of the terrain surface and obstacles that lead to resistance to the wind near the ground are referred to as the roughness of the terrain. Not all topographical features contribute to the roughness. For example, trees and buildings are roughness elements, whereas smooth hills are not because they do not cause an increase in the turbulence of the airflow.

The roughness change model in WAsP takes into account the influence of changes in roughness near sites of interest. Roughness changes close to sites of interest are generally said to be important for distances up to 10 km (Mortensen, 2003). However, if there is significant roughness change further away, such as at a coastline, in the direction of a prevailing wind, then the mapped area should be extended to include them, up to 20 km away (Bowen and Mortensen, 1996). In a study over the southern North Island of New Zealand where wind climate predictions were made for some specific locations, it was shown that the inclusion of a coastline around 200 km away, in the roughness and topographic map file, improved the results in a WAsP analysis (Reid, 1997).

The sub-program of WAsP models the downstream effects of surface roughness on the airflow. The roughness classifications applied in the WAsP program are made up of 36 azimuth sector divisions from the site (or grid point) of interest, with up to 10 roughness changes permitted in each of these 36 sectors (Mortensen, 2003). These roughness classifications for each site can be viewed as a roughness rose, but for this study roughness changes are specified in a map file format (see Figure 3.10) that indicate the roughness change boundaries over the area of interest. The sub-program uses this map file to generate a roughness classification for each grid point calculation. In general, the roughness length is considered a climatological parameter, due to the variations in foliation, snow cover and vegetation, for example. Table 3.1 below describes the roughness criteria that were used in this study.

**Table 3.1: Roughness criteria used in this study of the Bank Peninsula area.**

| Roughness length | Terrain description |
|---|---|
| 0 | Sea and inland water |
| 0.005 | Smooth land surfaces such as sand and bare ground |
| 0.03 | Open farmland |
| 0.1 | Less open farmland with trees and buildings |
| 0.4 | Rough surface with trees and buildings |
| 0.8 | Forests and built up urban regions |

In the wind atlas files generated by WAsP, the roughness criteria are divided into four standard classes. This allows for wind and energy calculations to be done in the same area but for varying land cover characteristics. These classes correspond to the roughness lengths shown in Table 3.2 below.

**Table 3.2: Standard roughness classes for which wind atlas files are generated by WAsP.**

| Roughness class | Roughness length (m) | Terrain description |
|---|---|---|
| 0 | 0.0002 | Smooth land and water surfaces |
| 1 | 0.03 | Farmland with very few buildings/trees |
| 2 | 0.1 | Less open farmland with trees and buildings |
| 3 | 0.4 | Rough surface with trees and buildings |

## The Orographic Model

WAsP utilises the 'BZ-model' Troen (1990) to calculate the wind velocity perturbations induced by orographic features such as single hills or more complex terrain. The linear model is limited to neutrally stable airflows over low, smooth hills with attached flows. WAsP predictions in such conditions compare well with measured field data from two benchmark studies at Askervein and Blashval (Bowen and Mortensen, 1996). The model was developed specifically for wind energy siting and has the following features:

- It employs a high resolution, zooming polar grid. This allows for increasing detail in the calculation of flow perturbation profiles close to the sites (or grid points in a wind or energy resource analysis) of interest.

- It incorporates the roughness conditions of the terrain in the vicinity of the sites of interest.
- Its uses a boundary layer thickness of approximately 1000 m to force large-scale airflow around high elevation areas (Mortensen, 2003).

The zooming grid is illustrated in Figure 3.9. The top left map has dimensions of 25 km by 25 km, while the bottom right map area has dimension of about 200 m by 200 m. The grid resolution at the centre of the model is 4 m.

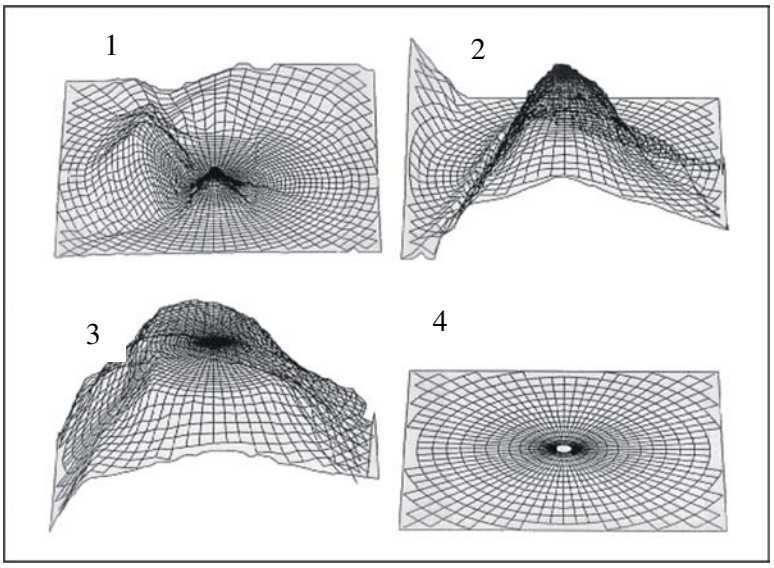


**Figure 3.9: Illustration of the zooming grid (from 1 to 4) of the B-Z model used in the WAsP model (Mortensen, 2003).**

### 3.2.2 WAsP in complex terrain

The WAsP program generalises a long-term wind data time series at a reference site, which is stored as a wind atlas file and then used to predict the wind climate at other sites. Accurate predictions using WAsP can be obtained if the reference and predicted sites meet the following criteria:

- They are subject to the same weather regime.
- The prevailing weather conditions are close to being neutrally stable.
- The surrounding terrain is sufficiently gentle and smooth to ensure mostly attached flows, and with minimal large-scale terrain effects, such as channelling.

The prediction accuracy also depends on the reliability of the reference site wind data, the methods used to do preliminary data processing and the correct use of the WAsP program (Bowen and Mortensen, 1996).

Areas of wind energy potential assessment are not always going to fit the above criteria. The Banks Peninsula study area has a large spatial variation of climates that can be illustrated during certain synoptic situations. For example, in a westerly flow over the South Island, the upper parts of Banks Peninsula can experience strong and relatively unstable westerly winds and at the same time, lower elevations are in a stable northeast regime. Climatic stability and wind patterns are complicated further by seasonal and diurnal variations. Also, much of Banks Peninsula is associated with steep terrain resulting in flow separation and channelling.

***Factors affecting the prediction process***

The analysis and application procedures in WAsP can be considered as a transfer function model linking the winds from a reference site to a predicted site (Bowen and Mortensen, 2004). WAsP assumes that there are different and unique speed-up ratios between the two sites for each direction sector. These speed-up ratios are dependent on surface roughness and the orography surrounding the sites, and are independent of the wind speed and climatic conditions that are assumed to be neutrally stable. For a well-behaved transfer function model, a high cross-correlation of the wind conditions must exist between the reference site and predicted site. (Bowen and Mortensen, 2004) (This condition also applies to measure-correlate-predict (MCP) prediction methods). However, Bowen (2004) suggests that there is limited importance in this cross-correlation dependence since WAsP deals with mean wind statistics, which should remain unaffected by spatial effects.

Bowen (2004) stated that there are a number of factors that can contribute to the overall errors made in a WAsP prediction process. These were separated into the following four categories and are explained in more detail below:

1. Atmospheric conditions
2. Character of the orography
3. The forcing of wind speed data to fit a Weibull distribution
4. Dividing of winds into direction sectors.

**Atmospheric conditions**

It is accepted that errors in WAsP predictions that result from non-standard atmospheric conditions can be significant. The conditions that can cause the transfer function to deviate from the neutral WAsP model can be sorted into two categories:

1. When the two sites lie in different wind regimes as a result of one or more of the following:
    - Excessive horizontal separation relative to the scale of the prevailing weather systems.
    - Excessive vertical separation that transcends the interface between high and low altitude wind regimes.
    - Moderate separation, but with local strongly stable stratification, inversion layers, sea breezes or density driven flows prevailing.

2. When the two sites lie in the same weather regime, but the prevailing atmospheric conditions are not neutrally stable.

The individual effect that each of the climate phenomena have on WAsP predictions is complex and requires further investigation (Bowen and Mortensen, 2004). Bowen (2004) proposed that WAsP errors were likely to be slightly higher if the predicted site was in a relatively unstable environment, such as on a hilly area, but errors would be much less when the predicted site was subjected to stable conditions. This is likely to be because the orographic model used in WAsP assumes a neutrally stable atmosphere, and in a stable environment, airflows behave in a similar way compared to airflow in unstable conditions.

**Character of the orography**

The other significant category of factors affecting WAsP predictions are those associated with the terrain at both the reference and predicted sites. Errors could be created by the following factors:

- Individual site ruggedness. Ruggedness is defined as the steepness of the terrain surrounding a site (Mortensen, 2003).
- Extensive flow separation
- Topographic features beyond the terrain map considered by WAsP
- Site elevation
- Hill height relative to the boundary-layer height
- Effective surface roughness length due to the ruggedness of terrain
- The degree of turning due to large-scale terrain effects and the resulting changes in the frequencies of occurrence in each wind direction sector.

The area covered by the topographic maps used in the wind energy assessment analysis is considered to be a factor in reducing WAsP prediction errors. It is recommended that maps should extend at least 10 km from any reference site or site of interest within the map region. However, if there is a major roughness change, such as a coastline in a frequent wind direction, then this distance should extend further, perhaps 20 km away (Mortensen, 2003). It is important to account for major roughness changes since the orographic flow model of WAsP responds to terrain variations on a smaller scale than the roughness change model (Frank et al., 2001).

In a study by (Reid, 1997), it was shown that WAsP was better able to predict mean speed and direction for particular locations if large-scale topography features were included in the map domain. For predictions of winds at Wellington Airport, the ranges well to the east had a greater effect on WAsP calculations than closer but relatively low hills.

Also, since WAsP responds to detailed changes in topography and surface roughness, the quality of these data will also have an impact on WAsP predictions. In an evaluation of WAsP in the Lyttelton Harbour region, (Saba, 1999) suggested that a lack of accurate or high-resolution topographic data had a negative effect on WAsP calculations for a site at Godley Heads.

**Weibull curve fitting**

In general, wind speed data for most sites fit a Weibull distribution that is shaped using the scale and shape parameters. Sometimes wind data for a direction sector may not fit closely to this distribution. For example, there may be a double wind speed maximum for a particular direction sector. Such forcing of the wind data to fit the Weibull distribution can cause errors in wind climate predictions.

**Direction sectors**

Usually WAsP predictions are made for 12 directions sectors. In the WAsP application process, winds may fall into adjacent sectors when they are interacting with complex terrain features. This effect can be seen when predictions for the wind-monitoring site are generated at sites in or surrounded by steep terrain. Here the predicted wind climate at the observed site can have different direction sector frequencies than the observed wind climate. The mean

wind speed might also be different due to different weightings applied to the speed-up ratios in each direction sector.

***WAsP errors***

It has been shown that the size of WAsP errors in the analysis and prediction processes are predominately a function of the degree that the operational limits are violated by factors associated with atmospheric conditions and terrain (Bowen and Mortensen, 2004). Overall, the errors can be defined as the analysis error E1, when creating a wind atlas from the reference site, and the application error E2, when creating a wind climate for the predicted site. The overall prediction error of the wind climate will be determined by the difference in the two procedure errors (E2–E1).

As discussed in the overview of WAsP, the orographic component uses a linear model, which is limited to neutrally stable airflow over low smooth hills. It is suggested that the critical slope for flow separation to occur is above 0.3 (Wood, 1995). Bowen (1996) proposed an orographic performance indicator, which attempts to quantify the extent to which the terrain at a particular site exceeds the limits of the orographic model. The resulting ruggedness index (RIX) is a fraction of the surrounding terrain that exceeds a slope of 0.3. The index is calculated for each of the 12 sectors and the overall RIX is the mean RIX for all of the sectors. The radius from a site for which the RIX is calculated can be changed, but is usually set at a default value of 3500 m. Different radius values can yield different RIX values, especially when there is steep terrain within the area being analysed.

***Using the ruggedness index (RIX) to assess potential WAsP errors***

The ruggedness index (RIX) is described in detail in Bowen (1996), Mortensen (1997), and Bowen (2004). The following conclusions regarding RIX can be made:

- If the RIX is close to zero, then the terrain is generally less steep then 0.3 and the airflow in the region is likely to be attached.
- If the RIX is greater than zero, then parts of the terrain are steeper than 0.3 and flow separation may occur in some sectors.

Therefore, large RIX values can lead to significant errors in the modelling of the airflow.

The sign and magnitude of the prediction error (E2-E1) due to orography was found to be proportional to the difference in the ruggedness of the observed and predicted sites (Bowen and Mortensen, 1996). However, in complex terrain the errors in the analysis and application procedures can effectively cancel each other out, resulting in an accurate prediction. Therefore, if the terrain does differ between sites, an indication of either under-prediction and over-prediction of mean wind speeds can be made based on the difference of the RIX values at each site. It should be emphasised that few studies have provided information or application of this error indicator. Also, this error indicator ignores the effects of different atmospheric conditions at the two sites.

Bowen (1996) therefore proposed that the overall accuracy of WAsP predictions depends on the terrain characteristics near both the reference and predicted sites, and can be summarised as below.

1. If the observed and predicted sites have similar RIX values, then modelling errors are significant but will tend to cancel each other out. Both sites should have similar orientation and orography, and also experience similar wind climatic conditions.
2. If the observed site is less rugged than the predicted site, then modelling errors are significant and unequal. The overall prediction will be overestimated.
3. If the observed site is more rugged than the predicted site, then modelling errors are significant and unequal. The overall prediction will be underestimated.

Error indication maps will be given using RIX values in the results section. By calculating the difference between the RIX value at reference and predicted site, a quantitative indication of prediction errors can also be made. A study of wind predictions using WAsP in complex terrain in Portugal (Bowen and Mortensen, 2004) is the only documented paper on error indication. This study showed that if the difference in RIX values was within about 5%, the wind speed error should be less than 5%. If the absolute difference in RIX values between the sites is 10%, then the wind speed error could potentially be in excess of 30%.

### 3.2.3 Specific aims for combining prognostic and diagnostic modelling

It has been highlighted in previous sections that there are many factors that influence WAsP predictions. The effects from topography and atmospheric conditions are considered to be the most significant. Deviations from neutral stability, the forcing of wind speed data to fit the Weibull function, and winds falling in different direction sectors in the analysis and

application procedures of WAsP, are all limitations of the mathematical sub-models and will not be addressed directly in this study.

Considering the limitations that have been highlighted above, and the overall goals of this research, the methodology described below will address the following three issues:

1. Using wind data from the prognostic mesoscale meteorological model (TAPM) to generate a wind climate for WAsP in situations where there is no actual reliable wind data available.

2. Using prognostic model wind data to reduce potential errors that can result when using WAsP if the reference and predicted sites are located in different wind climate areas and/or topography.

3. Considering the relationship between the 'ruggedness' of sites and the size of the modelling errors, to assess the reliability of WAsP predictions in a complex terrain environment.

### 3.2.4 Combined modelling methodology

Wind data from other locations are often used when wind energy assessments are made at sites where there are no actual wind data. The observed and predicted sites may be in different wind climate and/or topographic environment. For example, an assessment of the Gebbies Pass area might use Christchurch Airport winds to generate a regional wind climate to be used in the WAsP analysis. This can lead to significant errors in predictions. This case study investigates using wind data from seven different sites to make a prediction of the wind climate at Gebbies Pass.

The analysis procedure of the WAsP program was used to generate a wind atlas file based on wind observations from seven sites. This process involves the elimination of terrain and roughness change effects around each of the observation sites to obtain the expected regional wind climate over flat, homogeneous terrain for neutral atmospheric conditions. The resulting wind atlas files were then applied to the Gebbies Pass region to account for detailed topography features and surface roughness changes, and to obtain a predicted wind climate and, hence, expected energy production (the WAsP analysis and application procedures are

described in detail in Section 3.2.1). The results were then compared with the reference data obtained from using actual winds from the Gebbies Pass site.

Figure 3.10 illustrates the detail of the topographic map file used by WAsP in the Gebbies Pass area. The elevation contours are at 20 m intervals and the surface roughness boundaries used in the map are given in Section 3.2.1. The same topographic detail was used to create the wind atlas files at the seven wind observations sites.

The Gebbies Pass site was chosen for this case study for the following reasons:

1. There was access to reliable actual wind data that could be used in the validation process.
2. The complex terrain at and surrounding the site is as difficult to model as any potential wind energy development site in New Zealand, and is therefore a 'good test' for the methodology.
3. This wider area has already been modelled by TAPM (mesoscale meteorological model) and the results validated reasonably well against actual wind data.
4. Error indication of the analysis based on the 'ruggedness' of the terrain could be applied in this area due to some of the terrain in the area exceeding the operational limits of the WAsP model.

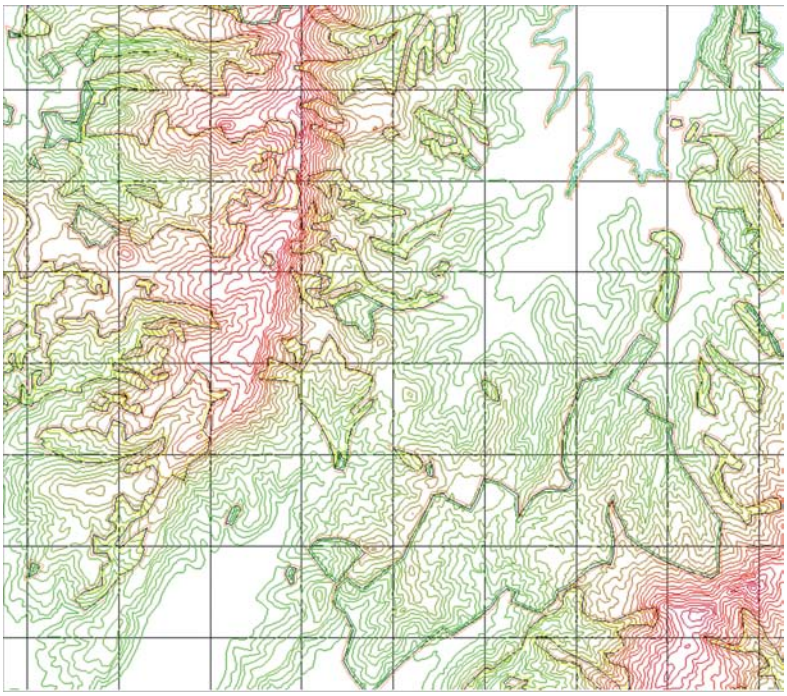

**Figure 3.10: A visual representation of part of the WAsP roughness and elevation contour map used in the Gebbies Pass case study. The map shows elevation contours at 20 m intervals and boundaries between areas of surface roughness in the region.**

The seven observed wind climates were all derived from hourly winds for the period 1 May to 31 December 2002. Wind data were obtained from either actual observations or output from TAPM inner grid points. Descriptions of these sites are given in the following section.

Analysis of the wind and annual energy predictions at the Gebbies Pass site (at 50 m above ground level) will be made using the seven derived wind regional wind atlas files. WAsP predictions will also be made for a wider area surrounding Gebbies Pass, as shown in Figure 3.11, using some of these regional wind atlas files. These maps of the Gebbies Pass area will illustrate spatial variations of mean wind speed and annual energy production predictions when using wind data from different sites. The analysis of wind and annual energy production for a sample wind farm will also be given to show an application of the combined modelling technique.

### 3.2.5 Description of the Gebbies Pass area

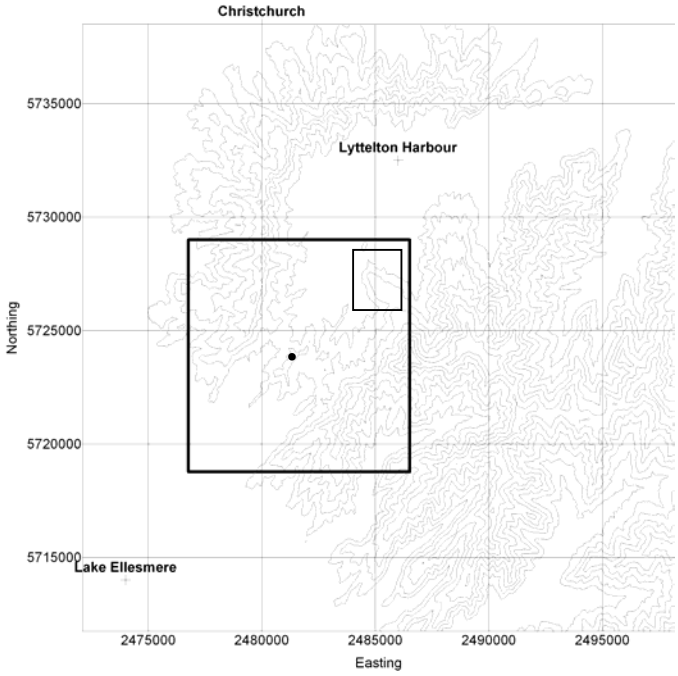


**Figure 3.11: The location of the Gebbies Pass case study site and surrounding area. The outer box represents the wider Gebbies Pass area within which the WAsP model was applied. The inner box indicates the where the sample wind farm will be located (see Conclusions chapter).**

The Gebbies Pass reference site is the current location of the Windflow Technology Ltd turbine. With access to reliable hourly wind data for the period 1 May 2002 to 31 December 2002, this was considered to be a good reference site for this case study. Details of the Gebbies Pass site and surrounding topography are given in Section 3.1.3. Figure 3.11 shows the Gebbies Pass case study site (and WAsP analysis area) within the wider region. Figures 3.12 and 3.13 provide a visual representation of the Gebbies Pass site and the map area used in the case study.

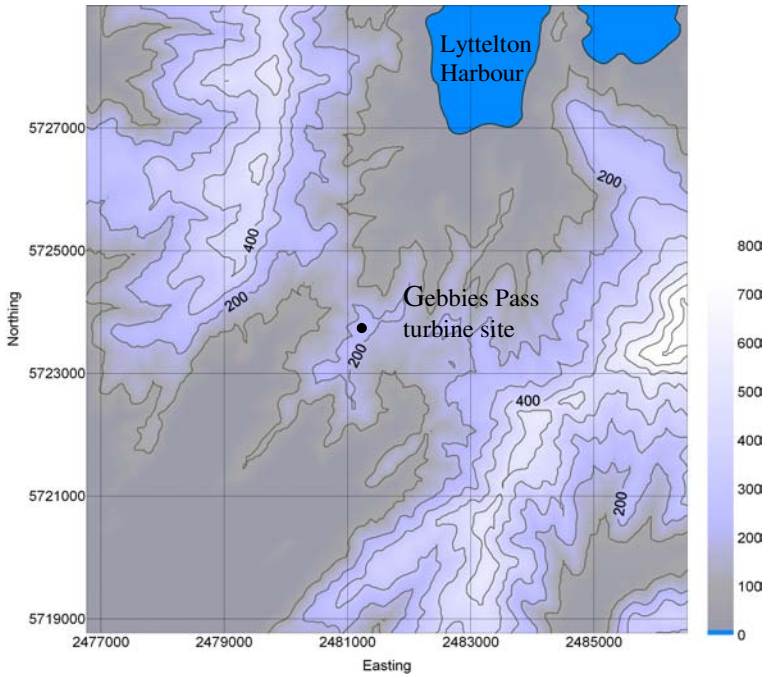


**Figure 3.12: Gebbies Pass reference site and surrounding area. Elevation contours are at 100 m intervals.**

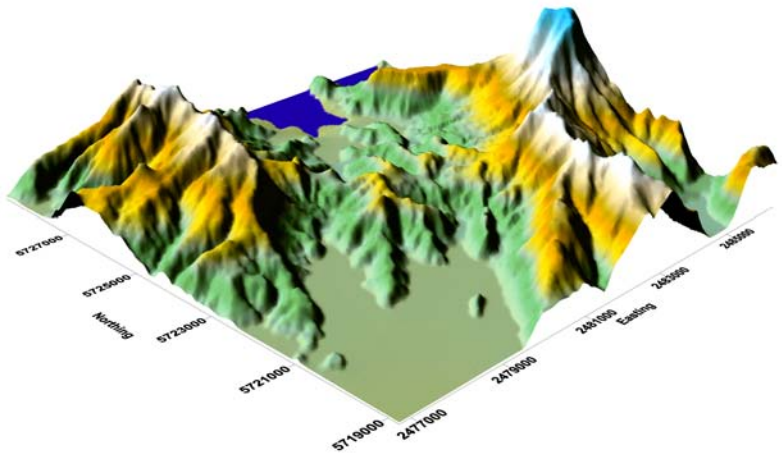


**Figure 3.13: Three-dimensional illustration of the Gebbies Pass area looking toward the northeast.**

### 3.2.6 Wind data site descriptions

As described in Section 2.3, airflow can be significantly enhanced when channelled between topographic features and over hills and ridges. Results from the high-resolution prognostic modelling (Section 4.2) completed for the Banks Peninsula region showed that at 800 m resolution, these effects are not likely to be fully accounted for when topographic features have dimensions less than 3 – 5 km, resulting in an under-estimation of the modelled winds. The results suggest that the Gebbies Pass area and the elevated ridges around Lyttelton Harbour area affected by these model limitations.

As part of this case study, modelled winds from sites where under-prediction of wind speeds was likely, a correction factor was applied (This correction factor will be discussed in full in the Results chapter). These wind data were then used to create a regional wind atlas to be applied to the Gebbies Pass site. The regional wind atlas files used were based on hourly wind data from the seven sites listed below. The location of each of the sites is shown in Figure 3.14.

1. Christchurch Airport, actual data, 10 m (CHA)
2. Le Bons Bay automatic weather station, actual data, 10 m (LBA)
3. Gebbies Pass, TAPM model data, 10 m (GP10M)
4. Gebbies Pass, TAPM model data, 50 m (GP50M)
5. Port Hills site, TAPM model data, 25 m (PHM)
6. Sea site, TAPM model data, 10 m (SSM)
7. Interpolator generated file, from TAPM model data combining wind atlas files from three sites in the Lyttelton Harbour area (LHM)

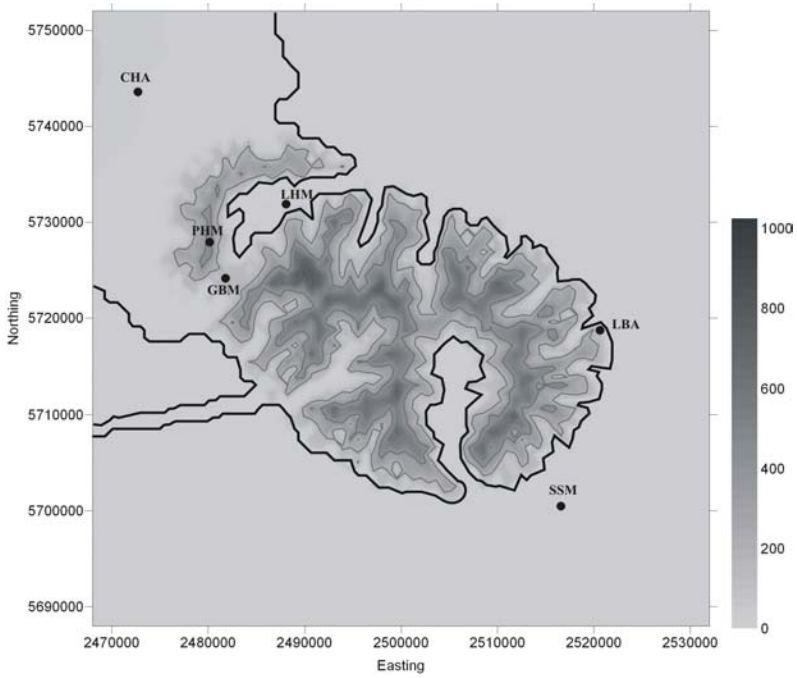


**Figure 3.14: Map of Banks Peninsula showing the location of the wind data sites used in the WAsP analysis for the Gebbies Pass area. Note that the GBM site is associated with two TAPM wind data levels (GB10M and GB50M) and the LHM site is used as part of the interpolator derived wind atlas file.**

1. Christchurch Airport 10 m (CHA)

Data from this site were also used in the validation of the TAPM model and are described in detail in Section 3.1.3. Christchurch Airport lies about 26 km north-northwest of Gebbies Pass. Winds from here have been used in wind energy assessments for the Banks Peninsula area (Cherry 1987) and are therefore of interest in this case study.

2. Le Bons Bay 10 m (LBA)

Le Bons Bay was included in this case study as it provided reliable actual wind data from the far east of Banks Peninsula about 40 km east of the Gebbies Pass site. This site was used in the validation of TAPM and is also described in detail in Section 3.1.3.

3. Gebbies Pass 10 m (GP10M)

This wind data were obtained from TAPM at 10 m above ground level at the closest grid point to the Gebbies Pass observation site. These data were used in the validation of the high-resolution prognostic model at the Gebbies Pass site.

4. Gebbies Pass 50 m (GP50M)

This wind data were obtained from TAPM at 50 m above ground level at the closest grid point to the Gebbies Pass observation site (same grid point as the GP10M site). These data were also used in the validation process of the high-resolution prognostic modelling at the Gebbies Pass site.

5. Port Hills 25 m (PHM)

This dataset was derived from the TAPM model at a site at an elevation of 300 m on the summit of the Port Hills about 5 km northwest of Gebbies Pass. The winds were taken from a height of 25 m above ground level to account for the likely under-prediction of modelled wind speeds at 10 m above ground level.

6. Sea site 10 m (SSM)

Wind data from this site were obtained from the TAPM model at 10 m above sea level from a location over the sea near the southeast coast of Banks Peninsula. The grid point was located about 40 km east-southeast of Gebbies Pass.

7. *Wind Atlas Interpolator* generated file from the Lyttelton Harbour region (LHIM)

This wind atlas file combined three wind atlas files from the Gebbies Pass region using an interpolator function of WAsP. Wind data for individual wind atlas files were obtained from the following TAPM grid points:

- Gebbies Pass 50 m (GP50M)
- Port Hills 25 m (PHM25)
- A site in Lyttelton Harbour 50 m (LHM).

This wind atlas file was used to investigate if combining wind atlas files could improve the wind climate prediction at Gebbies Pass. A description of the *Wind Interpolator* is given below.

***The Library Interpolator***

The LIB interpolator is a feature of WAsP that combines up to three wind atlas (*.lib) files. Although the interpolator was designed more for wind atlas mapping rather than individual site predictions, there was interest in this study to see if combining wind atlas files in the Lyttelton Harbour region could better represent the channelling effects at Gebbies Pass.

The weighting of each wind atlas file used can be specified by the user or can default to values determined by the relative distance of each wind atlas file from the specified location of the interpolated wind atlas file. More detail of the interpolation methods used to create the interpolated wind atlas files are given in Mortensen (1999). Figure 3.15 shows the relative positions and weightings given to the three wind atlas files used to generate the Lyttelton Harbour wind atlas file (LHM). The weighting ratio of the three original wind atlas files, Gebbies Pass, Port Hills and Lyttelton Harbour; was specified as 2:1:1, respectively.

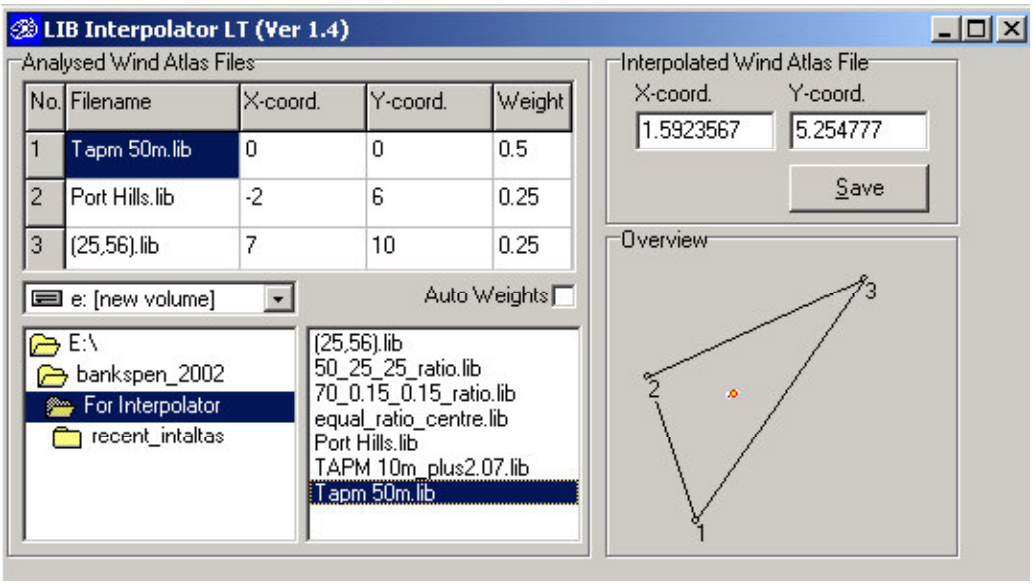


**Figure 3.15: The user interface of the Library Interpolator used to generate the LHM wind atlas file.**

### 3.2.7 Wind atlas assessment methodology

To make an assessment of the seven different wind climates used to make a prediction of the 10 m above ground wind climate at Gebbies Pass, wind atlas files generated from each of the sites given above were applied to the Gebbies Pass site. The results from each analysis will be measured against reference data (as described below). The model output results and reference data consist of the frequency of occurrence and annual energy production for the twelve 30-degree sectors. While comparing the direction sectors gives a general comparison of the predicted and reference wind climates for the Gebbies Pass site, the AEP calculations also account for the distribution of wind speed in the 12 sectors (As described in Section 2.2.3, AEP calculations are based on the frequency of occurrence and the Weibull distribution for each of the 12 sectors).

The statistics used in the analysis were the absolute mean error (AME) and the root mean square error (RMSE) between the reference and predicted values for the frequency of occurrence and AEP for the twelve sectors. The general equations for these two statistics are given below.

$$\text{AME} = \frac{\sum_{i=1}^{12} |P_i - R_i|}{12} \qquad \text{RMSE} = \sqrt{\frac{\sum_{i=1}^{12} (P_i - R_i)^2}{12}}$$

Here, $P_i$ is the predicted direction frequency of occurrence or predicted AEP, and $R_i$ is reference direction frequency of occurrence or AEP.

Maps for the Gebbies Pass area (see Figures 3.12 and 3.13) were also used to illustrate the spatial differences of mean wind speed and AEP when using three sources of wind data in the analysis. These maps were generated using wind atlas files based on winds from Christchurch Airport, output from the meteorological mesoscale model TAPM at the Gebbies Pass site and actual winds from Gebbies Pass. The maps are based on 50 m above ground mean wind speed and AEP calculations at 100 m resolution. AEP calculations were based on a 1 MW rated turbine. Three-dimensional surface maps are also used to illustrate the results obtained from using different sources of wind data.

### 3.2.8 Obtaining reference data

Reference data were required for the statistical analysis. The reference (or validation) data were based on 'best' wind and energy predictions for the Gebbies Pass site using actual wind data from the same site. Because all energy calculations performed by WAsP use the analysis and application procedures, the 'best' predictions were used as reference data. In this case, the procedure for obtaining the reference data is called a 'self-site' analysis. The steps used to obtain the reference data for Gebbies Pass and the results are:

1. Analysis of the observed wind climate
2. Generation of regional wind atlas based on the observed wind climate
3. Application of wind atlas to the Gebbies Pass site.

***The Gebbies Pass observed wind climate***

Tables 3.3 and 3.4 and Figure 3.16 illustrate the nature of the observed wind climate at Gebbies Pass site for the period from 1 May to 31 December 2002. The wind climate is based on hourly observations for this period. The tables and diagram clearly show that the prevailing wind is from the 030 – 060° sector with 32.2% of the winds from this direction,

and with a secondary maximum from the southwest sectors. Table 3.4 also shows that the strongest mean winds come from the northerly quarter, the highest from the 330 – 360° sector with 9.95 m $s^{-1}$, although the frequency of winds from this sector is low. The high mean wind speeds from the northwest are due to strong synoptic flows required from this direction to overcome the channelling effects of Lyttelton Harbour, which is orientated to the north-northeast of Gebbies Pass.

**Table 3.3: Sectorised wind speed summary of the Gebbies Pass observed wind climate.**

| U | 0 | 30 | 60 | 90 | 120 | 150 | 180 | 210 | 240 | 270 | 300 | 330 | Total |
|---|---|---|---|---|---|---|---|---|---|---|---|---|---|
| **1.00** | 0 | 2 | 18 | 113 | 49 | 124 | 26 | 17 | 16 | 11 | 5 | 1 | 15 |
| **2.00** | 5 | 14 | 106 | 301 | 190 | 271 | 91 | 106 | 104 | 160 | 54 | 8 | 70 |
| **3.00** | 17 | 35 | 134 | 173 | 174 | 121 | 73 | 138 | 229 | 146 | 38 | 11 | 90 |
| **4.00** | 27 | 65 | 130 | 67 | 95 | 113 | 64 | 101 | 196 | 189 | 94 | 13 | 90 |
| **5.00** | 65 | 84 | 68 | 139 | 95 | 89 | 75 | 133 | 93 | 121 | 66 | 19 | 87 |
| **6.00** | 88 | 110 | 55 | 72 | 55 | 45 | 84 | 78 | 64 | 112 | 45 | 25 | 83 |
| **7.00** | 96 | 152 | 53 | 22 | 48 | 48 | 65 | 72 | 56 | 41 | 38 | 66 | 91 |
| **8.00** | 116 | 154 | 62 | 61 | 83 | 4 | 76 | 66 | 57 | 53 | 75 | 107 | 99 |
| **9.00** | 156 | 125 | 60 | 17 | 123 | 30 | 107 | 71 | 41 | 67 | 78 | 133 | 98 |
| **10.00** | 85 | 90 | 59 | 22 | 24 | 35 | 101 | 52 | 44 | 45 | 134 | 125 | 77 |
| **11.00** | 144 | 56 | 34 | 0 | 24 | 13 | 83 | 34 | 38 | 24 | 66 | 114 | 59 |
| **12.00** | 93 | 38 | 28 | 6 | 20 | 15 | 51 | 25 | 27 | 12 | 87 | 120 | 44 |
| **13.00** | 53 | 34 | 47 | 0 | 12 | 11 | 41 | 33 | 12 | 5 | 49 | 106 | 36 |
| **14.00** | 23 | 19 | 53 | 6 | 8 | 11 | 25 | 26 | 10 | 0 | 71 | 57 | 24 |
| **15.00** | 13 | 9 | 36 | 0 | 0 | 19 | 20 | 18 | 5 | 0 | 28 | 46 | 15 |
| **16.00** | 8 | 6 | 15 | 0 | 0 | 45 | 7 | 20 | 4 | 0 | 21 | 22 | 10 |
| **17.00** | 5 | 2 | 26 | 0 | 0 | 0 | 5 | 12 | 0 | 5 | 16 | 8 | 6 |
| **18.00** | 5 | 3 | 7 | 0 | 0 | 0 | 6 | 1 | 3 | 0 | 0 | 6 | 3 |
| **19.00** | 0 | 1 | 6 | 0 | 0 | 7 | 0 | 0 | 1 | 5 | 0 | 3 | 1 |
| **20.00** | 0 | 0 | 4 | 0 | 0 | 0 | 0 | 0 | 0 | 0 | 9 | 6 | 1 |
| **21.00** | 2 | 0 | 0 | 0 | 0 | 0 | 0 | 0 | 0 | 0 | 9 | 0 | 1 |
| **22.00** | 0 | 0 | 0 | 0 | 0 | 0 | 0 | 0 | 0 | 0 | 9 | 0 | 0 |
| **23.00** | 0 | 0 | 0 | 0 | 0 | 0 | 0 | 0 | 0 | 5 | 0 | 3 | 0 |
| **24.00** | 0 | 0 | 0 | 0 | 0 | 0 | 0 | 0 | 0 | 0 | 5 | 0 | 0 |

**Table 3.4: Weibull parameters (A and k), mean wind speed (U) and mean power density (P) for the 12 direction sectors.**

| | 0 | 30 | 60 | 90 | 120 | 150 | 180 | 210 | 240 | 270 | 300 | 330 | Total |
|---|---|---|---|---|---|---|---|---|---|---|---|---|---|
| **A** | 9.6 | 8.3 | 7.8 | 3.5 | 5.2 | 4.0 | 8.4 | 6.7 | 4.9 | 5.1 | 10.4 | 11.1 | 8.0 |
| **k** | 3.13 | 2.62 | 1.62 | 1.29 | 1.54 | 0.97 | 2.38 | 1.56 | 1.31 | 1.37 | 2.52 | 3.31 | 2.14 |
| **U** | 8.58 | 7.36 | 7.00 | 3.21 | 4.69 | 4.08 | 7.48 | 6.02 | 4.55 | 4.65 | 9.26 | 9.95 | 7.09 |
| **P** | 531 | 372 | 512 | 70 | 165 | 271 | 420 | 342 | 196 | 194 | 764 | 806 | 391 |
| **Freq** | 7.4 | 32.2 | 4.5 | 1.5 | 2.2 | 2.3 | 11.0 | 14.5 | 11.7 | 3.5 | 3.6 | 5.4 | 100 |

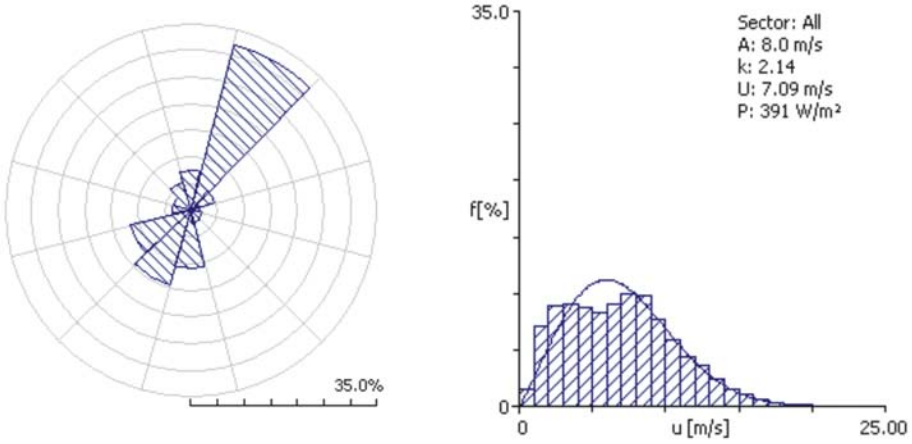


**Figure 3.16: Summary wind rose and Weibull curve for all direction sectors.**

***The Gebbies Pass wind atlas***

Table 3.5 below shows a summary of the wind atlas for the Gebbies Pass region based on the observed wind climate from the Gebbies Pass site. The wind atlas is summarised into the four roughness criteria and four standard heights above ground level.

**Table 3.5: Regional wind atlas summary based on Gebbies Pass observed wind climate.**

| Height | Parameters | 0.00 m | 0.03 m | 0.10 m | 0.40 m |
|---|---|---|---|---|---|
| **10.0 m** | Weibull A [m/s] | 7.3 | 5.0 | 4.4 | 3.5 |
| | Weibull k | 2.24 | 1.91 | 1.91 | 1.93 |
| | Mean speed U [m/s] | 6.42 | 4.47 | 3.90 | 3.08 |
| | Power density P [W/m$^2$] | 279 | 110 | 73 | 35 |
| **25.0 m** | Weibull A [m/s] | 7.9 | 6.0 | 5.4 | 4.6 |
| | Weibull k | 2.31 | 2.04 | 2.03 | 2.04 |
| | Mean speed U [m/s] | 7.03 | 5.35 | 4.81 | 4.06 |
| | Power density P [W/m$^2$] | 357 | 175 | 128 | 77 |
| **50.0 m** | Weibull A [m/s] | 8.5 | 7.0 | 6.4 | 5.5 |
| | Weibull k | 2.36 | 2.26 | 2.22 | 2.20 |
| | Mean speed U [m/s] | 7.55 | 6.18 | 5.64 | 4.90 |
| | Power density P [W/m$^2$] | 435 | 247 | 191 | 126 |
| **100.0 m** | Weibull A [m/s] | 9.2 | 8.3 | 7.6 | 6.7 |
| | Weibull k | 2.30 | 2.39 | 2.42 | 2.47 |
| | Mean speed U [m/s] | 8.19 | 7.33 | 6.73 | 5.91 |
| | Power density P [W/m$^2$] | 566 | 394 | 302 | 202 |
| **200.0 m** | Weibull A [m/s] | 10.2 | 10.3 | 9.4 | 8.1 |
| | Weibull k | 2.19 | 2.30 | 2.33 | 2.39 |
| | Mean speed U [m/s] | 9.04 | 9.10 | 8.30 | 7.22 |
| | Power density P [W/m$^2$] | 794 | 777 | 583 | 376 |

***Self-site analysis and reference data***

Figure 3.16 shows an illustration of the predicted wind climate for the Gebbies Pass site, based on the observed wind climate from the same site (self-site analysis). Through the analysis and application procedure, reference wind direction and annual energy production data has been obtained, as shown in Table 3.6.

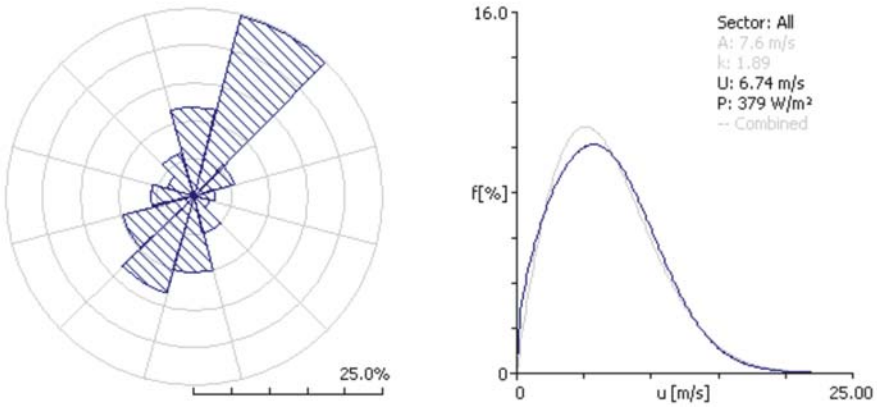


**Figure 3.17: The Weibull curve and wind rose for the self-site prediction at Gebbies Pass.**

**Table 3.6: Reference data for wind direction frequency and annual energy production from the self-site analysis at the Gebbies Pass site.**

| Gebbies Pass 10m reference data (from self-site analysis) | | |
|---|---|---|
| Sector | Direction Frequency (%) | AEP (GWh) |
| 1 | 11.8 | 0.414 |
| 2 | 24.7 | 0.667 |
| 3 | 5.5 | 0.135 |
| 4 | 2.7 | 0.046 |
| 5 | 2.2 | 0.026 |
| 6 | 4.9 | 0.106 |
| 7 | 9.9 | 0.227 |
| 8 | 13.1 | 0.262 |
| 9 | 9.8 | 0.132 |
| 10 | 5.7 | 0.087 |
| 11 | 3.8 | 0.138 |
| 12 | 5.9 | 0.269 |
| Total | 100 | 2.509 |

**Limitations of the self-site analysis and effects on the reference data**

Table 3.7 and Figure 3.17 highlight some differences between the observed and predicted climates for the Gebbies Pass site. These differences occur for WAsP predictions in complex terrain environments, such as in the Gebbies Pass area.

**Table 3.7: Observed and self-site predicted wind direction sector frequency and mean wind speed for the Gebbies Pass site.**

| Gebbies Pass 10m wind self site analysis | | |
|---|---|---|
| Sector | Observed Frequency (%) | Predicted Frequency (%) |
| 1 | 7.4 | 11.8 |
| 2 | 32.2 | 24.7 |
| 3 | 4.5 | 5.5 |
| 4 | 1.5 | 2.7 |
| 5 | 2.2 | 2.2 |
| 6 | 2.3 | 4.9 |
| 7 | 11 | 9.9 |
| 8 | 14.5 | 13.2 |
| 9 | 11.7 | 9.9 |
| 10 | 3.5 | 5.7 |
| 11 | 3.6 | 3.8 |
| 12 | 5.4 | 5.9 |
| Mean speed | 7.09 m $s^{-1}$ | 6.74 m $s^{-1}$ |

There are two main differences between the observed and self-site prediction wind climates — the overall mean wind speed and the frequencies of occurrence in sectors 1 and 2. The predicted mean wind speed is 0.35 m $s^{-1}$ lower than the observed mean wind speed. It is worth considering here that the under-prediction of the mean wind speed by 0.35 m $s^{-1}$ equates to a 16% lower AEP estimate for the reference data (this is based on the assumption that the speed-up ratios are equal for each direction sector).

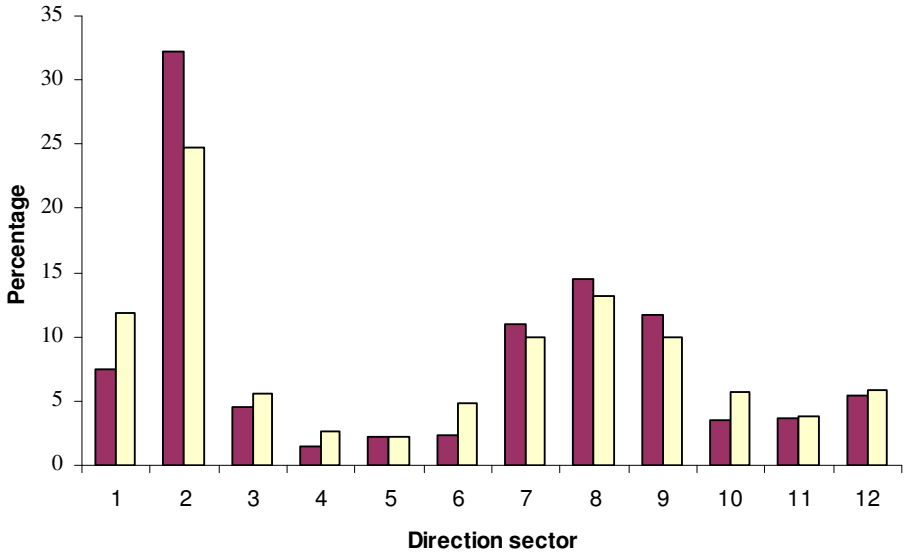


**Figure 3.18: Bar graph illustrating the differences of the observed (red) and predicted (yellow) wind direction frequency for the Gebbies Pass site.**

Two reasons have been identified as to why there are these differences in the observed and self-site predictions. The first is that in the wind atlas analysis and application procedures of WAsP, some winds are falling into neighbouring direction sectors due to the complex terrain environment. This results in different weightings being applied to the speed-up ratios in each sector in the application procedure of the WAsP analysis. Second is that the overall observed wind climate frequency graph for the Gebbies Pass site shows two wind speed maxima (see the histogram in Figure 3.16). Therefore, in its application procedure when WAsP uses the modelled Weibull distribution in its calculations, higher wind speeds for some of the sectors may not have been proportionally accounted for.

**Investigating changing parameters of WAsP to force channelling**

WAsP has a simple procedure that can enhance the effects of channelling airflow and therefore increase the mean wind speed for a site. This can be achieved by adjusting a height inversion parameter, usually set at a default value of 1000 m, and a 'softness' parameter, which is usually set at 1.0.

By reducing the vertical perturbations in WAsP calculations, the horizontal motions can be increased. Enhancement of these horizontal motions effectively increases channelling in a region. By reducing the inversion height in the model, the effects of channelling can be increased and the degree of this enhancement is determined by the softness parameter. Reid

(1997) found that by adjusting these parameters in WAsP analyses for the Wellington and Manawatu regions, mean wind speeds could be increased to the observed values. Reid could not identify any reason for choosing one softness value over another, so 0.5 was adopted for all calculations and different inversion heights were tested.

Because the 10 m above ground level winds at Gebbies Pass were underestimated for the self-site analysis, the inversion height and softness parameters were adjusted to see if there was any effect on the mean wind speed and direction frequency distribution. The effects from changing parameters on the 10 m and 50 m mean wind speeds are given in the Table 3.8.

**Table 3.8: The effect of adjusting the stability parameters on mean wind speed at 10 m and 50 m in the self-site analysis for Gebbies Pass.**

| Softness parameter | Inversion height (m) | 10m mean wind speed ($ms^{-1}$) | 50m mean wind speed ($ms^{-1}$) |
|---|---|---|---|
| *1.0 | *1000 | 6.74 | 7.64 |
| 0.5 | 1000 | 6.74 | 7.60 |
| 0.2 | 1000 | 6.76 | 7.62 |
| 0.0 | 1000 | 6.77 | 7.63 |
| 1.0 | 500 | 6.74 | 7.64 |
| 0.5 | 500 | 6.76 | 7.57 |
| 0.2 | 500 | 6.79 | 7.56 |
| 0.0 | 500 | 6.81 | 7.54 |
| 1.0 | 300 | 6.74 | 7.64 |
| 0.5 | 300 | 6.80 | 7.51 |
| 0.2 | 300 | 6.82 | 7.43 |
| 0.0 | 300 | 6.86 | 7.42 |
| 1.0 | 100 | 6.74 | 7.64 |
| 0.5 | 100 | 6.87 | 7.27 |
| 0.2 | 100 | 6.89 | 7.20 |
| 0.0 | 100 | 6.92 | 7.18 |

*default parameters

Decreasing the softness parameter and inversion height can increase the mean wind speed for the self-site analysis at Gebbies Pass to within 0.17 m $s^{-1}$ of the observed mean when the softness parameter is set to 0.0 and inversion height to 100 m. However, increasing the 10 m

mean wind speed impacted on the mean wind speed at higher levels. For example, the predicted 50 m mean wind speed for the standard WAsP parameters was 7.64 m $s^{-1}$, but this was reduced to 7.18 m $s^{-1}$ when the stability parameters were set at 0.0 and 100 m.

It was also found that reducing the inversion height and softness parameters improved the self-site wind direction frequency results at Gebbies Pass by predicting a higher frequency of winds from the prevailing northeast and southwest direction sectors. This is closer to the observations data wind rose, as shown in Figure 3.19.

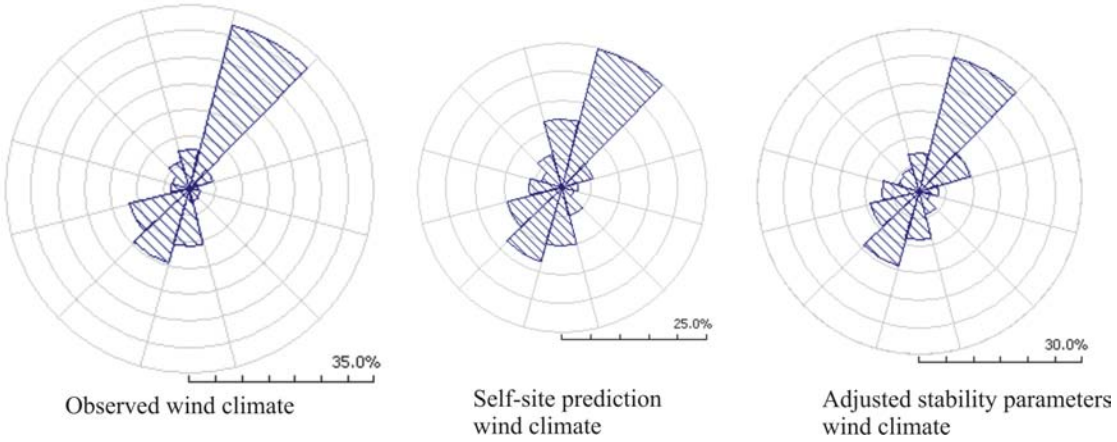


**Figure 3.19: Wind rose diagrams showing comparison of Gebbies Pass observed wind climate, self-site predicted wind climate and adjusted stability parameter (0.0, 100 m) predicted wind climate. All of the wind rose diagrams are for 10 m above ground level.**

Limitations of the reference (validation) data used in this case study have been identified. Some of these limitations can be overcome at 10 m above ground level by adjusting stability parameters used by the WAsP program, but there are implications for how this would affect energy production estimates at higher levels – a key function of WAsP. Applying changes to the stability parameters needs to be done with caution due to the resulting changes of the vertical wind profile. This will have implications on wind and energy predictions at higher levels above the ground. Although it is important to understand these limitations of the WAsP program, further research needs to be done to incorporate changes of the stability parameters in WAsP in regions of complex terrain. It was decided that it was outside the scope of this study to investigate this any further.

## 3.3Methodology Summary

Methodologies for the high and low resolution prognostic modelling were introduced first in this chapter. The validation for the higher resolution prognostic modelling was more comprehensive, using hourly wind data from four sites over the Banks Peninsula region. The combined prognostic and diagnostic modelling methodology involved using both the TAPM and WAsP models to predict wind and energy in areas where there are no reliable wind data. Limitations of the WAsP model were discussed in detail in this chapter. Recognising and understanding the model limitations is important to help overcome and be aware of when errors are likely to occur. Finally reference data was obtained to measure the relative performance of WAsP when using different sources of wind data to make a wind and energy prediction at the Gebbies Pass site.

# Chapter 4

## Results

This chapter is given in two sections, dealing with the prognostic modelling results, and the combined prognostic and diagnostic modelling results, respectively. The prognostic modelling section covers the low and high-resolution modelling separately, with a more rigorous evaluation of the high-resolution modelling. Evaluation of the combined modelling work involves the application of statistical techniques, and uses maps to help illustrate the strengths and weaknesses of the modelling approaches.

### 4.1 Prognostic modelling – low-resolution

Maps of mean wind speed at 50 m above ground level for the Canterbury and Otago regions based on the 2000 m resolution prognostic modelling are provided in Figures 4.1 and 4.2. Associated with each of the maps is a table with predicted 50 m mean wind speeds from The Wind Energy Resource Survey of New Zealand (Cherry, 1987) and estimated mean wind speeds from the maps (Tables 4.1 and 4.2).

**Canterbury region**

There are some obvious patterns identified in the mean wind speed map for the Canterbury region, with stronger mean 50 m winds offshore and in elevated regions to the northwest, and relatively lower mean wind speeds over the Canterbury Plains, and particularly over the Christchurch area. Eastern parts of Banks Peninsula lie within the zone of stronger offshore winds, with a region where mean speed is above 9 m $s^{-1}$ at higher elevations to the east of Akaroa. It is also clear that winds above elevated ridges of Banks Peninsula are stronger than other areas.

In general, the modelled winds were less than those estimated in the Wind Energy Resource Survey study. The difference was less over more homogeneous terrain, such as over the Canterbury Plains. The mean winds speeds over Banks Peninsula are likely to be under-estimated by the model, especially in exposed locations. However, based on wind data obtained for 2002 from Gebbies Pass, it is more likely that the actual 50 m mean wind speed here is closer to 8.8 m $s^{-1}$ (and not the 10.3 m $s^{-1}$ estimated from the Wind Energy Resource Study). Note the low mean wind speeds over Christchurch city, which is accounted for by the higher surface roughness values incorporated into the model. The speed-up of airflow over terrain features is likely to be represented better in the higher resolution modelling.

**Table 4.1: A comparison of 50 m modelled winds for the Canterbury region with estimated 50 m mean wind speeds from the Wind Energy Resource Survey of New Zealand (Cherry, 1987). The sites in the table are identified on the wind map in Figure 4.1.**

| Site | Estimated 50 m 'well exposed' mean wind speed (m $s^{-1}$) | Estimated 50 m mean wind speed from model data (m $s^{-1}$) |
|---|---|---|
| 1. Birdlings Flat | 7.7 | 7.3 |
| 2. Christchurch (Bromley) | 6.0 | 6.4 |
| 3. Darfield | 7.1 | 7.0 |
| 4. Godley Head | 7.7 | 6.7 |
| 5. Gebbies Pass | 10.3 | 7.3 |
| 6. Lincoln College | 7.9 | 7.2 |
| 7. Lyttelton | 6.9 | 6.8 |
| 8. Marleys Hill | 7.3 | 7.4 |
| 9. Mount Herbert | 10.2 | 8.1 |
| 10. Quail Island | 7.4 | 7.1 |
| 11. Rakaia Huts | 7.7 | 7.4 |

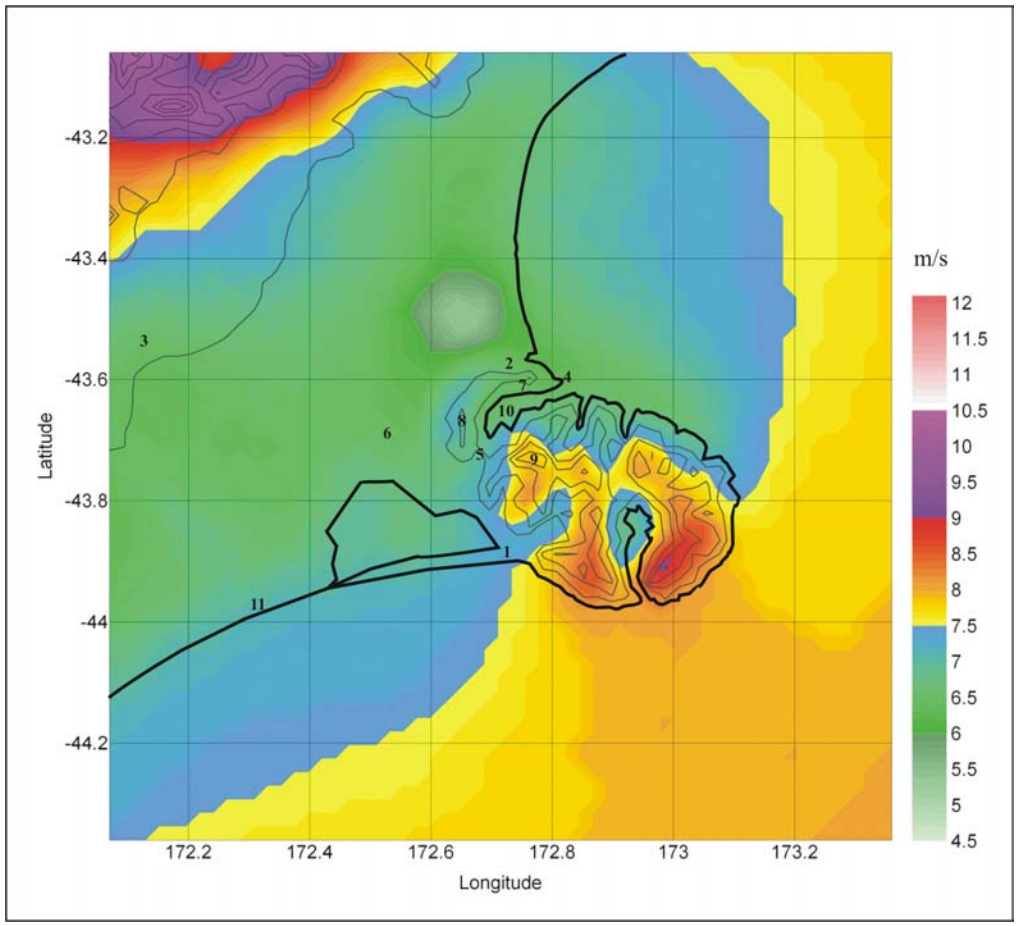


**Figure 4.1: Contour map of mean wind speed at 50 m above ground for the Canterbury region based on hourly average wind speeds for 2002 calculated at 2 km resolution. The elevations contours are at 150 m intervals.**

**Otago region**

The 50 m mean wind speed distribution of the eastern Otago shows a similar pattern to Canterbury, with a belt of relatively strong winds offshore, and with the Otago Peninsula extending into this area. In offshore areas to the southeast, the model predicted mean wind speeds greater than 9 m $s^{-1}$ at 50 m above ground level. The 8.5 m $s^{-1}$ mean wind speed contour extends along the coast south of the Otago Peninsula. Mean wind speeds winds are lower north of the peninsula and in sheltered inland areas. The strongest mean wind speeds for this region are over elevated terrain to the west and northwest of Dunedin, where modelled mean wind speed exceeds 12 m $s^{-1}$ in some places. When comparing this map to the Canterbury region, it is clear that the coastal area south of about the Otago Peninsula is significantly more exposed to low-level synoptic scale flows affecting the South Island. This is illustrated by the 8.5 m $s^{-1}$ mean wind speed contour extending offshore north of the Otago Peninsula. This map also suggests that inland areas of the South Island need to utilise the stronger higher-level winds to make wind energy developments viable.

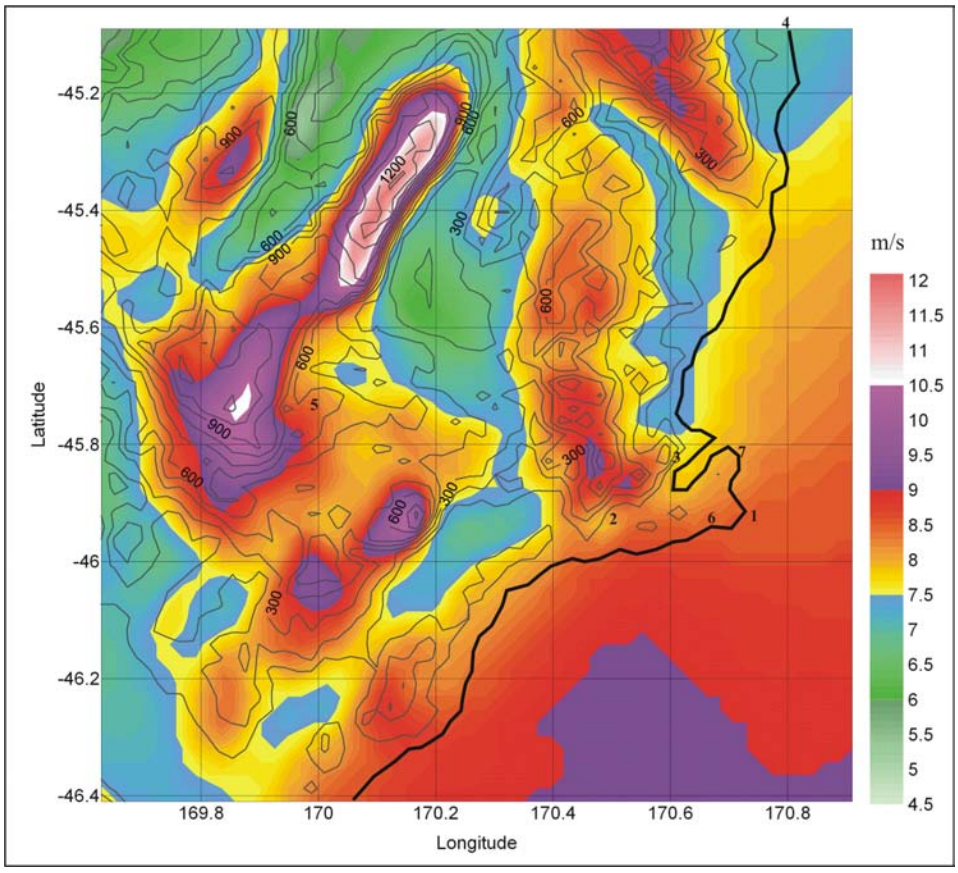


**Figure 4.2: Contour map of mean wind speed at 50 m above ground for the Otago region based on hourly average wind speeds for 2002 calculated at 2 km resolution. The elevations contours are at 100 m intervals.**

From the simple comparisons made here it is evident that the model resolution is not fully accounting for terrain features that give rise to local sheltering and enhancements of the winds in the area. For example, at Dunedin Airport the mean wind speed is likely to be over-estimated by the model due to the sheltering of hills close to this site not being represented accurately by the model. However, the map gives a good overall picture of the wind climate of the region.

There were two regions identified for good wind energy potential in the Wind Energy Resource Survey. These were the Otago Peninsula and Rocklands (an elevated plateau region 40 to 60 km west of Dunedin). The model appears to under-estimating the winds at the three Otago Peninsula sites (Cape Sanders, Sandymount and Taiaroa Heads), while the Rocklands area is better represented. It needs to be reinforced that the modelled wind results and comparisons from the Wind Energy Resource Survey of New Zealand are from very different periods and durations.

**Table 4.2: A comparison of 50 m modelled winds for the Otago region with estimated 50 m mean wind speeds from the Wind Energy Resource Survey of New Zealand (Cherry, 1987). The sites in the table are identified on the wind map.**

| Site | Estimated 50 m 'well exposed' mean wind speed (m $s^{-1}$) | Estimated 50 m mean wind speed from model data (m $s^{-1}$) |
|---|---|---|
| 1. Cape Sanders | 9.0 | 8.5 |
| 2. Dunedin Airport | 6.5 | 7.6 |
| 3. Mount Cargill | 10.0 | 8.0 |
| 4. Oamaru | 6.3 | 6.9 |
| 5. Rocklands | 8.6 | 8.6 |
| 6. Sandymount | 9.8 | 8.5 |
| 7. Taiaroa Head | 8.5 | 8.1 |

## 4.2 Prognostic modelling – high-resolution

The maps in Figure 4.3 illustrate the annual mean wind speeds for the Banks Peninsula region for 2002 at 10 m, 25 m, 50 m, and 100 m above ground level. Although limitations of the modelling process will be discussed below, overall the statistical and wind rose plot comparisons show that at 800 m-resolution the mesocscale modelling provides a good indication of the annual mean wind speed climate for this region. Also, the four map levels provide a useful picture of the mean wind speed increasing with height.

The mean wind speed distribution follows a similar pattern at each level. Stronger wind speeds occur over the higher parts of Banks Peninsula, especially in eastern parts. These areas are exposed to stronger higher-level synoptic winds and are also influenced by speed-up over the large-scale topographic features. These effects appear to be modelled reasonable well by TAPM at 800 m resolution. The maps indicate that the mean wind speed at 50 m above ground level exceeds 9 m $s^{-1}$ at some locations on the ridges east of Mt Herbert, and also over some eastern areas of Banks Peninsula. Large areas of Banks Peninsula experience mean wind speeds above 9 m $s^{-1}$ at 100 m above ground level. At 800 m resolution TAPM is not resolving small-scale features of the topography all that well and as a result the actual mean wind speeds at many sites are likely to be higher than indicated by these results.

The sea area east of Banks Peninsula, especially to the southeast, experiences relatively high wind speeds. Here the model is simulating channelling of the wind around the steep coastal terrain in this area. Also, eastern parts of Banks Peninsula are often exposed to synoptic winds

that have a lesser effect on areas further west, which are sheltered from them. These situations can occur in southwest flows aligned with the South Island when land areas (particularly the Southern Alps) provide sheltering for most areas except along the exposed eastern coasts.

The model is also clearly indicating regions of low mean wind speed. These areas tend to be away from the coast or in sheltered valleys and harbours on Banks Peninsula. The lower relative wind speeds over the Christchurch city area (in the northwest of the map area) result from the higher surface roughness values assigned to the model.

Some inconsistencies can be seen in the wind speed contours close to the map boundary. It is most likely that these inconsistencies are a result of the Kriging interpolation method used when generating contours using a larger number of grid points. The same inconsistency is not seen in the low-resolution wind maps, even though the same interpolation method is used.

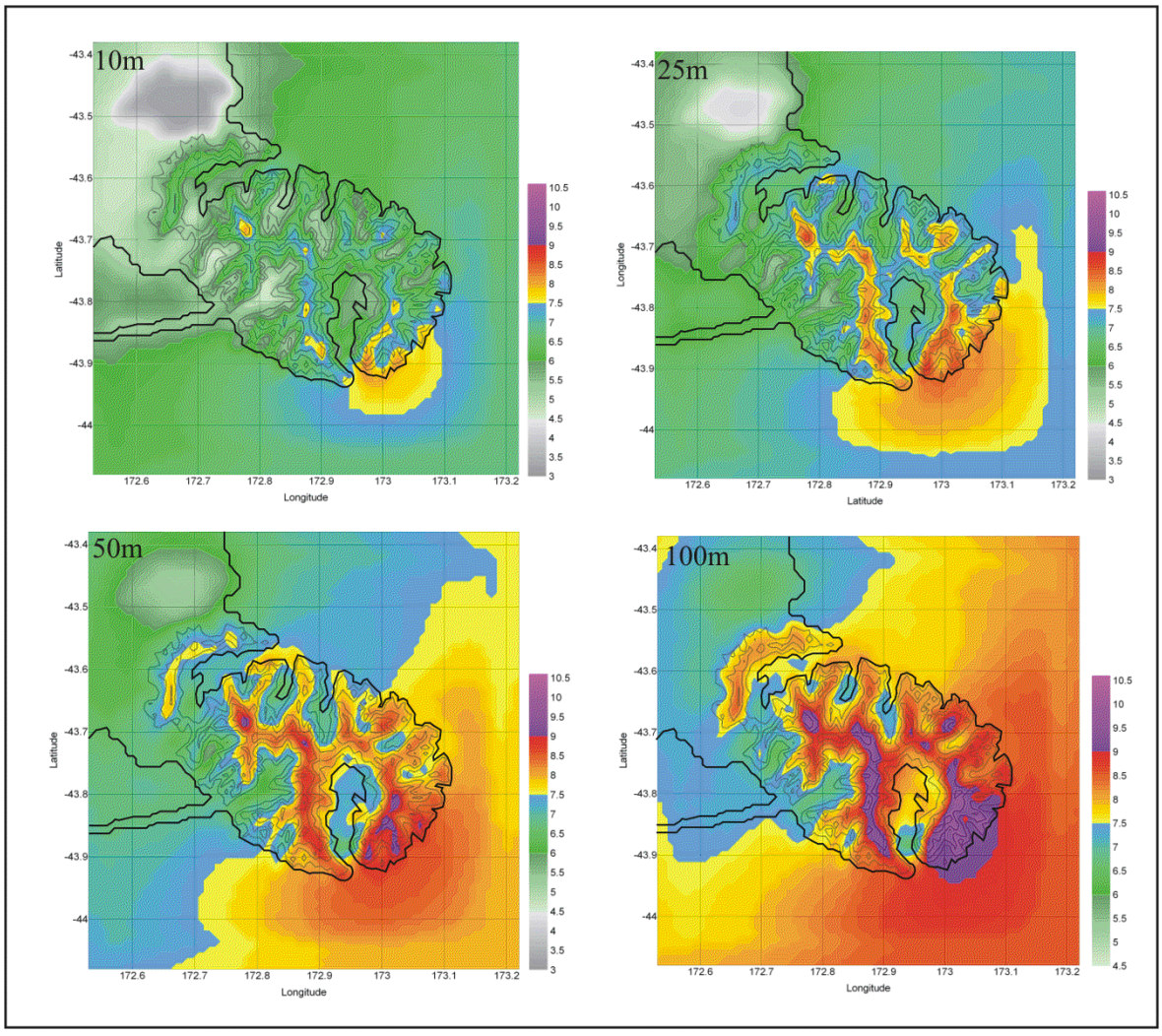


**Figure 4.3: Contour analyses for Banks Peninsula based on the 800 m-resolution model runs for 10 m, 25 m, 50 m and 100 m above ground level.**

### 4.2.1 High-resolution prognostic model evaluation

Wind rose plots and a statistical validation summary are used to evaluate the performance of the model output and the reliability of the wind maps shown in Figure 4.3.

**Comparison of wind rose plots - validation at a glance**

Wind rose plots are given for the four validation sites in Figures 4.4, 4.5, 4.6 and 4.7. Although the wind rose diagrams do not indicate the frequency of the speed of winds for each sector, this information was gained from another wind rose plotting program and therefore some reference will be made to this in the discussions below.

**Christchurch Airport**

The observed wind rose shows a prevailing wind direction from the northeast and a secondary maximum frequency from the southwest (Figure 4.4). Although the modelled wind rose shows a similar pattern, with higher frequency of winds from the northeast and southwest, the prevailing direction is from the southwest quadrant.

The model over-predicts winds from the westerly quarter. This is likely due to TAPM's inability to accurately simulate some situations that produce northeast winds over the coastal Canterbury region. These situations can arise during stable westerly flows, when the existence of an orographic trough east of the Southern Alps can maintain northeast winds near the coast. Northeast sea breezes during summer in westerly type situations may also be under-represented by the model. Other wind directions have a similar observed and modelled frequency distribution, although the model was over-predicting stronger winds from the west/northwest directions.

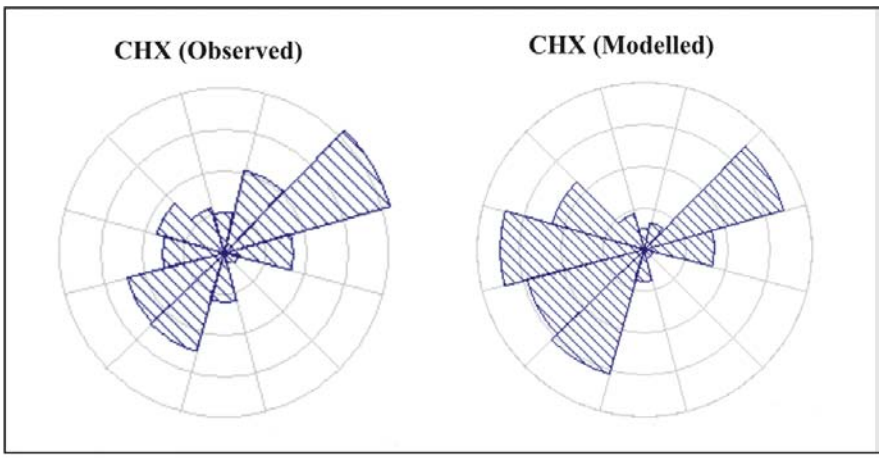


**Figure 4.4: Comparison of the observed and TAPM modelled winds for Christchurch Airport for all of 2002.**

**Gebbies Pass**

The Gebbies Pass observed wind rose shows a distinct wind direction maximum from the northeast (Figure 4.5). The prevailing northeast winds in this region and the channelling of other northerly component flows by Lyttelton Harbour cause this maximum to occur. There is also a secondary maximum frequency of winds from the south and southwest. The modelled wind rose shows that TAPM accounts for some of the channelling effects at Gebbies Pass, but there is a significant under-representation of winds from the northeast. This is probably due to the same reasons as discussed earlier for Christchurch Airport.

When animating the 10 m modelled wind field, it was observed that northeast flows were sometimes deflected around Banks Peninsula and up Gebbies Pass as a southwest wind. In reality, this is not likely to occur due to the known enhancement of northeast wind in that area. The model was also under-predicting stronger winds from the northwest and north.

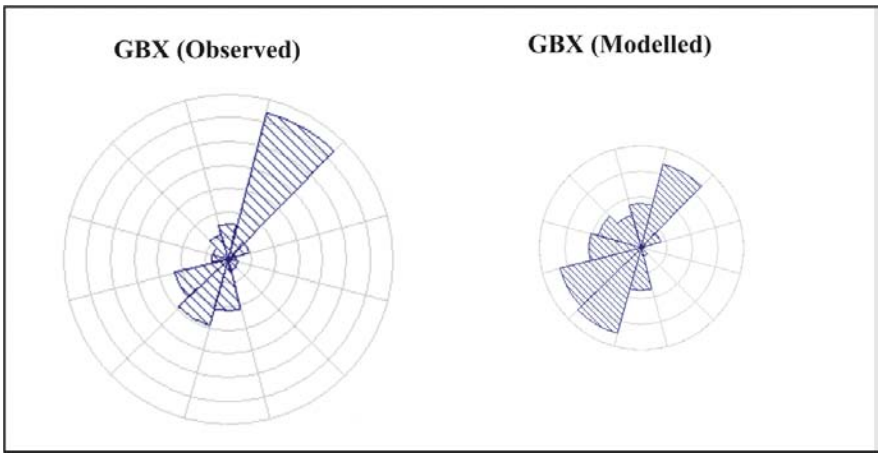


**Figure 4.5: Comparison of the observed and TAPM modelled winds for Gebbies Pass for the period 1 May 2002 to 31 December 2002.**

**McQueens Valley**

Although the McQueens Valley site is close to Gebbies Pass, it seems that TAPM better represented the wind regimes at this site (Figure 4.6). This is likely to be due to less influence from local channelling and better exposure to higher level synoptic scale flows. The observed and modelled wind rose diagrams are similar, with maximum frequencies from the northeast and southerly directions. The model does under-predict winds from the north and there is also a lower frequency of stronger winds from the north and south sectors.

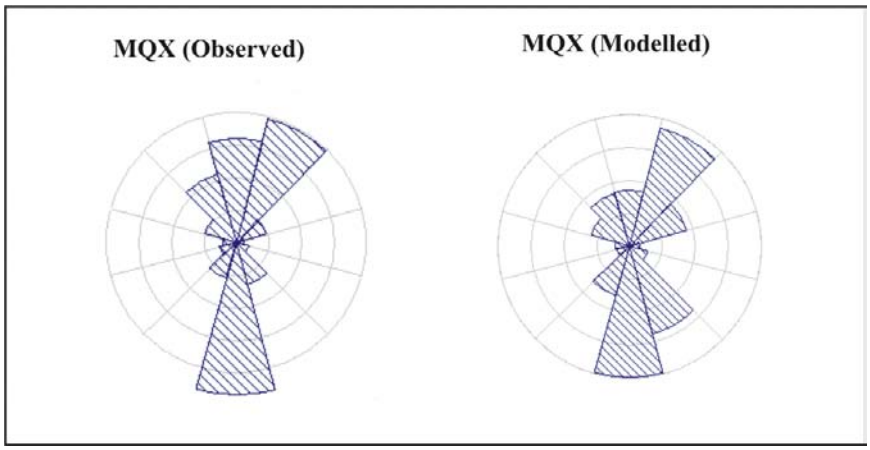


**Figure 4.6: Comparison of observed and TAPM modelled winds for the McQueens Valley site for the period 1 January to 31 March 2002.**

**Le Bons Bay**

The Le Bons Bay observed wind climate is characterised by two maxima in the direction frequency, from the north to northwest and southwest sectors (Figure 4.7). These maxima are most likely due to the forcing of wind around the eastern side of Banks Peninsula from both directions. The modelled wind rose indicates that TAPM is not consistently resolving these terrain-forced effects of winds from the northerly direction. This dominance of northerly

airflow is likely to occur in west or even southwest type synoptic situations, when resulting winds can be driven by regional-scale pressure gradients to produce a northerly component wind. The model simulated strong wind frequencies well for the southwest sector, but there were a conservative number of such events from the northerly quarter.

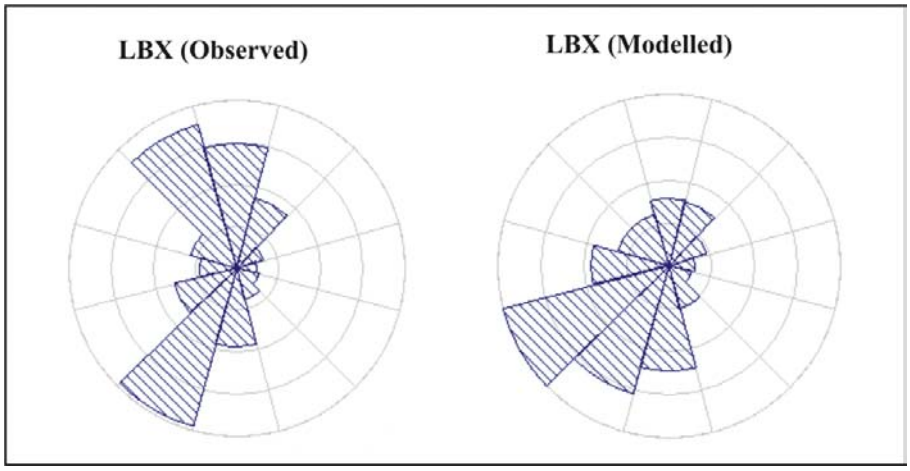


**Figure 4.7: Comparison of observed and TAPM modelled winds for Le Bons Bay for all of 2002.**

**Table 4.3: Summary statistics for TAPM simulations over varying periods of 2002 for four validation sites in the Banks Peninsula region**

| **WIND SPEED (m $s^{-1}$)** | | | | | | | | | | |
|---|---|---|---|---|---|---|---|---|---|---|
| SITE | NUM_OBS | MEA_OBS | MEA_MOD | STD_OBS | STD_MOD | CORR | RMSE | RMSE_S | RMSE_U | IOA |
| CHX | 8283 | 4.3 | 4.8 | 2.7 | 3.1 | 0.55 | 2.81 | 1.10 | 2.58 | 0.73 |
| LBX | 8481 | 6.7 | 6.1 | 4.8 | 3.3 | 0.58 | 3.98 | 2.98 | 2.65 | 0.73 |
| MQX | 2051 | 7.4 | 5.5 | 4.0 | 2.8 | 0.52 | 3.98 | 3.21 | 2.35 | 0.66 |
| GBX | 5810 | 6.9 | 5.6 | 3.7 | 3.0 | 0.48 | 3.26 | 2.05 | 2.16 | 0.74 |
| AVERAGE | 6272 | 6.1 | 5.5 | 3.8 | 3.0 | 0.55 | 3.59 | 2.43 | 2.53 | 0.71 |
| | | | | | | | | | | |
| **U-COMPONENT OF WIND (m $s^{-1}$)** | | | | | | | | | | |
| SITE | NUM_OBS | MEA_OBS | MEA_MOD | STD_OBS | STD_MOD | CORR | RMSE | RMSE_S | RMSE_U | IOA |
| CHX | 8283 | -0.1 | 1.7 | 3.8 | 4.4 | 0.65 | 3.91 | 2.04 | 3.33 | 0.77 |
| LBX | 8481 | 2.2 | 2.8 | 3.9 | 4.1 | 0.66 | 3.36 | 1.42 | 3.05 | 0.81 |
| MQX | 2051 | -0.3 | -1.3 | 3.6 | 3.0 | 0.66 | 2.92 | 1.48 | 2.52 | 0.80 |
| GBX | 5810 | 0.1 | 1.7 | 4.2 | 3.9 | 0.52 | 4.63 | 2.49 | 4.03 | 0.70 |
| AVERAGE | 6272 | 0.6 | 1.1 | 3.8 | 3.8 | 0.66 | 3.40 | 1.65 | 2.97 | 0.79 |
| | | | | | | | | | | |
| **V-COMPONENT OF WIND (m $s^{-1}$)** | | | | | | | | | | |
| SITE | NUM_OBS | MEA_OBS | MEA_MOD | STD_OBS | STD_MOD | CORR | RMSE | RMSE_S | RMSE_U | IOA |
| CHX | 8283 | -0.2 | 0.1 | 3.3 | 3.3 | 0.72 | 2.50 | 1.00 | 2.29 | 0.84 |
| LBX | 8481 | -0.1 | 2.0 | 6.9 | 4.5 | 0.83 | 4.59 | 3.83 | 2.53 | 0.84 |
| MQX | 2051 | -1.5 | 1.1 | 7.5 | 4.9 | 0.82 | 4.62 | 3.59 | 2.91 | 0.86 |
| GBX | 5810 | -1.5 | 0.2 | 6.4 | 4.6 | 0.73 | 5.22 | 3.48 | 3.29 | 0.78 |
| AVERAGE | 6272 | -0.6 | 1.1 | 5.9 | 4.2 | 0.79 | 3.90 | 2.80 | 2.58 | 0.85 |

**KEY:**

OBS=Observations
MOD=Model Predictions
MEAN=Arithmetic mean
STD=Standard Deviation
CORR=Pearson Correlation Coefficient (0=no correlation,1=exact correlation)
RMSE=Root Mean Square Error
RMSE_S=Systematic Root Mean Square Error
RMSE_U=Unsystematic Root Mean Square Error
IOA=Index of Agreement (0=no agreement, 1=perfect agreement)

This discussion is based on the wind rose plot comparisons and summary statistics for the four validation sites illustrated in Table 4.3. The Canterbury region is a difficult place to model mesoscale airflow[9]. Large-scale topographic features such as the Southern Alps, Banks Peninsula and Cook Strait impact on the airflow patterns over the entire Canterbury region. Interactions of the effects of these topographic features on the wind fields are complex and are also influenced by spatial variations of atmospheric stability and the scale of weather systems. The simulation of mesoscale wind flows over the complex region of Banks Peninsula is therefore a challenging task.

Table 4.3 shows that the modelled mean wind speeds are lower than the actual mean wind speeds at all three sites in complex terrain by 0.6 m $s^{-1}$ at LBX, 1.9 m $s^{-1}$ at MQX and 1.3 m $s^{-1}$ for GBX. However, the modelled wind speed is higher than the actual mean wind speed at CHX by 0.5 m $s^{-1}$. This indicates that the model is not resolving the finer scale features that cause speed-up effects at sites in complex terrain, which is to be expected for 800 m-grid spacing. In particular, there are limitations in accounting for the significant channelling effects that occur at the MQX and GBX sites. The high modelled mean wind speed at CHX may be due to the under-estimation of the frequency of winds from the northeast direction, as these will be influenced by higher surface roughness used to represent the Christchurch city area to the east and northeast of the CHX site.

The standard deviation of the hourly winds is higher for the actual winds at the sites in complex terrain due to the smoothing of airflow patterns in time and space by the model at 800 m-grid spacing. This 'dampening' of wind speed can be illustrated by the sample mean wind speed time series graph for Le Bons Bay for a 10-day period (Figure 4.8). The graph shows that the general trend for the predicted wind speed is simulated reasonably well, but the extreme high and low wind speed events tend to be smoothed out. This graph also suggests that in general the model is under-estimating the wind speeds in this complex environment. This time series example is typical for wind speed, and the u and v vector components at all of the validation points, especially those located in complex terrain. When the topography resolution of the model is given at 800 m resolution, the model is unlikely to resolve local variations in the airflow caused small-scale topographic features.

Overall, the IOA scores in table 4.3 are very good with an average of 0.71, 0.79 and 0.85 for wind speed and u and v components respectively. (Emery et al., 2001) suggests that IOA

[9] Steve Reid NIWA pers. comm. Dec 11 2003.

scores above 0.6 indicate good model performance. The correlation coefficients also show a moderately strong relationship between modelled and actual winds, although the v-component relationship is stronger. The IOA for the v-component winds are very high (average of 0.85), showing that the model is resolving north-south component winds well. This is due to less of an effect of topography features, at both a local and regional scale, than for east-west component winds. From the component winds, TAPM over-predicts the westerly winds at CHX and GBX, while MQX is biased towards the easterly component, and there is an over-prediction of winds from the south, especially at the sites in complex terrain.

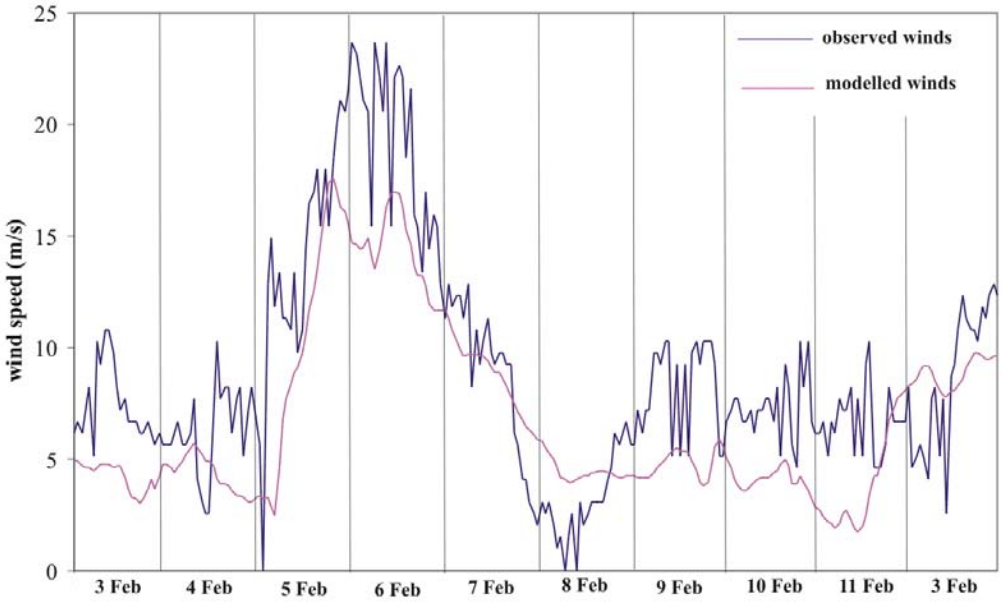


**Figure 4.8: Time series graph of hourly observed and modelled wind speeds for Le Bons Bay (LBX) for a 10-day period during February 2002.**

The RMSE values shown in Table 4.3 tend to be higher at the complex sites, although the RMSE is also large for the u-component at CHX. As suggested in (ENVIRON, 2004), RMSE values can be easily distorted by the heavy weighting (from squaring) of a relatively few but large differences between actual and modelled values. This can easily occur when attempting to model winds in complex terrain. The systematic and unsystematic error components of the RMSE are generally similar, indicating that the model errors are caused by a combination of the effects described in the definitions of $RMSE_s$ and $RMSE_u$. $RMSE_s$ errors might be reduced through improvements of the model input or use of different grid nesting, or use of more appropriate model options, while the $RMSE_u$ results from factors such as the requirement of new algorithms, or higher resolution grids, or that the phenomena being simulated cannot be fully resolved by the model. However, the $RMSE_u$ values for the u-

component are generally high, suggesting that a significant proportion of model errors here are caused by factors that cannot be accurately resolved by the model.

Considering the complexity of the terrain of Banks Peninsula and wider region, TAPM appears to have done reasonably well to simulate the wind climates at the four sites for 2002. However, based on the actual and modelled mean wind speed comparisons at MQX and GBX, the model does not adequately resolve the channelling effects. This is likely to be due to the few number of grid points (at 800 m-grid spacing) that represent the topography. Modelling at a higher resolution would improve the ability of the model to resolve channelling effects in the Gebbies Pass area or other valleys and harbours of similar dimensions. However, it was found that TAPM became unstable when the grid spacing was less than 800 m. Similar model instability has been documented for the MM5 model, when the model became unstable in mountainous terrain at grid resolutions less than 1000 m (Pinard, 1999). However, the use of smaller grid spacing might have reduced the systematic ($RMSE_s$) component of the RMSE.

A report completed by the UK Met Office (Met Office, 2005) suggests that a meteorological model requires 4 - 6 grid points to represent a hill and its effects on airflow patterns. Based on this, at 800 m-grid spacing, topographic features need to have dimensions of 3 - 5 km to be accurately accounted for by TAPM. The widths of most major valley systems on Banks Peninsula are generally less than this, with Gebbies Pass and Lyttelton Harbour being about 2 - 4 km wide. In case studies using the RAMS mesoscale model, results were significantly improved using smaller grid spacing to better represent topography features (Salvador et al., 1999). While areas affected by channelling are likely to have modelled mean wind speeds lower than what is actually measured, the channelling effects at Gebbies Pass are likely to be extreme in this region due to the parallel alignment of the steep topography to the prevailing winds, and also due to the low elevation of the pass and the low surface roughness on either side of the pass.

The wind rose plot comparisons and the statistical analysis both illustrate that a significant limitation of TAPM when modelling airflow patterns in the Banks Peninsula region is an under-prediction of winds from the north at the expense of a higher frequency of winds from the west and southwest. This is likely to be caused by the model not simulating regional scale pressure driven winds that can occur in westerly synoptic situations.

**Applying a correction factor to the wind data**

In the previous validation and discussion of the TAPM modelled wind data, it was shown that overall the model performed reasonably well at the four validation sites, especially considering how complex the airflow patterns are over the Banks Peninsula region. However the model under-estimated the overall mean wind speed at the sites in complex terrain. In fact any mesoscale meteorological model will encounter these problems when attempting to simulate airflow in such complex terrain at a resolution of 800 m. These limitations and reasons why they arise were discussed in the previous section. Based on the results from the validation at the complex terrain sites on Banks Peninsula, and on knowledge of airflow patterns in complex terrain, a proposed correction factor will be discussed as a way to better represent the wind climate at a site.

By recognising when wind data are being affected by model limitations, a correction factor can be applied. In this study the correction factor was obtained by using data output from a higher model level at the site of interest to see how the observed and modelled winds compared. Table 4.4 shows the same statistical analysis as in the previous section but using wind data with a correction applied at the three sites located in complex terrain. The following TAPM model data were used to represent the wind data for the same site at 10 m above ground level:

1. CHX 10 m (no change)
2. LBX 25 m
3. MQX 50 m
4. GBX 50 m.

**Table 4.4: Summary statistics for TAPM simulations over varying periods of 2002 for four validations sites in the Banks Peninsula region, using adjusted model output heights.**

| **WIND SPEED (m $s^{-1}$)** | | | | | | | | | | |
|---|---|---|---|---|---|---|---|---|---|---|
| SITE | NUM_OBS | MEA_OBS | MEA_MOD | STD_OBS | STD_MOD | CORR | RMSE | RMSE_S | RMSE_U | IOA |
| CHX (10 m) | 8283 | 4.3 | 4.8 | 2.7 | 3.1 | 0.55 | 2.81 | 1.10 | 2.58 | 0.73 |
| LBX (25 m) | 8481 | 6.7 | 7.0 | 4.8 | 3.7 | 0.59 | 4.00 | 2.63 | 3.01 | 0.76 |
| MQX (50 m) | 2051 | 7.4 | 7.0 | 4.0 | 3.7 | 0.53 | 3.78 | 2.10 | 3.14 | 0.73 |
| GBX (50 m) | 5810 | 6.9 | 7.0 | 3.7 | 3.7 | 0.53 | 3.39 | 1.72 | 2.82 | 0.71 |
| AVERAGE | 6272 | 6.1 | 6.3 | 3.8 | 3.5 | 0.56 | 3.53 | 1.94 | 2.91 | 0.74 |
| | | | | | | | | | | |
| **U-COMPONENT OF WIND (m $s^{-1}$)** | | | | | | | | | | |
| SITE | NUM_OBS | MEA_OBS | MEA_MOD | STD_OBS | STD_MOD | CORR | RMSE | RMSE_S | RMSE_U | IOA |
| CHX | 8283 | -0.1 | 1.7 | 3.8 | 4.4 | 0.65 | 3.91 | 2.04 | 3.33 | 0.77 |
| LBX | 8481 | 2.2 | 3.3 | 3.9 | 4.6 | 0.66 | 3.74 | 1.41 | 3.46 | 0.79 |
| MQX | 2051 | -0.3 | -1.0 | 3.6 | 4.2 | 0.66 | 3.65 | 0.42 | 3.62 | 0.79 |
| GBX | 5810 | 0.1 | 1.9 | 4.2 | 5.1 | 0.53 | 5.90 | 2.26 | 5.38 | 0.66 |
| AVERAGE | 6272 | 0.6 | 1.3 | 3.8 | 4.4 | 0.66 | 3.76 | 1.29 | 3.47 | 0.78 |
| | | | | | | | | | | |
| **V-COMPONENT OF WIND (m $s^{-1}$)** | | | | | | | | | | |
| SITE | NUM_OBS | MEA_OBS | MEA_MOD | STD_OBS | STD_MOD | CORR | RMSE | RMSE_S | RMSE_U | IOA |
| CHX | 8283 | -0.2 | 0.1 | 3.3 | 3.3 | 0.72 | 2.50 | 1.00 | 2.29 | 0.84 |
| LBX | 8481 | -0.1 | 2.1 | 6.9 | 5.1 | 0.83 | 4.51 | 3.48 | 2.87 | 0.86 |
| MQX | 2051 | -1.5 | 2.0 | 7.5 | 5.8 | 0.82 | 4.96 | 3.42 | 3.59 | 0.87 |
| GBX | 5810 | -1.5 | 0.0 | 6.4 | 5.7 | 0.74 | 5.28 | 2.57 | 4.08 | 0.81 |
| AVERAGE | 6272 | -0.6 | 1.4 | 5.9 | 4.7 | 0.79 | 3.99 | 2.63 | 2.92 | 0.85 |

**KEY:**

OBS=Observations
MOD=Model Predictions
MEAN=Arithmetic mean
STD=Standard Deviation
CORR=Pearson Correlation Coefficient (0=no correlation,1=exact correlation)
RMSE=Root Mean Square Error
RMSE_S=Systematic Root Mean Square Error
RMSE_U=Unsystematic Root Mean Square Error
IOA=Index of Agreement (0=no agreement, 1=perfect agreement)

The following discussion relates to the statistical analysis using the adjusted model output heights in Table 4.4. At the Gebbies Pass and McQueens Valley sites, the 50 m modelled mean wind speed and standard deviation were closer to the observed 10 m mean wind speed and standard deviation. The IOA for the wind speed and vector components were similar to the previous analysis for most of the sites, although the McQueens Valley IOA for wind speed increased from 0.66 to 0.73.

The Le Bons Bay 25 m-modelled winds were more representative of the actual 10 m winds. The mean speed increased from 6.1 m $s^{-1}$ to 7.0 m $s^{-1}$ (the observed mean was 6.7 m $s^{-1}$), while the standard deviation went from 3.1 m $s^{-1}$ to 3.7 m $s^{-1}$ (the observed standard deviation was 4.8 m $s^{-1}$). The IOA has increased for the wind speed and v-component, but was a little lower for the u-component.

A simple correction factor has been proposed to overcome some of the TAPM model limitations when simulating the airflow in a very complex terrain environment. There has been some improvement in the representation of the wind climatology at the 'complex' sites when using the model wind data. However knowledge and experience of airflow over complex terrain and of also of the model limitations in unique locations is essential when applying such corrections.

### 4.2.2 Seasonal variation of mean wind speed

The seasonal variation of the TAPM mean wind speeds over the Banks Peninsula region is given in Figure 4.9. The discussion below will focus on the spatial distribution of mean wind speed for the four seasons of 2002 at 50 m above ground level. Spring months were categorised as the months September, October and November, summer as December to February, autumn as March to May and winter as June, July and August.

The maps provide some interesting spatial patterns in the mean wind speed distribution for different times of the year. It is clear from the top left and bottom right maps in Figure 4.9 that there are stronger winds over higher elevations of Banks Peninsula and over the sea area during the winter and spring periods. This will be due to stronger synoptic flows over New Zealand as the mid-latitude westerlies generally extend further north during these periods. Westerly flows are characterised by increasing wind speed with height, which supports the distribution of areas of stronger mean wind speeds on the maps for these periods.

The winter months also show the lowest mean wind speeds over low elevations, in particular to the northwest of the analysis region. Due to low-level inversion, from either radiative cooling or from strong subsidence at this time of the year, it can sometimes be difficult for synoptic flows to penetrate to the surface at low elevation.

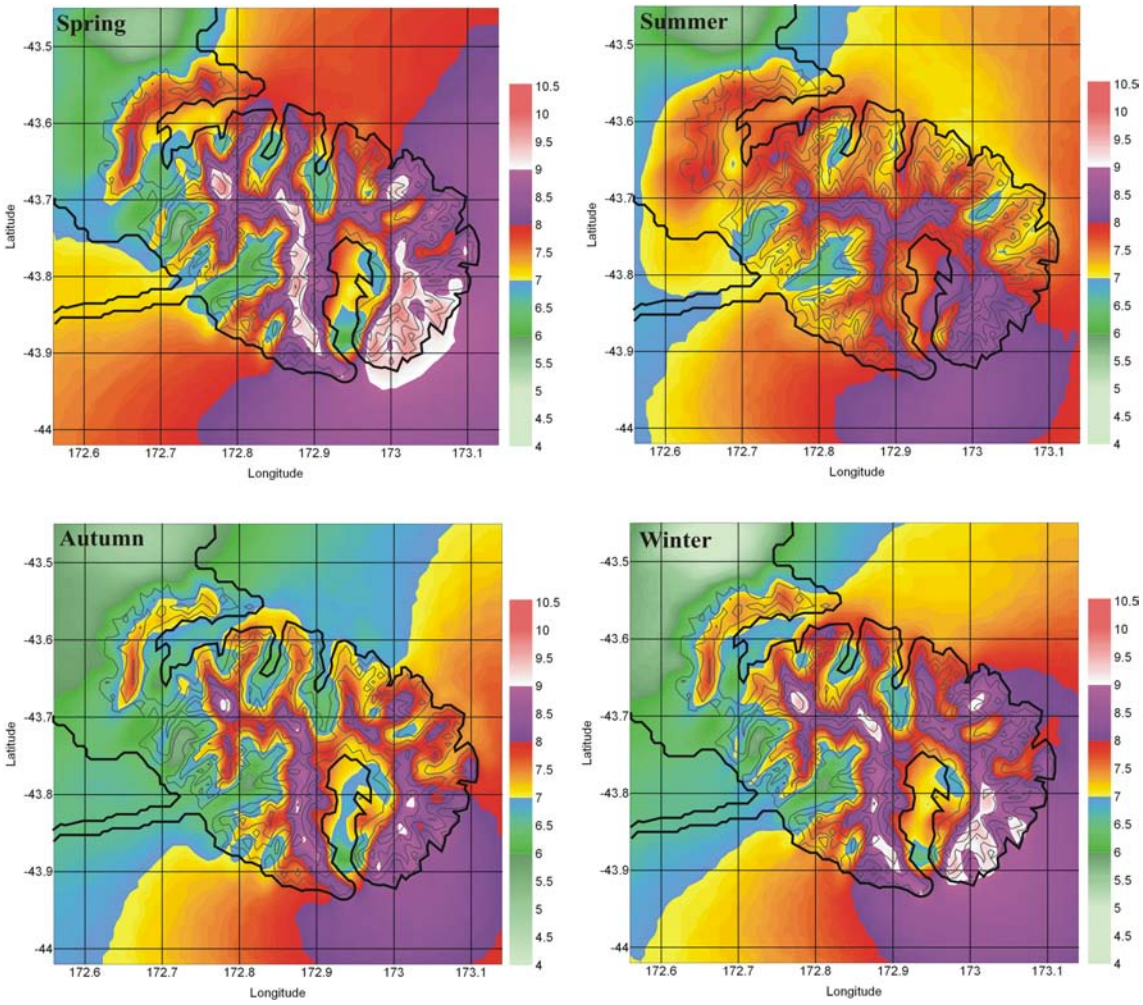


**Figure 4.9: Seasonal wind maps for the Banks Peninsula region for 2002 at 50 m above ground level based on TAPM modelled wind data.**

There is less difference in the relative mean wind speed during the summer months. This is illustrated in the Lyttelton Harbour / Port Hills and Akaroa Harbour areas of the summer map where higher mean wind speeds extend over a wider area and to low elevations. During the summer months there is likely to be less pronounced increasing wind speed with height and low-level winds are likely to be enhanced by the sea breeze over land areas.

## 4.3 Combined diagnostic and prognostic modelling results

The combined diagnostic and prognostic results are presented in three sections. First are the results of the wind and annual energy prediction analyses for the Gebbies Pass site. Here seven regional wind atlases were derived from different wind data and used to make wind and annual energy predictions at the Gebbies Pass wind measuring site. The next section illustrates how using different wind data can affect the spatial distribution of wind and energy predictions over the wider areas about Gebbies Pass. In both of these sections the results of the analyses are compared with the wind and energy predictions derived from the actual wind data from the Gebbies Pass site. Finally the results of an error analysis for the Gebbies Pass map area are presented. As discussed in section 3.2.2, errors in a WAsP analysis can result from a number of factors. The following error analysis is based on the model limitations resulting from the steepness of the terrain.

### 4.3.1 Wind and Energy Prediction Analysis for the Gebbies Pass site

The seven wind atlas files (as described in Section 3.2.6) were used to predict the wind direction frequency of occurrence and annual energy production (AEP) for each sector at the Gebbies Pass site. The results for these analyses and the reference data are given in Tables 4.5 and 4.6. Each sector spans 30° so that sector 1 is from 0 - 30°, sector 2 is from 30 – 060°, sector 11 is from 300 – 330°, etc.

Table 4.5 shows the wind direction frequency of occurrence (as a percentage) resulting from a WAsP analysis when applying the seven wind atlases to the Gebbies Pass site. The mean wind speeds for the Gebbies Pass site resulting from using the wind atlas files are also given. Table 4.6 gives the results of the annual energy production (AEP) for each direction sector when using the seven wind atlas files in a WAsP analysis for the Gebbies Pass site. The total expected AEP are given for each of the analyses in the bottom row of the table. The reference data (from the ‘self-site’ analysis) are given in the first column of the tables.

**Table 4.5: Wind direction frequency of occurrence (%) – the percentage of winds falling into the 12 direction sectors for the seven WAsP analyses. The overall mean wind speeds for each analysis are also given.**

| Site<br>Wind direction sector | Ref. | CHA | LBA | GP10M | GP50M | PHM | SSM | LHIM |
|---|---|---|---|---|---|---|---|---|
| 1 | 11.8 | 5.6 | 8.8 | 10.3 | 9.2 | 7.5 | 5.5 | 7.5 |
| 2 | 24.7 | 7.5 | 5.3 | 14.8 | 13.8 | 10.3 | 7.6 | 9.7 |
| 3 | 5.5 | 14.2 | 3.2 | 4.0 | 4.7 | 6.0 | 6.5 | 7.1 |
| 4 | 2.7 | 11.5 | 3.0 | 1.5 | 2.0 | 2.6 | 5.7 | 4.0 |
| 5 | 2.2 | 4.5 | 4.5 | 0.6 | 0.8 | 0.5 | 4.3 | 1.2 |
| 6 | 4.9 | 2.7 | 6 | 3.4 | 3.8 | 3.2 | 3.1 | 3.4 |
| 7 | 9.9 | 5.4 | 8.2 | 8.6 | 8.7 | 9.7 | 4.3 | 8.3 |
| 8 | 13.2 | 7.9 | 11 | 13.9 | 13.6 | 16.2 | 6.4 | 13.3 |
| 9 | 9.9 | 10.4 | 9.7 | 14.1 | 13.7 | 13.1 | 12.6 | 14.4 |
| 10 | 5.7 | 10.4 | 8.9 | 11.6 | 11.8 | 11.2 | 19 | 12.8 |
| 11 | 3.8 | 12.8 | 14.2 | 9.6 | 10.5 | 10.6 | 18.3 | 10.8 |
| 12 | 5.9 | 7 | 17.2 | 7.6 | 7.4 | 9 | 6.8 | 7.2 |
| Mean ($m\ s^{-1}$) | 6.74 | 8.38 | 6.65 | 5.29 | 6.71 | 7.02 | 10.11 | 6.87 |

**Table 4.6: Annual energy production sector totals (GWh) - total annual energy production and by wind direction sector for the seven WAsP analyses. The reference data is in the second column.**

| Site<br>Wind direction sector | Ref | CHA | LBA | GP10M | GP50M | PHM | SSM | LHIM |
|---|---|---|---|---|---|---|---|---|
| 1 | 0.414 | 0.096 | 0.088 | 0.111 | 0.174 | 0.183 | 0.215 | 0.155 |
| 2 | 0.667 | 0.121 | 0.038 | 0.208 | 0.345 | 0.224 | 0.204 | 0.213 |
| 3 | 0.135 | 0.553 | 0.019 | 0.092 | 0.196 | 0.082 | 0.094 | 0.19 |
| 4 | 0.046 | 0.507 | 0.013 | 0.029 | 0.069 | 0.023 | 0.059 | 0.101 |
| 5 | 0.026 | 0.169 | 0.023 | 0.001 | 0.005 | 0 | 0.027 | 0.024 |
| 6 | 0.106 | 0.096 | 0.086 | 0.025 | 0.056 | 0.099 | 0.031 | 0.084 |
| 7 | 0.227 | 0.231 | 0.218 | 0.123 | 0.205 | 0.328 | 0.09 | 0.245 |
| 8 | 0.262 | 0.319 | 0.403 | 0.259 | 0.386 | 0.515 | 0.18 | 0.405 |
| 9 | 0.132 | 0.308 | 0.334 | 0.224 | 0.367 | 0.297 | 0.537 | 0.379 |
| 10 | 0.087 | 0.273 | 0.274 | 0.169 | 0.297 | 0.261 | 1.215 | 0.326 |
| 11 | 0.138 | 0.548 | 0.495 | 0.115 | 0.231 | 0.31 | 1.32 | 0.275 |
| 12 | 0.269 | 0.239 | 0.453 | 0.054 | 0.104 | 0.281 | 0.412 | 0.146 |
| Total AEP | 2.509 | 3.46 | 2.444 | 1.41 | 2.435 | 2.603 | 4.384 | 2.543 |

Tables 4.7, 4.8, 4.9 and 4.10 show the results of the absolute mean error (AME) and root mean square error (RMSE) statistical analyses for the seven wind atlas files used in the WAsP prediction of the wind climate and annual energy production at the Gebbies Pass site. As described in Section 3.2.7, these tables combine all of the errors from each of the 12 direction sectors for each of the wind atlas files used to make the predictions. The AME and RMSE statistics will provide evidence of the relative accuracy of the wind climate predictions for Gebbies Pass when using the seven different wind atlas files, compared to the reference data that was obtained from the 'self-site' analysis for the Gebbies Pass site. (The 'self-site' analysis used observed wind data from the Gebbies Pass site see Section 3.2.8; Obtaining reference data). The smaller the AME and RMSE values, the closer the prediction is to the reference data.

Table 4.8 and 4.10 use adjusted AEP reference data values to base the AME and RMSE statistics on for the seven wind atlas files. The use of this correction was applied because in the 'self-site' analysis of the Gebbies Pass site to obtain the reference data, there was a 16 % under-prediction in the mean wind speed (see Section 3.2.8). The adjusted AEP values were used to determine if it would significantly change the results of the analysis based on the non-adjusted reference data.

**Table 4.7: Summary absolute mean error (AME) statistics for each of the wind atlas files used to make a wind and energy prediction for the Gebbies Pass site against the AEP reference data.**

| Site | Direction AME | Rank | AEP AME | Rank |
|---|---|---|---|---|
| CHA | 6.68 | 6 | 0.230 | 6 |
| LBA | 6.10 | 5 | 0.184 | 5 |
| GP10M | 3.77 | 1 | 0.121 | 1 |
| GP50M | 3.85 | 2 | 0.131 | 2 |
| PHM | 4.16 | 3 | 0.138 | 3 |
| SSM | 6.91 | 7 | 0.332 | 7 |
| ILHM | 4.56 | 4 | 0.146 | 4 |

**Table 4.8: Summary AME statistics for each of the wind atlas files used to make a wind and energy prediction for the Gebbies Pass site against the adjusted AEP reference data.**

| Site | AEP (+16%) AME | Rank |
|---|---|---|
| CHA | 0.237 | 6 |
| LBA | 0.197 | 5 |
| GP10M | 0.145 | 2 |
| GP50M | 0.139 | 1 |
| PHM | 0.146 | 3 |
| SSM | 0.341 | 7 |
| ILHM | 0.152 | 4 |

**Table 4.9: Summary of the root mean square error (RMSE) statistics for each of the wind atlas files used to make a wind and energy prediction for the Gebbies Pass site against the AEP reference data.**

| Site | Direction RMSE | Rank | AEP RMSE | Rank |
|---|---|---|---|---|
| CHA | 7.36 | 5 | 0.295 | 6 |
| LBA | 7.37 | 6 | 0.254 | 5 |
| GP10M | 4.08 | 2 | 0.179 | 2 |
| GP50M | 4.38 | 1 | 0.163 | 1 |
| PHM | 5.30 | 3 | 0.186 | 3 |
| SSM | 8.28 | 7 | 0.512 | 7 |
| ILHM | 5.60 | 4 | 0.194 | 4 |

**Table 4.10: Summary RMSE statistics for each of the wind atlas files used to make a wind and energy prediction for the Gebbies Pass site against the adjusted AEP reference data.**

| Site | AEP (+16%) RMSE | Rank |
|---|---|---|
| CHA | 0.311 | 6 |
| LBA | 0.280 | 5 |
| GP10M | 0.214 | 3 |
| GP50M | 0.185 | 1 |
| PHM | 0.207 | 2 |
| SSM | 0.517 | 7 |
| ILHM | 0.217 | 4 |

The absolute mean error (AME) and root mean square error (RMSE) statistics for the wind direction frequency of occurrence and annual energy production (AEP) were used to determine what wind data (seven wind datasets were considered in this study) are best used in a WAsP analysis at the Gebbies Pass site in the absence of actual data. The statistical analysis used the reference data from a 'self-site' analysis at Gebbies Pass (using observed wind data) and predicted results for wind direction frequency of occurrence and AEP for the twelve 30-degree direction sectors. The overall mean wind speed and AEP in each analysis also need to be considered.

The statistics show that the TAPM modelled data from the grid point closest to the Gebbies Pass site gave the best predictions. Using GP10M and GP50M wind data consistently gave the least error for the wind direction frequency of occurrence and for AEP. The 10 m above ground modelled wind climate (GP10M) gave the least error for wind direction frequency for both statistics, while the best results for AEP were from GP10M for the AME statistics and GP50M for the RMSE statistic. Tables 4 and 6 used AEP reference data that had been increased by 16% to account for the 5% under-prediction in the mean wind speed in the self-site analysis. When this reference data was used in the statistical analyses, both the AME and RMSE errors were least for the GP50M wind data sets. Using the wind atlas derived from GP50M wind data also gives the best overall estimates of the mean wind speed and AEP, as shown in the bottom rows of Tables 4.5 and 4.6

In general, the further away the wind data were derived from the Gebbies Pass site, using either actual or modelled wind data, the less accurate the prediction of the wind climate at the Gebbies Pass site. This is illustrated by the relatively large statistical errors generated when using CHA, LBA and SSM wind data. Tables 4.5 and 4.6 show that the predicted mean wind speeds (and hence the total AEP) when using wind data from CHA and SSM were very high.

Therefore, when considering the overall mean wind speed, the total AEP production estimate, and the statistical comparisons, the wind dataset obtained from TAPM at the closest grid point to the prediction site but with a correction factor applied (using a model output level 50 m above the ground) was the best representation of the 10 m wind climate to use in the WAsP model (in absence of actual wind data).

### 4.3.2 Wind and energy resource map comparisons

The following wind and annual energy production (AEP) maps illustrate the effects of using wind data from difference sources when performing a wind energy resource analysis for the Gebbies Pass area (Figure 4.10). The following wind data were used in each of the map:

1. Gebbies Pass actual winds. These were used to generate reference data used in the previous section. These wind and energy maps should provide the 'best' analysis for the Gebbies Pass area.

2. TAPM 10 m winds from a grid point near the Gebbies Pass site. This is considered the best wind data source when there is no actual or reliable wind data from near the area of interest. This wind dataset was referred to as GP10M in the previous section.

3. Christchurch Airport winds (CHA). These wind data are likely to have been used in such an analysis if there had been no actual wind data available.

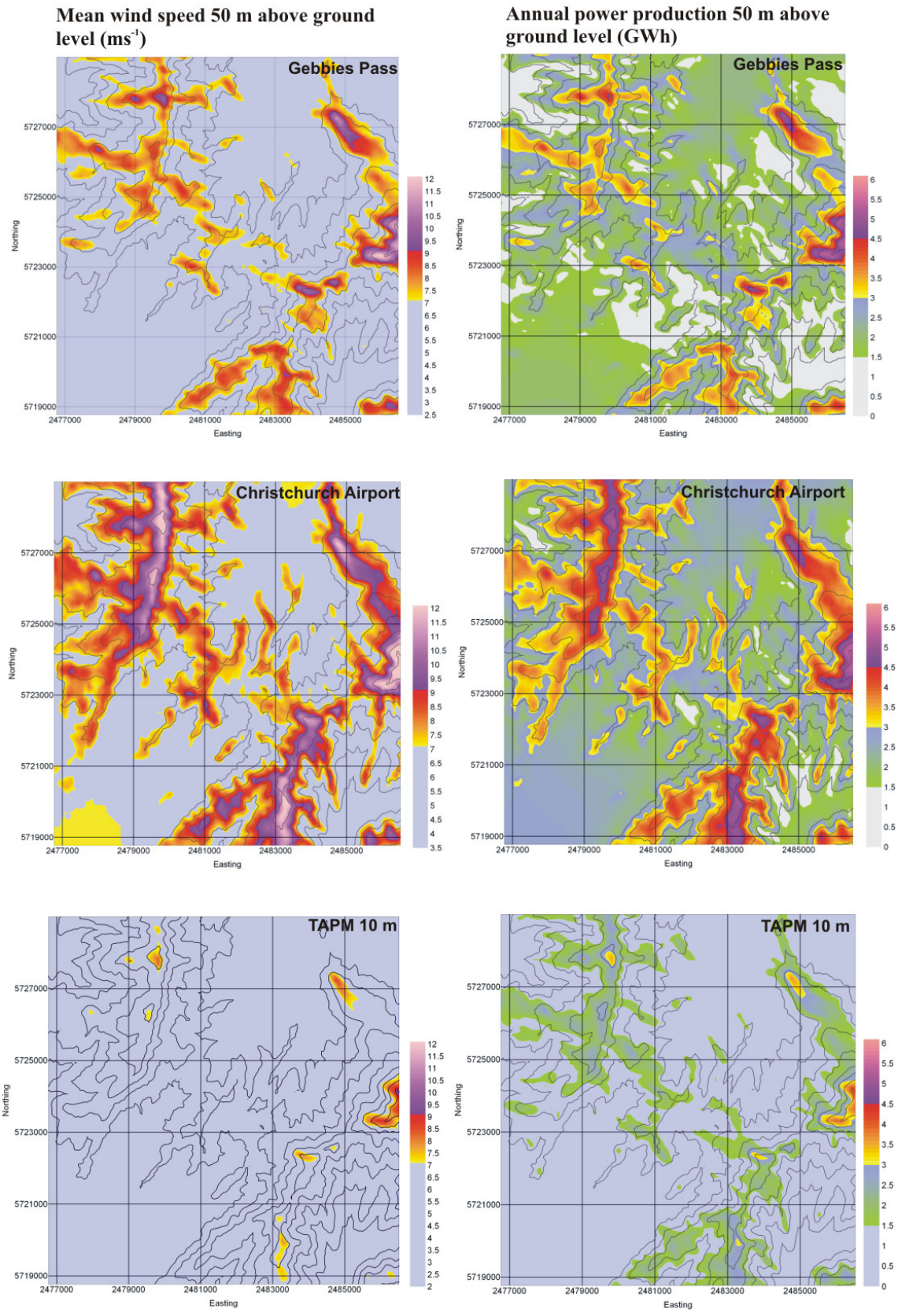


**Figure 4.10: Mean wind speed and AEP resource maps for the Gebbies Pass area using the three different wind data sources.**

Compared to the maps based on the Gebbies Pass actual winds (top two maps in Figure 4.10), the maps derived from the TAPM 10 m wind data (bottom two maps) indicate significantly lower mean wind speed and AEP predictions over the map area. This is due to the low mean wind speed predicted by the TAPM model in the Gebbies Pass areas because of the limitations of the mesoscale model to accurately simulate the channelling effects at the scale it occurs in this area. As would be expected from the results using the CHA to predict the wind climate at Gebbies Pass, the maps derived using the Christchurch Airport winds (middle two maps in Figure 4.10) over-predict the mean wind speed and AEP.

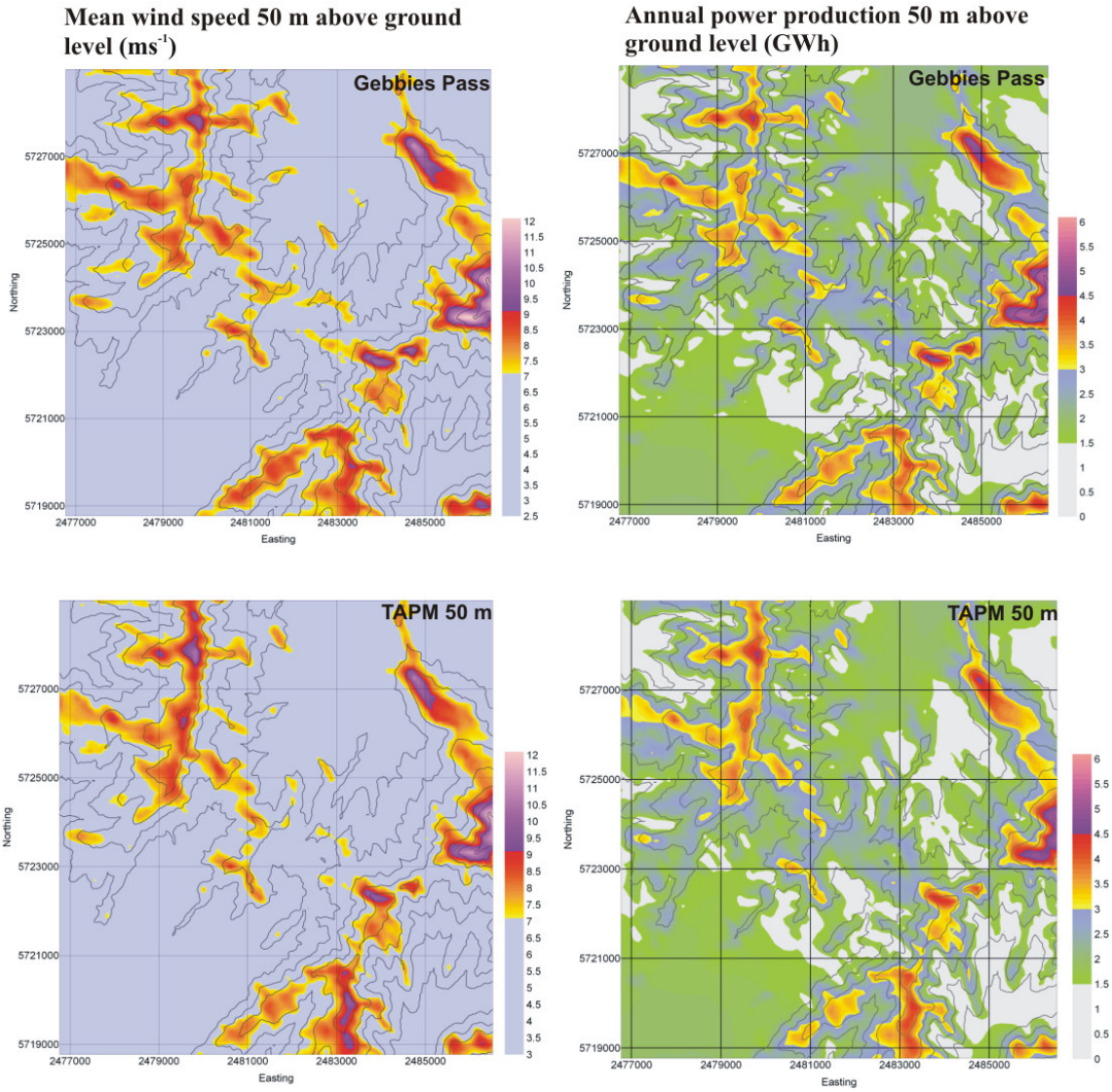


**Figure 4.11: Mean wind speed and AEP resource maps for the Gebbies Pass area using observed wind data from the Gebbies Pass site (GBA) and adjusted TAPM data, referred to as GP50M in the previous section.**

Figure 4.11 illustrates the wind and annual energy maps for the Gebbies Pass using the actual winds data from the Gebbies Pass site and from adjusted TAPM model data. Regions of both low and high mean wind speed (and AEP) are closely aligned in these maps. With experience and knowledge of the limitations of mesoscale models to represent channelling and flow over complex terrain, such maps can be used to make a useful and reliable mean wind speed and energy resource assessment for an area of interest when there is no actual data available.

Figure 4.12 shows a three-dimensional view of the 50 m mean wind speed predictions for the Gebbies Pass area based on the Gebbies Pass actual winds and TAPM 50 m wind data. The three-dimensional maps also highlight the low mean wind speed areas, which have similar spatial distributions over the map area.

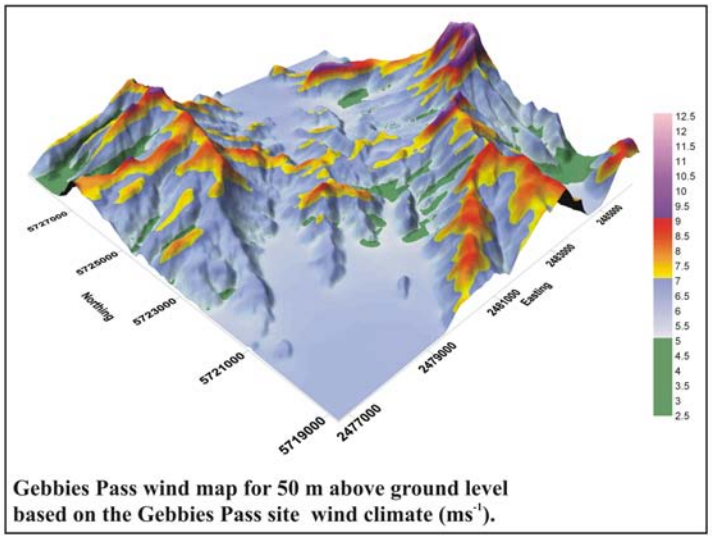


Gebbies Pass wind map for 50 m above ground level based on the Gebbies Pass site wind climate ($ms^{-1}$).

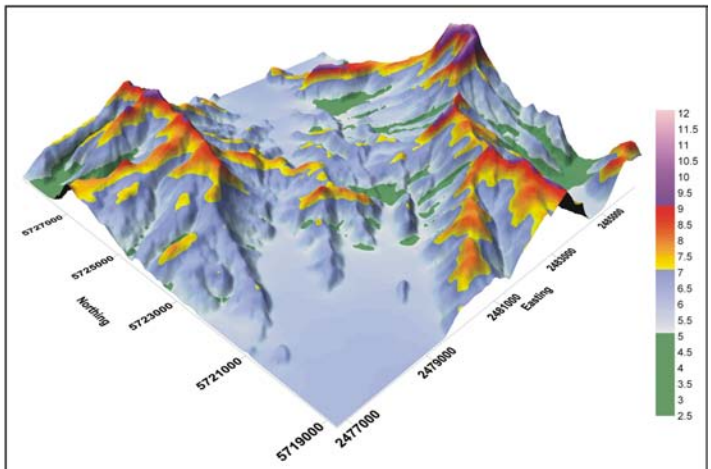


Gebbies Pass wind map for 50 m above ground level based on the TAPM 50 m wind climate ($ms^{-1}$).

**Figure 4.12: Three-dimensional illustrations of 50 m mean wind speed based on actual wind data from the Gebbies Pass site and using wind dataset TAPM 50 m.**

### 4.3.3 RIX and error indication maps for the Gebbies Pass area

The RIX and error indication maps in this section will provide a level of confidence of the wind and energy maps for the Gebbies Pass area. As discussed in the methodology chapter, a significant proportion of WAsP errors can be accounted for by the steepness of the terrain at either the observed or predicted sites. Because the wind data used in a WAsP analysis is independent of topography, RIX and error indication maps should also be able to be applied when using wind data from chosen grid points from a mesoscale meteorological model. The

similarity of the wind and energy maps in Figure 4.11 and 4.12, also suggest that potential errors that result from steep topography are independent of the wind data used.

Figure 4.13 shows the RIX values for the Gebbies Pass area. The RIX calculations are based on a 3500 m radius from each 100 m spaced grid point, and indicate the proportion of the topography that exceeds a slope of 0.3. For example, if the RIX value at a location is 35, then 35% of the topography within 3500 m of that grid point has slope in excess of 0.3. The highest RIX values are over the complex topography to the east and southeast of Gebbies Pass. An area of relatively high RIX values is also located over the Port Hills to the northwest. Flow splitting and separation are likely to occur at these locations.

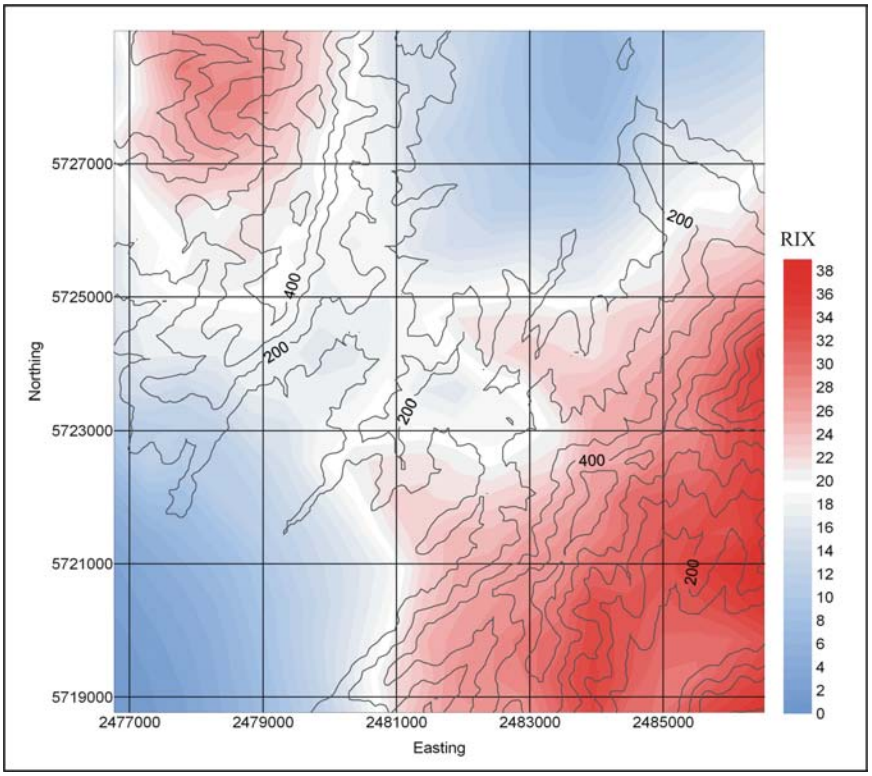


**Figure 4.13: RIX map for the Gebbies Pass area based on 20 m interval contour height data.**

An indication of potential errors in the mean wind speed predictions by WAsP, are given in Figure 4.14. Bowen (2004) suggested that accurate predictions are likely if the observed and predicted sites have similar RIX values. Given that the RIX value near the Gebbies Pass site is 19, the regions with no shading have RIX values in the range of 14 and 24, therefore suggesting that the WAsP predictions are accurate for these areas. When the deviation of RIX values is more than this, then under or over-prediction is likely to occur. For example, there is potential for significant over-prediction of the mean wind speed over some of the elevated and steep terrain to the east and southeast of Gebbies Pass. Also, there is potential for under-

prediction of the mean wind speed over the flat terrain and sea areas to the northeast and southwest of Gebbies Pass.

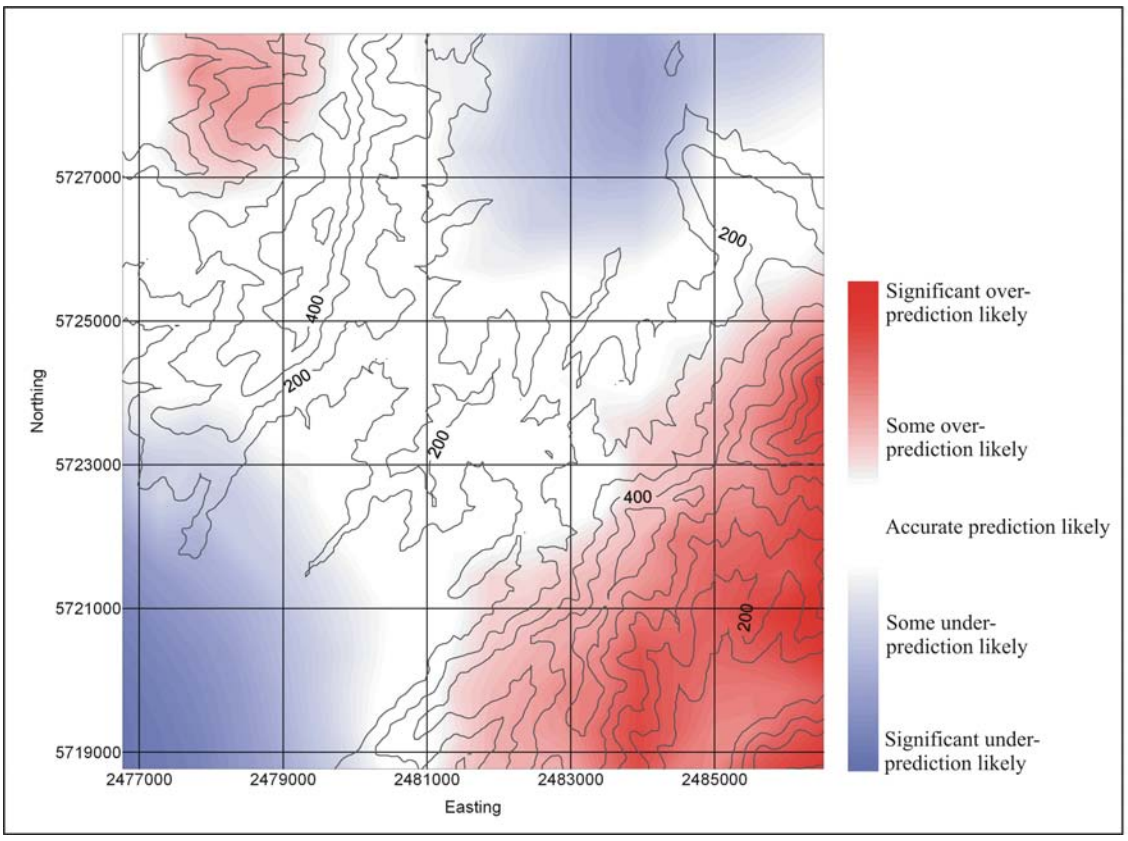


**Figure 4.14: Error indication map for the Gebbies Pass area. The degree of likely under or over prediction is based on the relative difference in the RIX values between the Gebbies Pass site and grid points over the map area at 100 m intervals.**

It is difficult to put quantitative error values on WAsP predictions due to limited research on this topic, and also because other factors affect the prediction process. Reliable wind data at sites of different 'ruggedness' over the map area and for the same period would be useful to assess these quantitative errors of a WAsP prediction in complex terrain.

### 4.3.4 An application for the combined prognostic and diagnostic modelling - a wind farm simulation

High-resolution mean wind speed and annual energy production maps have been presented in previous sections of this study. Also using the WAsP model, a simulated wind farm case study is given below. This wind farm case study applies the results of the combined prognostic and diagnostic modelling technique. A simulated wind farm analysis was completed for a ridge on the northeast of the Gebbies Pass analysis map area, as shown in

bordered areas in Figure 3.11 and Figure 5.2. The wind and annual energy production results on the ridgeline indicate that this location has good wind energy potential. The evidence of tree deformation shown in Figure 5.3 also supports the model results. The analysis was based on corrected wind data for the TAPM model. (The corrected wind data was used to account for the limitations of the prognostic model (TAPM) to fully simulate the effects of channelling at the Gebbies Pass site, as previously discussed in detail).

Ten simulated 1 MW Vestas turbines at a hub height of 50 m above ground level were positioned along the ridgeline. The turbines were positioned to optimise the wind resource (as illustrated by the wind map in Figure 5.2) and also perpendicular to the prevailing wind directions (northeast and southwest), to reduce the wake effects from neighbouring turbines. For this case study, the separation distances between turbines were not rigorously considered. Figure 4.15 shows the positions of the ten turbines that extend along the ridge from 185 m to 295 m above mean sea level.

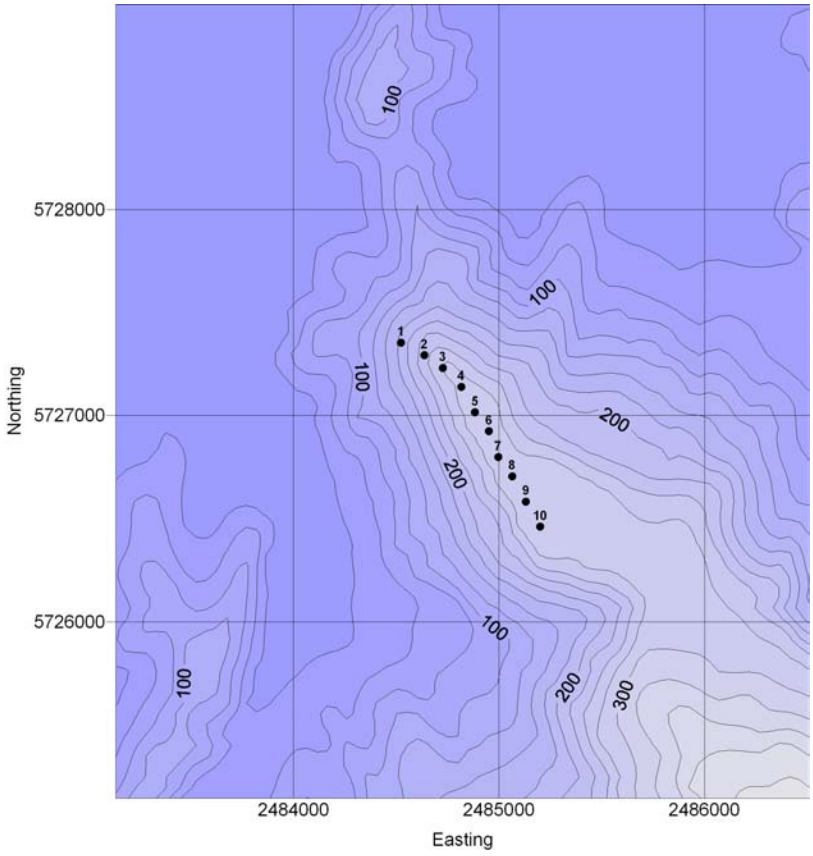


**Figure 4.15: Position of the ten Vestas 1 MW turbines in the simulated wind farm**

The results from the wind farm simulation are given in Table 4.11, 4.12, and 4.13 below. Table 4.11 gives the positions and elevations for each of the turbines. Table 4.12 gives the

mean wind speed and annual energy production (AEP) and the wake loss at each turbine site. (The net AEP accounts for the wake loss.) The final table (4.13) gives an overall summary of the energy output from the wind farm. Note that the wake loss is very low for this simulated wind farm due to the prevailing wind directions, from the northeast and southwest, being across the line of turbines.

**Table 4.11: Locations and elevations of the ten Vestas 1 MW turbines in the simulated wind farm.**

| Site | Location (NZMG) | Elevation (m) |
|---|---|---|
| 1 | (2484523, 5727354) | 181 |
| 2 | (2484636, 5727292) | 238 |
| 3 | (2484726, 5727231) | 275 |
| 4 | (2484816, 5727139) | 280 |
| 5 | (2484883, 5727015) | 284 |
| 6 | (2484951, 5726923) | 287 |
| 7 | (2484996, 5726800) | 289 |
| 8 | (2485064, 5726707) | 291 |
| 9 | (2485131, 5726584) | 292 |
| 10 | (2485401, 5726462) | 295 |

**Table 4.12: Predicted mean wind speed and energy production from the ten turbines. Note that the net AEP accounts for the wake effects from the other turbines.**

| Site | Mean wind speed ($m\ s^{-1}$) | Gross AEP (GWh) | Net AEP (GWh) | Wake loss [%] |
|---|---|---|---|---|
| 1 | 9.12 | 3.536 | 3.535 | 0.03 |
| 2 | 10.16 | 3.919 | 3.865 | 1.38 |
| 3 | 10.89 | 4.113 | 4.059 | 1.31 |
| 4 | 10.56 | 4.015 | 3.972 | 1.07 |
| 5 | 10.10 | 3.886 | 3.843 | 1.1 |
| 6 | 9.95 | 3.822 | 3.774 | 1.26 |
| 7 | 9.78 | 3.767 | 3.730 | 0.96 |
| 8 | 9.42 | 3.643 | 3.617 | 0.71 |
| 9 | 9.14 | 3.532 | 3.508 | 0.68 |
| 10 | 8.85 | 3.414 | 3.393 | 0.6 |

**Table 4.13: Summary annual energy production from the simulated wind farm.**

| | Total | Mean | Min. | Max. |
|---|---|---|---|---|
| **Net AEP (GWh)** | 37.298 | 3.730 | 3.393 | 4.059 |
| **Gross AEP (GWh)** | 37.647 | 3.765 | 3.414 | 4.113 |
| **Wake loss (%)** | 0.93 | - | - | - |

## 4.4 Results Summary

The results in this study highlighted the difficulties of modelling airflow in a complex terrain environment, at both a regional and local scale. The steep character of the topography of the Banks Peninsula area, and also the scale of topographic features, provided one of the most challenging regions to simulate mesoscale airflow patterns. There were also complex interactions on the wider regional scale airflow by other significant topographic features, such as the Southern Alps and Cook Strait. Applying the WAsP program in the Gebbies Pass area also identified limitations of using this model in a very complex environment. However valuable results were gained in all of the case studies completed above. When using wind data from one mesoscale model as input into another, being aware of model limitations, and also of the behaviour of wind in complex terrain, is important in being able to identify and overcome such limitations.

# Chapter 5

## Conclusions

This chapter provides conclusions from the prognostic modelling, and the combined prognostic and diagnostic modelling work. Discussions will cover the strengths and limitations of these modelling processes, and also propose ways to overcome and reduce these limitations so to make reliable wind and energy predictions.

### 5.1 Prognostic modelling – Low-resolution

The aim of this aspect of the research was to investigate whether low-resolution prognostic modelling could be used to produce wind maps that would be useful in identifying general regions favourable for wind energy generation. The TAPM model was run for the year 2002 to simulate the overall wind climatology for two 120 km by 120 km areas (covering parts of Canterbury and Otago) at 50 m above ground level. Simple comparisons were made with 50 m mean wind speed estimates from The Wind Energy Resource Survey of New Zealand (Cherry, 1987).

Using this low-resolution modelling, broad regions favourable for wind energy generation were able to be located. At 2000 m grid spacing, larger scale topographic features, with dimensions greater than about 10 km could be accounted for in the modelling process, so that the wind climatology over reasonably large regions could be identified. However, the effects of small-scale terrain features on the airflow patterns were not accurately modelled. This is significant, because such features are likely to have a significant impact on the local scale variations of mean wind speed, especially in more complicated terrain. As seen in the simple comparisons with Cherry's (1987) work, the modelled 50 m mean wind speeds in complex terrain appear to be underestimate. However, over homogeneous terrain, mean wind speeds appeared to be modelled more accurately.

### 5.2 Prognostic modelling – High-resolution

There to were two aims of this part of the prognostic modelling programme. The first was to determine if a reliable wind map could be generated for a region of complex terrain. The second aim was to assess if wind data from specific locations (grid points) of the modelled region could be successfully used in the high-resolution industry-standard wind energy assessment model, WAsP, when no actual reliable wind data were available.

The TAPM model was run for a one-year period (2002) for the Banks Peninsula region at a resolution of 800 m. Wind maps were generated for heights of 10 m, 25 m, 50 m, and 100 m above ground level. A detailed validation analysis was carried out at four sites where there were actual wind data available for either all or part of the modelled period.

When comparing the 2000 m and 800 m resolution wind maps for the Banks Peninsula area, it is clear that the higher resolution maps provide much more spatial detail of the spatial variation of the mean wind speed. Smaller regions can be identified for potential wind energy developments and more accurate quantitative assessments can also be made. However, as discussed in the results section, the scale of many topographic features in the Banks Peninsula region means that they are still not represented perfectly at this model resolution. The results and validation analysis provide the following conclusions for the TAPM prognostic modelling at 800m-resolution:

- A good overall indication of the mean wind speed climate and the spatial patterns of the mean wind speed can be obtained in regions of complex terrain.

- It is likely that the mean wind speeds over elevated terrain and at locations that experience local channelling of airflows are under-estimated by the model. Channelling of wind is not likely to be represented accurately when the scale of topography features is less than about 3–5 km (as suggested in (Met Office, 2005).

- The model does not always accurately represent short duration extreme high or low wind speed events. The end result is a smoother depiction of the wind speed by the model compared to the actual winds over a period of time.

- There are limitations of modelling winds over the Canterbury region that result from regional scale pressure distortions in many westerly synoptic scale situations. This has resulted in a higher frequency of westerly and southerly component winds being modelled than actually occurs.

- It is limited by the 800m-grid spacing in its ability to resolve local scale speed-up effects from topography features such as hills and smaller ridges. This is likely to result in conservative modelled mean wind speeds in these areas.

Based on theory of airflow in complex terrain, and experience and knowledge gained from the prognostic modelling in this study, the following conclusions have been made for the 800 m-resolution wind maps specific to the Banks Peninsula region:

1. For exposed locations that are influenced by significant local channelling of airflows, 50 m modelled winds are likely to better represent 10 m observed winds. This would apply to smaller scale features such as harbour entrances and passes aligned with the prevailing wind directions.

2. For exposed sites not affected by channelling of airflows, 25 m modelled winds are likely to better represent 10 m observed winds. This would apply to areas such as near the Port Hills summit and other lower level ridges in Banks Peninsula.

3. A 75 m level wind map is likely to give a better representation of mean wind speeds at 50 m over exposed and higher terrain. This would apply to the high ridges east of Mt Herbert and around Akaroa Harbour.

Modelling was run at higher resolutions to improving the simulation of channelling and effects from smaller scale topography features. However, it was found that TAPM became unstable at grid spacing less than 800 m for this area. Similar model instability has been documented for the MM5 model, when the model became unstable in mountainous terrain at resolutions less than 1000 m (Pinard, 1999).

As discussed in the results chapter, there are limitations in the prognostic modelling of airflow over areas of complex terrain, such as for parts of the Banks Peninsula region. However, by recognising when these limitations are likely to occur, it is possible to apply a correction factor so that mesoscale derived wind data can be used with confidence in the higher resolution wind assessment model, WAsP. The statistical analysis, and the wind and energy maps for the Gebbies Pass area in the previous chapter illustrate that this can be done. In the combined prognostic and diagnostic modelling methodology, TAPM data from a grid point near the Gebbies Pass site from 50 m level was used to represent the 10 m above ground wind climate for the Gebbies Pass site. This correction factor was used to overcome TAPM's limitations to accurately simulate the channelling of airflow in the Gebbies Pass area. Further discussion and the implications of these results will be provided in the following section.

## 5.3 Combined prognostic and diagnostic modelling conclusions

The overall aim of the combined prognostic and diagnostic modelling work was to assess if wind data derived from the prognostic model TAPM, could be used as input to the diagnostic model WAsP to make reliable predictions of wind and energy for an area in complex terrain. After considering the limitations of the WAsP model, this aim was divided into the following three parts (as also given in Section 3.2.3).

4. Use wind data derived from the prognostic mesoscale meteorological model (TAPM) to generate a wind climate for WAsP when there is no actual reliable wind data available. Ideally the results from TAPM should have been previously validated using other reliable wind monitoring sites within the inner grid of the modelled area.

5. Use prognostic mesoscale modelled wind data to reduce potential errors that can result in WAsP predictions due to the situation when the observed and predicted sites are located in different climate zones and/or 'ruggedness' areas.

6. Assess the relationship between the 'ruggedness' of sites and the size of the modelling errors, to assess the reliability of WAsP predictions in a complex terrain environment.

As discussed in the results, the best wind data available for a wind energy assessment (in the absence of actual wind data) were derived from the prognostic model TAPM, from the closest grid point to the validation (or prediction) site (rather than the nearest wind monitoring site located 20 km or so away). Limitations of the prognostic modelling were identified and discussed in results chapter (and also in Section 5.2 above), and measures were applied to overcome these. These measures were based on the statistical analysis of the sectorised wind direction frequency of occurrence and annual energy production, and also the overall mean wind speed and total annual energy production predictions. For example, the 50 m level TAPM winds were found to better simulate the 10 m actual winds at the Gebbies Pass site. Similar judgements would need to be made when using modelled wind data for WAsP predictions in other areas. Experience of the prognostic model limitations and knowledge of wind processes in complex terrain are essential to make such judgements.

It is relevant here to refer to conclusions made in the study by Bowen and Mortensen (1996), where it was suggested that accurate predictions using WAsP could be obtained provided that the following criteria are satisfied:

- Both the reference and predicted sites are subject to the same weather regime.
- The prevailing weather conditions are close to being neutrally stable.
- The terrain surrounding the reference and predicted sites is sufficiently gentle and smooth to ensure mostly attached flows.
- The reference data are reliable.

In the same study, Bowen and Mortensen (1996) concluded that if the 'ruggedness' around the observed and predicted sites were similar, then the prediction errors resulting from unattached flow could cancel each other out resulting in accurate predictions.

The use of prognostic mesoscale meteorological models to generate wind data can address some of the issues highlighted above, to make WAsP predictions more reliable. First, wind data can be obtained from appropriately located grid points so that the observed and predicted sites are subject to the same weather regimes. For example, if a wind energy development spans a range of elevations, prognostic model wind data could be obtained from selected grid points at high and low elevations. WAsP predictions could then be made with each of these input data to maintain the 'same weather regime' requirement. Another advantage using wind data from the prognostic model is that wind data can be obtained from sites of similar 'ruggedness' to the predicted site (or area). The 'ruggedness index' (RIX) map could be used to identify grid points from which wind data can be obtained.

It is likely that the same grid points could satisfy the climate and ruggedness requirements to obtain a reliable WAsP prediction. Figure 5.1 shows the RIX map for the Gebbies Pass area and possible locations of six grid points from which TAPM wind data could be obtained to generate wind and energy production maps for the Gebbies Pass map region. It may be necessary to use an interpolation procedure such as Kriging to smooth any discontinuities at the boundaries of each of the WAsP 'small-area prediction' areas that will make up the whole map.

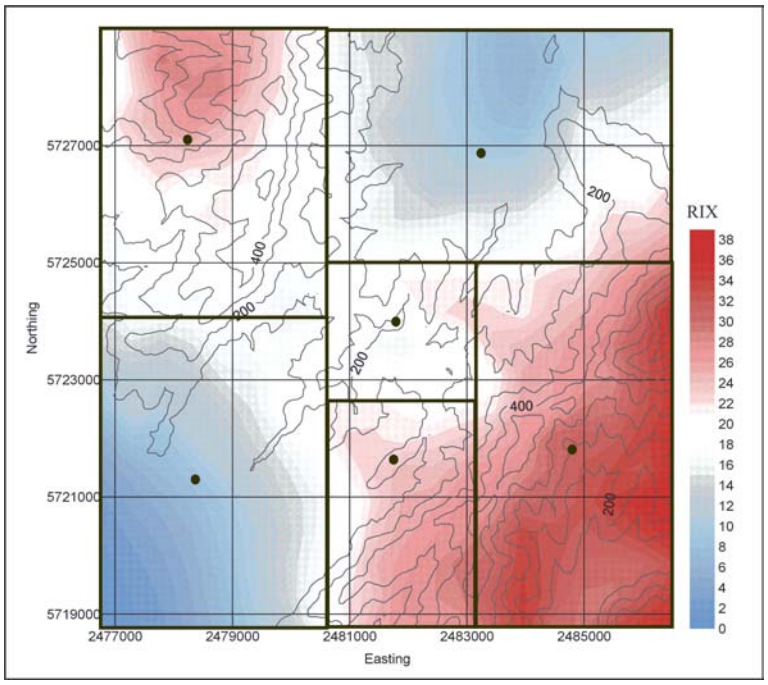


**Figure 5.1: A possible mosaic of WAsP prediction areas used to generate wind or energy maps for the whole area. The dots indicate possible grid points from which prognostic mesoscale wind data could be obtained.**

Therefore RIX and error indication maps could be used in two ways:

- To identify areas where there is likely to be under or over-prediction of the mean wind speed in a WAsP area analysis.
- To help locate sites from which wind data could be obtained from a prognostic model to reduce the potential errors in a WAsP analysis.

The reliability of the reference data is a key component of a WAsP analysis. Obtaining wind data from a prognostic mesoscale meteorological model, that has had limitations identified in complex terrain, could be argued as adding another level of uncertainty to the wind and energy predictions. However, there is evidence in this study that it is more reliable to use this wind data than to use actual wind data from a site in a different climate or topographic environment (often some distance away from the potential wind farm site). It should be noted that the number of existing wind measurement sites in New Zealand is very limited. The KAMM/WAsP methodology follows a similar approach (Petersen (1996) and Frank (2001)) when making wind and energy predictions, but there is no reference to its use in a complex terrain environment.

Bowen (2004) suggested that there is much further potential to investigate the ruggedness index (including varying the parameters in RIX value calculations) and its relationship with

the prediction errors of WAsP. However, with a new version of WAsP due to be released that incorporates a non-linear orographic model, there will be a need to conduct new case studies to assess this relationship how well the new model handles the effects of topographic complexity.

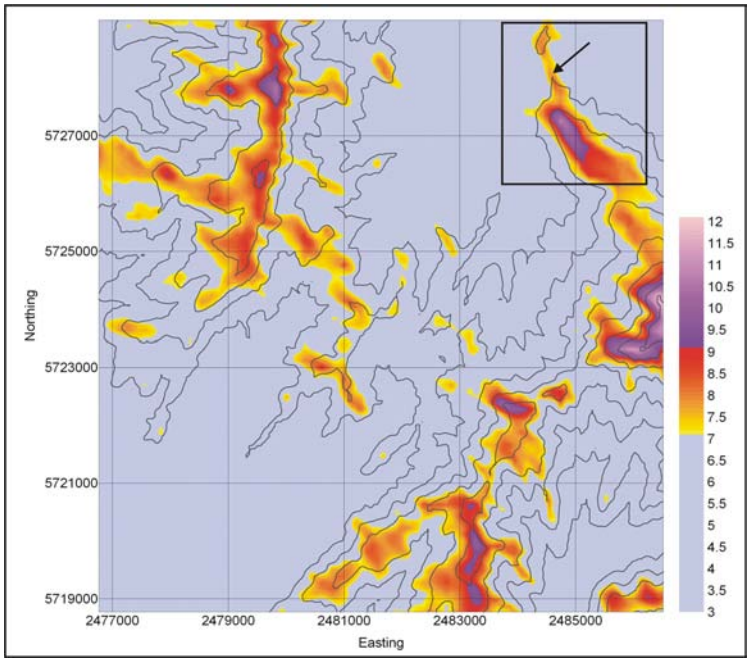


**Figure 5.2: 50 m wind map for the Gebbies Pass area generated using TAPM wind data derived from the closest grid point to the Gebbies Pass site. The region within the border at the top right of the map will be used to simulate a small wind farm. The arrow in this area shows the position of the tree in Figure 5.3.**

The 50 m wind map for the Gebbies Pass area (Figure 5.2) was generated using the TAPM wind data from near the Gebbies Pass site. Some of the highlighted region appears to be favourable for wind energy generation due to the relatively high mean wind speeds, easy access and smooth terrain. Figure 5.3 provides a photograph of a tree that has been deformed by the wind in this area. The arrow in Figure 5.2 shows the approximate position of the tree. Using the Griggs-Putnam Index (described in Section 2.4.3 to estimate the mean wind speed from the deformation of coniferous type trees), the 7 m above ground mean wind speed was estimated to be 6.1 m $s^{-1}$. Using the logarithmic vertical profile model (see Section 2.6.1), this equates to a 50 m mean wind speed about 7.8 to 8.3 m $s^{-1}$, which is in good agreement with the wind map prediction.

Evidence of tree deformation was also sought for the higher mean wind speed area to the east, but the area was covered in dense young trees. However, there was some evidence on the

corner of the forested area of the bending of trunks of small trees away from the southwest on the southern side of the ridge, and away from the northeast on the northern side of the ridge.

**Figure 5.3: Evidence of tree deformation near 100 m elevation, as indicated in the map region in Figure 5.2.**

## 5.4 In summary

This thesis demonstrated that sophisticated computer models can be powerful tools to identify and quantify regions of good wind energy potential. Awareness of model limitations and knowledge of airflow in complex terrain are also key requirements to confidently assess the mean wind speed and energy potential. The use of simple empirical techniques can still be useful tools in the identification and validation of 'windy' sites.

Wind maps derived from prognostic mesoscale modelling at about 800 m resolution are valuable for assessing the mean wind speed climate over a wide area, and also for generating wind data at specific sites.

Recent assessment studies in less complex terrain (compared to the Gebbies Pass region) have shown that wind data from a mesoscale meteorological model at specific sites validated very well with actual data from those sites. The ability to obtain reliable wind data at sites where there are no actual wind data and use it to drive the higher resolution industry standard model, WAsP, could result in significant savings of both time and money for wind energy developers.

# References


Angle, R. P. and S. K. Sakiyama (1991) Plume dispersion in Alberta, Edmonton. Standards and approval division, Alberta Environment.

Barry, R. G. (1992) *Mountain weather and climate,* New York, Routledge, Chapman and Hall, Inc.

Beckrakis, D. A. and P. D. Sparis (2000) Simulation of the wind speed at different heights using artificial neural networks. *Wind Engineering* 24(2): 127-136.

Bowen, A. J. & Mortensen, N. G. (1996) Exploring the limits of WAsP: the Wind Atlas Analysis and Application Program. *Proceedings of the 1996 European Union Wind Energy Conference.* Gotenburg, Sweden.

Bowen, A. J. & Mortensen, N. G. (2004) WAsP prediction errors due to site orography. Roskilde, Denmark, Riso National Laboratory.

Brower, M., J. W. Zack, et al. (2002). Mesoscale modeling as a tool for wind energy assessment and mapping.

Cherry, N. (1987) Wind energy resource survey of New Zealand. Lincoln College.

Cook, N. J. (1997) The Deaves and Harris ABL model applied to heteorgeneous terrain. *Journal of Wind Engineering and Industrial Aerodynamics,* 66**,** 179-196.

Coppin, P. A., Ayotte, K. W., Steggel, N. & Hurley, P. J. (2000) Recent advances in wind energy resource assessment. IN DURIE, D. J. (Ed.) *CSIRO Energy Technology, Electricity Supply Association of Australia, IEA Greenhouse Gas Programme.* Cairns.

Coppin, P. A., E. F. Bradley, et al. (1994). Measurements of flow over a elongated ridge and its
thermal stability dependence: the mean field. *Boundary Layer Meteorology* 69: 173-199.

Corbet, D. C. (1993) Viability of a wind farm in an area of low wind speed. IN PITCHER, K. F. (Ed.) *Fifteenth BWEA Wind Conference.*

Danish Wind Energy Association (2005a) *Describing wind variations: Weibull distribution. Available from: www.windpower.org/en/tour/wres/weibull.htm.*

Danish Wind Energy Association (2005b) *The power coefficient. Available from: http://www.windpower.org/en/tour/wres/cp.htm.*

Dunbar, C. & Inan, D. (1996) Investigation of wind energy application possibilities for a specific island (Bozcaada) in Turkey. *Renewable Energy,* 9**,** 822-826.

Dvorak, P. (2001) Wind power is getting too good to resist. *Future Technology Energy - Machine Design***,** 84-90.

Emery, C. A., Tai, E. & Yarwood, G. (2001) Enhanced meteorological modeling and performance evaluation for two Texas ozone episodes. Novato, ENVIRON International Corporation.

Environ (2004) Draft protocol. 2002 annual MM5 simulations to support WRAP CMAQ visibility modeling for the section 308 SIP/TIP. Novato, ENVIRON International Corportation.

Finardi, S., Tinarelli, G., Faggian, P. & Brusasca, G. (1998) Evaluation of different wind field modeling techniques for wind energy applications over complex topography. *Journal of Wind Engineering and Industrial Aerodynamics,* 74-76**,** 283-294.

Frank, H. P., Rathman, O., Mortensen, N. G. & Landberg, L. (2001) *The numercial wind atlas: the KAMM/WAsP method*, Riso National Laboratory.

Gardiner, M. W. & Dorling, S. R. (1998) Artificial neural networks (the multi-layer perceptron): a review of applications in the atmospheric sciences. *Atmospheric Environment,* 32**,** 2627-2636.

Greenpeace (2005). *Greenpeace urges hearing to say yes to West Wind. Available from: http://www.greenpeace.org.nz/news/news_main.asp?PRID=854.*

Hewsen, E. W. & Wade, J. E. (1979) *A handbook for the use of trees as indicators of wind power potential,* Springfield, Virginia, National Technical Service.

Hunt, J. C. R. (1980) Wind over hills. IN WYNGAARD, J. C. (Ed.) *Workshop on the planetary boundary layer.* American Meteorological Society.

Hurley, P. J. (2002) The air pollution model (TAPM) version 2. Part 1: Technical description. Aspendale, CSIRO Atmospheric Research.

Hurley, P. J., Physick, W. L. & Luhar, A. K. (2002) The air pollution model (TAPM) version 2. Part 2: Summary of some verification studies. Aspendale, CSIRO Atmospheric Research.

Jacobson, M. Z. (1999) *Fundamentals of atmospheric modeling,* Cambridge, Cambridge University Press.

Lalas, D. P., Ratto, C. F. & Walmsley, J. L. (1996) Glossary. IN Lalas, D. P. & Ratto, C. F. (Eds.) *Modelling of atmostpheric flow fields.* World Scientific Publishing Co Pte Ltd.

Luhar, A. K. & Hurley, P. J. (2003) Evaluation of TAPM, a prognostic meteorological and air pollution model, using urban and rural point-source data. *Atmospheric Environment,* 37**,** 2795-2810.

Mason, P. J. & King, J. C. (1984) Atmospheric flow over a sucession of neary two-dimensional ridges and valleys. *Quarterly Journal Royal Meteorological Society,* 110**,** 821-845.

McCauley, M. P. & Sturman, A. P. (1999) A study of orographic blocking and barrier wind development upstream of the Southern Alps, New Zealand. *Meteorology and Atmospheric Physics,* 70**,** 121-131.

Met Office (UK) (2005). *Representing orography in the forecasting model. Available from: http://www.metoffice.com/corporate/scitech0001/8_apr/3.html.*

Milborrow, D. (2002) Wind energy technology: the state of the art. *Journal of power and energy,* 216**,** 23-30.

Miller, C. A. (1996). Turbulent boundary layers above complex terrain. London, University of Western Ontario.

Mortensen, N. G., D. N. Heathfield, et al. WAsP 8 help facility 1987-2003. Wind atlas analysis and application program. Roskilde, Denmark, Riso National Laboratory.

Mortensen, N. G., L. Landberg, et al. (1999). Wind atlas analysis and application program (WAsP). Vol 3: Utility programs. Roskilde, Denmark.

Mortensen, N. G. and E. L. Petersen (1997). Influence of topographical input data on the accuracy of wind flow modelling in complex terrain. European Community Wind Energy, Dublin, Ireland.

Moussiopoulos, N. (1996) Mesoscale models and their use. IN Lalas, D. P. & Ratto, C. F. (Eds.) *Modelling of Atmospheric Flow Fields.* World Scientific Publishing.

Neale, A. A. (1987) *Weather forecasting in New Zealand,* Wellington, New Zealand Meteorological Service.

New Zealand Wind Energy Association (2005a) *The cost of wind energy. Available from: http://www.windenergy.org.nz/FAQ/cost_wind.htm*.

New Zealand Wind Energy Association (2005b) *Currently operational New Zealand wind farms. Available from: http://www.windenergy.org.nz/FAQ/proj_dom.htm*.

New Zealand Wind Energy Association (2005c) *Global installed [wind energy] capacities. Available from: http://www.windenergy.org.nz/FAQ/proj_glob05.htm*.

New Zealand Wind Energy Association (2005d) *Global warming: what it is and New Zealand's role. Available from: http://www.windenergy.org.nz/FAQ/warming.htm#kyoto*.

New Zealand Wind Energy Association (2005e) *Map of wind farms in New Zealand. Available from: http://www.windenergy.org.nz/FAQ/map.htm*.

New Zealand Wind Energy Association (2005f) *Transpower map of current and potential wind farms in New Zealand. Available from: http://www.windenergy.org.nz/FAQ/transmap.htm*.

New Zealand Wind Energy Association (2005g) *Wind energy, total domestic energy needs and electrical supply. Available from: http://www.windenergy.org.nz/FAQ/elecsupply.htm*.

Perera, M. D. (1981). Shelter behind two dimensional solid and porous fences. *Journal of Wind Engineering and Industrial Aerodynamics* 8: 93-104.

Petersen, E. L., Landberg, L. & Mortensen, N. G. (1996) European wind atlas. Vol. II: Measurements and modelling in complex terrain. Roskilde, Denmark, Riso National Laboratory.

Petersen, E. L., Troen, I., Frandsen, S. & Hedegaard, K. (1981) *Wind atlas for Denmark: a rational method for wind energy siting.,* Roskilde, Denmark, Riso National Laboratory.

Pinard, J. P. (1999) *Computer models for wind flow over mesoscale mountainous terrain applied to the Yukon. Available from:* http://www.polarcom.com/~jppinard/MesoscalesModels.pdf, University of Alberta.

Putnam, P. C. (1948) *Power from the wind,* New York, Van Nostrand Co. Inc.

Ratto, C. F. (1996) An overview of mass consistent models. IN Lalas, D. P. & Ratto, C. F. (Eds.) *Modelling of atmospheric flow fields.* World Scientific Publishing.

Reid, S. (1997) Modelling of channelled winds in high wind areas of New Zealand. *Weather and Climate,* 17**,** 3-21.

Reuters News Service (2003) NZ Government to back wind farms with carbon credits.

Rohatgi, J. (1996) An analysis of the influence of atmospheric stability on vertical wind profiles: its influence on wind energy and wind turbines. *Wind Engineering,* 20**,** 319-332.

Rohatgi, J. & Nelson, V. (1994) *Wind Characteristics: an analysis for the generation of wind power,* Canyon, Tx, Alternative Energy Institute.

Saba, T. (1999) The evaluation of software for wind turbine sitting in simple and complex terrain. *Engineering.* Christchurch, Canterbury University.

Salmon, J. R. & Walmsley, J. L. (1999) A two-site correlation method for wind speed, direction and energy estimates. *Journal of Wind Engineering and Industrial Aerodynamics,* 79**,** 233-268.

Salvador, R., Calbo, J. & McMillan, M. (1999) Horizontal grid size selection and its influence on mesoscale model simulations. *Journal of Applied Meteorology,* 38**,** 1311-3130.

Simmon, M. (2002) Wind turbines are sprouting off Europes shores. *New York Times.* New York.

Sims, R. E. (1992) Candidate wind farms sites in New Zealand.

Steggel, N., K. W. Ayotte, et al. (2002). Wind prospecting with windscape, Wind Energy Research Unit CSIRO Land and Water.

Sturman, A. P. and M. Kossmann (2003). Pressure-driven channelling effects in bent valleys. *Journal of Applied Meteorology* 42(1): 151-158.

Taylor, P. A., Mason, P. J. & Bradley, E. F. (1987) Boundary layer flow over hills. *Boundary Layer Meteorology,* 39**,** 107-132.

Troen, I. (1990). A high resolution spectral model for flow in complex terrain. Ninth Symposium on Turbulence and Diffusion, Roskilde, Denmark.

Troen, I., N. G. Mortensen, et al. Wind atlas and analysis program (WAsP), 1987-2003. Roskilde, Denmark, Riso National Laboratory.

Troen, I. & Petersen, E. L. (1989) *European wind atlas,* Roskilde, Denmark, Riso National Laboratory.

Walmsley, J. L. (1996) The Jackson-Hunt approach. IN LALAS, D. P. & RATTO, C. F. (Eds.) *Modelling of atmospheric flow fields.* World Scientific Publishing.

Whiteman, C. D. (2000) *Mountain meteorology: fundamentals and applications,* New York, Oxford Univeristy Press.

Whiteman, C. D. & Doran, J. C. (1993) The relationship between overlying synoptic-scale flows and winds in a valley. *Journal of Applied Meteorology,* 32**,** 1669-1682.

Willmott, C. J. (1982). Some comments on the evaluation of model performance. *Bulletin of the American Meteorological Society* 63(11): 1309-1313.

Winters, J. (2003) Winding up. *Mechanical Engineering,* 125**,** 36-39.

Wood, N. (1995) The onset of separation in neutral, turbulent flow over hills. *Boundary Layer Meteorology,* 76**,** 137-164.

Woods, J. C. & Watson, S. J. (1997) A new matrix method of predicting long-term wind roses with MCP. *Journal of Wind Engineering and Industrial Aerodynamics,* 66**,** 85-94.

Zaphiropoulos, Y., P. Dellaportas, et al. (1999). Prediction of wind speed and direction at potential sites. *Wind Engineering* 23: 167-175.